Recent Advances in the Chemistry of Carborane Metal Complexes Incorporating d- and f-Block Elements

Anil K. Saxena and Narayan S. Hosmane*

Department of Chemistry, Southern Methodist University, Dallas, Texas 75275

Received July 31, 1992 (Revised Manuscript Received November 18, 1992)

Contents

I. Introduction 1081
II. Metallacarboranes of d-Block Elements 1081
A. Early Transition Metal Complexes 1082
B. Middle and Late Transition Metal Complexes 1103
C. Linked-Cage and Multidecker Complexes 1109
D. Complexes of Arene and $C_8H_8^{2-}$ Ligands 1111
E. Complexes of Mono-, Tri-, and Tetracarbon Carborane Ligands 1113
III. Metallacarboranes of f-Block Elements 1117
IV. Metallacarboranes in Catalysis 1120
V. Current and Future Directions 1121
VI. Acknowledgment 1122
VII. References 1122

I. Introduction

There is a large and growing field of transition metal cluster chemistry in which carborane ligands are involved. Several monographs and review articles that adequately cover the earlier work are available.[1-5] In a recent issue of *Chemical Reviews* Grimes discussed small clusters that contain carborane or organoboron ring ligands,[3a] while Bregadze reviewed the chemistry of externally derivatized heterocarboranes in detail.[3b] The latest developments in the general area of metallacarboranes have not been gathered into a single review article. Therefore, this review has a very different focus from the recently published articles and hence discusses the most promising research that has been published during the past 10 years or so on the d- and f-block metal complexes derived from various carborane ligand systems.

Carboranes constitute one of the most studied classes of polyhedral molecules with a variety of structural arrangements that are well understood and depicted using various electron counting rules.[6] Most of the observed borane clusters can be grouped into three geometrically distinct classes: *closo*-$B_nH_n^{2-}$, *nido*-B_nH_{n+4}, and *arachno*-B_nH_{n+6}.[7] The electron counting rules of Wade suggest that clusters with $(2n + 2)$ skeletal electrons adopt a closo structure, and those with $(2n + 4)$ and $(2n + 6)$ skeletal electrons possess nido and arachno geometries, respectively. Increasingly, however, exceptions to these rules are being observed. Therefore, these electron counting rules[6,7] of Wade and Williams, although they predict accurate geometries of polyhedral boron hydrides, cannot be applied effectively in all cases of polyhedral complexes that incorporate heteroatoms.[1,4]

Metallacarboranes are cluster compounds that incorporate metal atoms or units, and hydrides of carbon and boron in their polyhedral skeletons. A large number of metals have been incorporated as cluster vertices. Figure 1 shows the d- and f-block elements of the periodic table which have formed complexes with carborane ligands.

The chemistry of metallacarboranes originated with the assumption that the dicarbollide ion ($C_2B_9H_{11}^{2-}$) is very similar to the cyclopentadienyl ligand (Cp^-).[8,9] For example, the dicarbollide ion has six delocalized electrons in π-type orbitals on the open C_2B_3 pentagonal face, as those found in the Cp^- ion. However, a number of important features of carborane dianions including the dinegative charge, the inward tilting of the frontier orbitals and the presence of heteroatoms on the bonding face, make them better ligands than Cp ligands. Consequently, a wide variety of metal complexes of the icosahedral and subicosahedral carborane ligand systems have been synthesized and characterized. The carborane ligands also seem to stabilize uncommon and high oxidation states of the metals, such as Cr(IV) and Sn(IV), more effectively than do their organic counterparts.[10,11]

A large number of metallacarboranes that have been synthesized during the last decade display unusual structural and bonding features. The potential general applications of the boron cluster compounds have been reviewed recently by Plešek.[12] In general, metallacarboranes are found in an increasing number of applications in catalysis,[13-18] boron neutron capture therapy (BNCT),[19,20] siloxane-linked polymers,[21] solvent extraction of radionuclides,[12] and ceramics.[22,23] The transition metal complexes are also used to catalyze polyhedral borane reactions, e.g., syntheses of multicage compounds and alkenyl carboranes and ring closures.[24] The isolated and characterized transition metal carborane complexes also help in understanding the mechanisms of these reactions. With the continued progress of metallacarborane chemistry, the day is not far away when their practical applications will ultimately be developed.

II. Metallacarboranes of d-Block Elements

Our discussion is restricted to metallacarboranes in which the d-block element is incorporated as an integral part of the polyhedral framework. No attempt is made to cover those compounds where the metal atom bridges several carborane polyhedra or is involved solely as member of a substituent group. However, exception is made in one or two cases in which the metal atoms are

0009-2665/93/0793-1081$12.00/0

Anil Saxena was born in Agra, India in 1958. He received a Ph.D. degree in Inorganic Chemistry from the University of Rajasthan, India. He was trained in organosilicon chemistry under the supervision of Professors Colin Eaborn, F.R.S., and Adrian Brook. He was a recipient of Alexander von Humboldt fellowship and worked with Professor F. Huber at Dortmund. After about two years of employment at Tata Institute of Fundamental Research and Indian Institute of Chemical Technology. He joined the research group of Professor Narayan Hosmane at Southern Methodist University in 1991. His research interests are in the field of organometallic chemistry of main group elements, catalysis, and molecular modeling. He has coauthored over 45 publications including 4 review articles and monographs.

Narayan S. Hosmane was born in Gokarn, India, in 1948. He is a B.S. and M.S. graduate of Karnatak University, located in the southern part of India. He obtained a Ph.D. degree in Inorganic Chemistry in 1974 from the University of Edinburgh, Scotland, under the supervision of Evelyn Ebsworth. After a brief postdoctoral research training in Frank Glockling's laboratory at the Queen's University of Belfast, he joined Lambeg Research Institute in Northern Ireland and then moved to United States to do research in the area of carboranes and metallacarboranes. After postdoctoral work with W. E. Hill and F. A. Johnson at Auburn University and Russell Grimes at the University of Virginia, in 1979 he joined the faculty at the Virginia Polytechnic Institute and State University. In 1982, he joined the faculty at Southern Methodist University, where he is currently Professor of Chemistry. In 1985, he was invited by Sheldon Shore to spend a sabbatical leave at the Ohio State University as a Visiting Professor. He was the organizer and cofounder of the first Boron USA (BUSA) workshop which was hosted in Dallas in April 1988. His research interests are in the synthesis and structure of carboranes, metallacarborane sandwich compounds, and organosilicon compounds, with particular emphasis on the electrochemical and catalytic studies.

in unusual coordinating sites. This restriction is dictated by the fact that the π-bonded metal atoms have unique properties that are not typical of their usual σ-bonding environment. A great deal of information on reactivity patterns and structures has recently become available on the metallacarboranes of d-block elements. Therefore, this section emphasizes

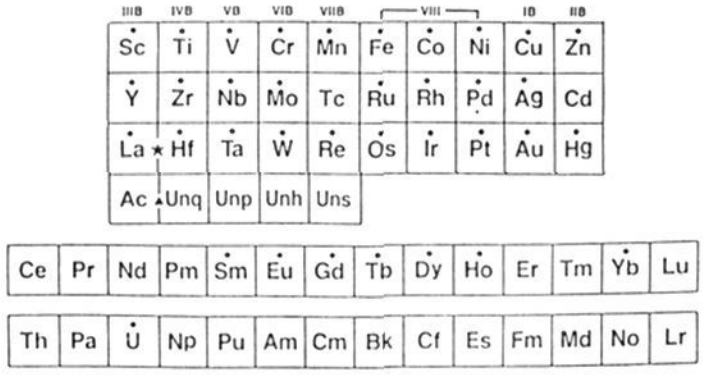

Figure 1. Periodic chart of the d- and f-block elements. (The asterisks denote the elements which have formed metallacarboranes.)

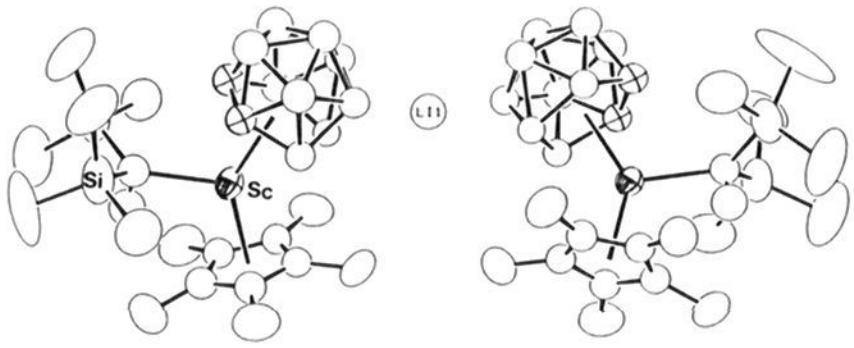

Figure 2. An ORTEP drawing of $\{[Cp^*(C_2B_9H_{11})\text{-}ScCH(SiMe_3)_2]_2Li\}\cdot Li(THF)_3$ showing the two anions with the bridging lithium atom. Reprinted from ref 26a. Copyright 1992 International Union of Crystallography.

as much the structural and bonding features of these complexes as their reaction chemistry. Earlier work is discussed only as background to current results or for purposes of comparison. Although the crystal structures of some of the complexes are discussed in the following subsections, the selected crystallographic parameters of most of the compounds published since 1982 are presented in Table I.

A. Early Transition Metal Complexes

Although the cyclopentadienyl π-complexes of scandium have been known for some time,[25] analogous carborane complexes were not known until recently. Bercaw et al. synthesized, in 1992, a novel permethylcyclopentadienyl dicarbollide scandium complex, $[Li(THF)_3]\cdot Li[Sc(C_2B_9H_{11})(Cp^*)CH(SiMe_3)_2]_2$, whose structure was determined by X-ray crystallography.[26] A precursor to this complex, $Cp^*[C_2B_9H_{11}]Sc(THF)_3$, can be synthesized either by the reaction of $[Cp^*Sc(Me)_2]_x$ with the neutral *nido*-carborane $C_2B_9H_{13}$, followed by treatment with THF or by the reaction between $[Cp^*ScCl_2]_x$ and $Na_2[C_2B_9H_{11}]$, followed by addition of THF. Alkylation of the precursor with $LiCH(SiMe_3)_2$ in toluene followed by precipitation in petroleum ether yields the novel scandium complex $[Li(THF)_3]\cdot[Sc(C_2B_9H_{11})(Cp^*)CH(SiMe_3)_2]$ that dimerizes upon diffusion of pentane in a concentrated toluene solution.[26] Figure 2 shows that each Sc atom is bonded to one Cp* and one dicarbollide ligand in η^5 fashion, with one $(SiMe_3)_2CH$ unit in the plane between the two η^5 ligands. The centroid–Sc–centroid angle of 137.8° is identical to that found in the corresponding $(Cp^*)_2Sc$ analogue.[27] An interesting structural feature of the complex is that a Li atom bridges the two units by loosely bonding to three boron atoms of each dicarbollide ligand resulting in a dimeric monoanion, while the $Li^+(THF)_3$ counterion resides outside the coordination sphere for charge balance.[26]

The alkylated, mononuclear Sc complex can also be converted to the corresponding dimeric hydride $[Li(THF)_n]_2[ScH(C_2B_9H_{11})(Cp^*)]_2$ by reacting with H_2 slowly. The crystal structure shows the presence of two Sc cores held together by a 2e⁻ dative bond between an electron-rich B–H unit and the Lewis acidic Sc center. Although the Sc-bound hydrogen has not been observed crystallographically, it could be detected by ^1H NMR spectroscopy (δ 5.23 broad).[26] The tremendous stability of the Sc–H bonds limits the utility of the Sc hydride species as olefin polymerization catalysts.

Although a mixed-ligand yttrium sandwich species is yet to be synthesized, the first carborane analogue of an yttrocene derivative $[Li(THF)_4][Y(Cl)(THF)\{\eta^5\text{-}(SiMe_3)_2C_2B_4H_4\}_2\cdot Li(THF)]$ was reported very recently.[28] The complex was synthesized, in 83% yield, by treatment of the dilithium salt of the $[2,3\text{-}(SiMe_3)_2\cdot 2,3\cdot C_2B_4H_4]^{2-}$ dianion with anhydrous YCl_3 in a molar ratio of 2:1 in dry benzene, followed by extraction and crystallization of the product from anhydrous *n*-hexane and THF solution. The yttrium complex is composed of a dianionic $\{Y(Cl)(THF)\{\eta^5\text{-}(SiMe_3)_2C_2B_4H_4\}_2\}^{2-}$ sandwich complexed with an exo polyhedral $Li(THF)^+$ cation, and the negative charge is balanced by a discrete cationic $Li^+(THF)_4$ unit outside the coordination sphere as found by X-ray structure analysis (see Figure 3).[28] The centroid–Y–centroid angle of 129.7°, Y–centroid distance of 2.38 Å, Y–Cl distance of 2.582 Å, Cl–Y–THF angle of about 90°, and the bent-sandwich geometry of this complex all resemble those of an yttrocene analogue. As in the Cp systems,[25] the average centroid–Y–THF and centroid–Y–Cl angles constitute a distorted-tetrahedral geometry of the Y metal. This work, together with the scandium complex described above, demonstrates that, by using a carborane ligand, a second metal atom such as lithium can be incorporated into the structure of bent-sandwich complexes as a counterion. One of the limitations of carborane ligands in metal chemistry is that, with two dianionic ligands and a 3+ charge on the metal, there is little possibility of adding reactive anionic ligands such as alkyls without forming a highly charged species. The complexes described above offer a convenient solution to that problem. It is, therefore, expected that monomeric, bent, anionic, and mixed carborane–Cp-complexed Sc species such as $[Cp^*Sc(R)C_2B_9H_{11}]^-$,[26] or a monomeric, anionic, and purely carborane-based Y bent-sandwich of the type $[\{\eta^5\text{-}(SiMe_3)_2C_2B_4H_4\}_2Y(R)Li]^-$,[28] should support α-olefin polymerization or oligomerization catalytic activity as in the cases of analogous neutral group 4 complexes (discussed below).[29-32]

Until mid 1970s there were no known examples of metallacarboranes of early transition metals, but in 1975 Salentine and Hawthorne reported the first π-complexes of Ti, Zr, and V that were prepared from the $[1,2\cdot C_2B_{10}H_{12}]^{2-}$ ion or its *C,C'*-dimethyl derivatives.[33] Subsequently, a number of metallacarboranes of early transition metals with the general formula $[M^{II}(C_2B_{10}H_{10}R_2)_2]^{2-}$ (M = Ti, V, Cr, Mn, R = H; M = Ti, Zr, Hf, V, R = CH_3) as well as the mixed-ligand titanacarboranes of the formula $[C_xH_xTiC_2B_nH_{n+2}]^{m-}$ ($x = 5$, $n = 10$, $m = 1$; $x = 8$, $n = 9$ or 10, $m = 0$ or 1) have been reported by the same authors.[34] The crystal structure of the titanium complex revealed that the titanium metal, in a formal oxidation state of +2, is

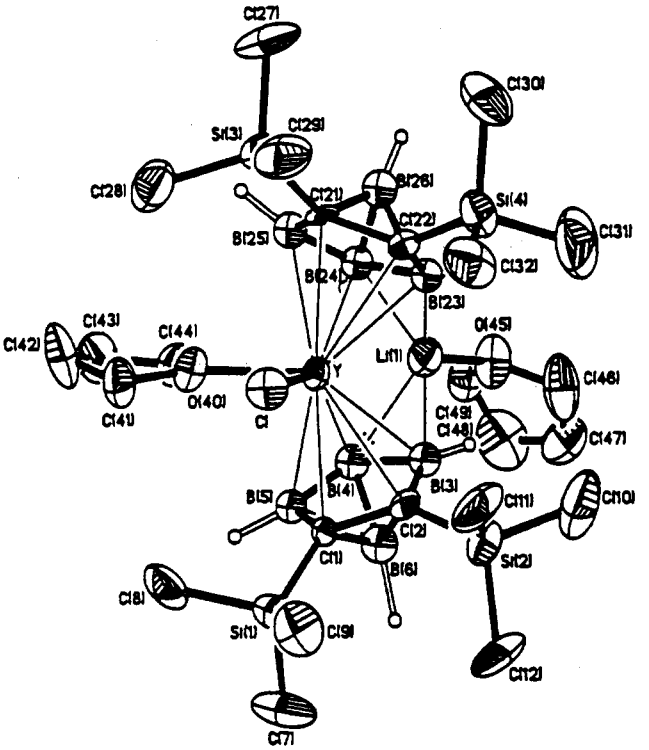

Figure 3. A perspective view of the yttracarborane $\{Li(THF)\text{-}1,1'\text{-}commo\text{-}Y(THF)Cl[2,3\text{-}(SiMe_3)_2\text{-}2,3\text{-}C_2B_4H_4]_2\}\text{-}\{Li(THF)_4\}$. Reprinted from ref 28. Copyright 1991 American Chemical Society.

sandwiched by two dinegative C_2B_{10} carborane cages, and hence the metal center represents a 14 interstitial electron system.[35] Apparently, the titanium, zirconium, and vanadium sandwich complexes are substantially more stable than the corresponding cyclopentadienyl analogues, which is consistent with the general trend of greater stability of the metallacarboranes compared to the corresponding metallocenes.[33-35] However, both the C_2B_9 and C_2B_{10} carborane systems failed to produce the group 4 metal sandwich species in which the metal atoms are in their formal highest oxidation state of +4. The synthesis of the first "zwitterionic" zirconium(IV) sandwich complex was reported very recently.[29] This synthesis involved the reaction between $ZrCl_4$ and the C_2B_4 carborane double salt in a molar ratio of 1:2 in dry benzene and subsequent extraction of the product from a solvent mixture of THF and *n*-hexane. Similarly, a number of other Zr(IV) and Hf(IV) sandwich complexes of a C_2B_4 carborane system have been synthesized according to the general reaction pathway, shown in eq 1.[29-31]

$$2Na^+(THF)Li^+[2\cdot(SiMe_3)\text{-}3\text{-}(R)\text{-}2,3\cdot C_2B_4H_4]^{2-} + MCl_4 \xrightarrow[\text{(ii) THF/hexane}]{\text{(i) } C_6H_6 \text{ at } 0\ ^\circ C} 2NaCl + LiCl + Li(THF)_n\cdot 1,1'\text{-}commo\text{-}M(THF)Cl[2\text{-}(SiMe_3)\cdot 3\text{-}(R)\cdot 2,3\text{-}C_2B_4H_4]_2$$

$n = 1$ or 2, M = Hf, Zr; R = $SiMe_3$, Me, H (1)

The crystal structure of a zirconium sandwich complex of a C_2B_4 carborane system is shown in Figure 4. The structure reveals that the zirconium atom is sandwiched by the two carborane cages with the metal to cage distances of 2.53–2.58 Å, which are comparable to the Zr–η^5-Cp distance of 2.49 Å in the structure of

Table I. Selected Crystallographic Data of d- and f-Block Metal–Carborane Complexes[a]

compound	M–X (length, Å)	X–Y–X′ (angle, deg)	ref
Early Transition Metal Complexes			
$[Li(THF)_3]\cdot Li]Sc(C_2B_9H_{11})(Cp^*)CH(SiMe_3)_2]_2$	Sc–Cnt_{cage} (2.12) Sc–C_{cage} (2.57) Sc–B (2.55) Sc–Cnt_{Cp} (2.20) Sc–C_{alkyl} (2.28)	Cnt_{Cp}–Sc–Cnt_{cage} (137.8) C_{alkyl}–Sc–Cnt_{cage} (111.2) C_{alkyl}–Sc–Cnt_{Cp} (110.9)	26a
$[Cp^*(C_2B_9H_{11})ScH]_2[Li(THF)_n]_2$	Sc–Cnt_{cage} (2.08) Sc–C_{cage} (2.51) Sc–B (2.52) Sc–Cnt_{Cp} (2.20) Sc–H (2.19)	Cnt_{cp}–Sc–Cnt_{cage} (136.2) H–Sc–Cnt_{cage} (107.6) H–Sc–Cnt_{Cp} (105.6)	26b
{Li(THF)-1,1′-*commo*-Y(THF)Cl[2,3(SiMe$_3$)$_2$-2,3-$C_2B_4H_4]_2$}-{Li(THF)$_4$}	Y–C_{cage} (2.71) Y–B (2.71) Y–Cnt_{cage} (2.38) Y–Cl(2.58) Y–O (2.35) Y···Li (3.34) Li–B (2.27–2.41)	Cl–Y–O (89.5) Cnt_{cage}–Y–O (103.3) Cnt_{cage}–Y–Cl (111) Cnt_{cage}–Y–Cnt_{cage} (129.7)	28
$(C_8H_8)Ti[Et_2C_2B_4H_4]$	Ti–C_{cage} (2.30) Ti–B (2.37) Ti–Cnt_{cage} (1.91) Ti–C_{arene} (2.29) Ti–Cnt_{arene} (NR)	Ti–C_{cage}–C_{Et} (127.6) Ti–C_{cage}–C_{Et} (134) Cnt_{cage}–Ti–Cnt_{arene} (177.2)	43
Li(THF)$_2$-1,1′-*commo*-Zr(THF)Cl[2,3-(SiMe$_3$)$_2$-2,3-$C_2B_4H_4]_2$	Zr–C_{cage} (2.57) Zr–B (2.54) Zr–Cnt_{cage} (2.17) Zr–O (2.29) Zr–Cl (2.46) Li–B (2.41–2.60)	Cnt_{cage}–Zr–O (104.5) Cnt_{cage}–Zr–Cl (104.1) Cnt_{cage}–Zr–Cnt_{cage} (130.4)	29
Li(THF)-1,1′-*commo*·Zr(THF)Cl[2-(SiMe$_3$)-3-(Me)-2,3-$C_2B_4H_4]_2$	Zr–C_{cage} (2.53) Zr–B (2.56) Zr–Cnt_{cage} (2.17) Zr–Cl (2.45) Zr–O (2.24) Li–B (2.34)	Cnt_{cage}–Zr–O (105.2) Cnt_{cage}–Zr–Cl (106.7) Cnt_{cage}–Zr–Cnt_{cage} (133.6) Cl–Zr–O (91.2)	31
$Cp^*(C_2B_9H_{11})Zr[C(Me)=CMe_2]$	Zr–Cnt_{cage} (2.04) Zr–H (2.29) Zr–C_{alkene} (2.19) Zr–Cnt_{Cp} (2.19) Zr–B (NR) Zr–C_{cage} (NR)	Cnt_{cage}–Zr–Cnt_{Cp} (141.3) Zr–C_{alkene}–C_{alkene} (147.8) Zr–C_{alkene}–C_{Me} (91.1)	32
$[(Cp^*)(C_2B_9H_{11})Zr]_2(\mu\text{-}CH_2)$	Zr–Cnt_{cage} (2.09) Zr–H (2.09) Zr–C_{CH_2} (2.18) Zr···B_{cage} (2.99) Zr–Cnt_{Cp} (2.23) Zr–B (NR) Zr–C_{cage} (NR)	Cnt_{cage}–Zr–Cnt_{Cp} (134.9)	32
Li(THF)·1,1′-*commo*-Hf(THF)Cl[2-(SiMe$_3$)3·(Me)-2,3-$C_2B_4H_4]_2$	Hf–C_{cage} (2.50) Hf–B (2.54) Hf–Cnt_{cage} (2.15) Hf–Cl (2.43) Li–B (2.35) Hf–O (2.19)	Cnt_{cage}–Hf–Cnt_{cage} (134.1) Cl–Hf–O (89.7) Cnt_{cage}–Hf–O (105.8) Cnt_{cage}–Hf–Cl (106.3) Bi–Li–B (77.9–96.7)	30
Li(THF)-1,1′-*commo*·Hf(THF)Cl[2-(SiMe$_3$)-3-(H)-2,3·$C_2B_4H_4]_2$	Hf–C_{cage} (2.45) Hf–B (2.57) Hf–Cnt_{cage} (2.13) Hf–Cl (2.45) Hf···Li (3.41) Li–B (2.29–2.42) Hf–O (2.20)	Cnt_{cage}–Hf–Cnt_{cage} (132.2) Cnt_{cage}–Hf–O (105.9) Cnt_{cage}–Hf–Cl (107.6)	31
$(C_8H_8)V[Et_2C_2B_4H_4]$	V–C_{cage} (2.23) V–B (2.30) V–Cnt_{cage} (1.83) V–C_{arene} (2.28) V–Cnt_{arene} (NR)	V–C_{cage}–C_{Et} (130.5, 133.5) Cnt_{cage}–V–Cnt_{arene} (177.2)	43
$(C_2B_9H_{11})TaCl_3$	Ta–C_{cage} (2.41) Ta–B (2.40) Ta–Cnt_{cage} (1.92) Ta–Cl (2.23)	Cl–Ta–Cnt_{cage} (116.2, 124) Cl–Ta–Cl (97.7) Cl–Ta–B (116.3, 124)	38
$Cp'(C_2B_9H_{11})TaCl_2$	Ta–C_{cage} (2.47) Ta–B (2.47) Ta–Cnt_{cage} (2.01) Ta–Cnt_{Cp} (2.10) Ta–Cl (2.36)	Cnt_{Cp}–Ta–Cnt_{cage} (133.48) Cl–Ta–Cl (92.0) Cl–Ta–Cnt_{cage} (108.9) Cl–Ta–Cnt_{Cp} (102.8)	38
$(C_7H_7)Cr[Et_2C_2B_4H_4]$	Cr–C_{cage} (2.17)	Cr–C_{cage}–C_{Et} (131.7, 133.2)	43

Table I. (Continued)

compound	M–X (length, Å)	X–Y–X′ (angle, deg)	ref
	Cr-B (2.25) $Cr–C_{arene}$ (2.18) $Cr–Cnt_{arene}$ (NR) $Cr–Cnt_{cage}$ (NR)	Cnt_{cage}-Cr·Cnt_{arene} (177.2)	
1,1′-*commo*-Cr[2,3-$(SiMe_3)_2$-2,3·$C_2B_4H_4]_2$	$Cr–C_{cage}$ (2.18) Cr–B (2.27–2.38) $Cr–Cnt_{cage}$ (1.80)	Cnt_{cage}–Cr–Cnt_{cage} (180)	10
$Li(THF)_4${1,1′-*commo*-Cr[2,3-$(SiMe_3)_2$-2,3-$C_2B_4H_4]_2$}	$Cr–C_{cage}$ (2.18) Cr–B (2.26) $Cr–Cnt_{cage}$ (1.77) Li–O (1.97)	Cnt_{cage}–Cr–Cnt_{cage} (180) O–Li–O (108.5)	42
$Li(TMEDA)_2${1,1′-*commo*-Cr[2·$(SiMe_3)$-2,3-$C_2B_4H_5]_2$}	$Cr–C_{cage}$ (2.18) Cr–B (2.21) $Cr–Cnt_{cage}$ (1.77) Li–N (2.11)	Cnt_{cage}–Cr–Cnt_{cage} (175.3) N–Li–N (121.2)	42
$[Mo_2Cu_2(\mu·CO)_4(CO)_2(\mu-H)_2(C_2B_9H_{10})_2]^{2-}$	Mo–Cu (2.65, 2.83) Cu···B (2.18) $Mo–C_{cage}$ (2.35) Mo–B (2.45) Cu–Cu (2.40) $Mo–C_{CO}$ (1.94) $Cu–C_{CO}$ (2.24) Cu–H (1.69) $Mo–Cnt_{cage}$ (NR)	Cu–Mo–Cu (51.7) Cu–H–B (97)	46
$[W_2(\mu·CC_6H_4Me\text{-}4)(CO)_3(\eta^5-C_2B_9H_9Me_2)(\eta^5-Cp)]$	W–B (2.33) $W–C_{cage}$ (2.40) W–W (2.65) $W–C_{CO}$ (1.99) $W–Cnt_{cage}$ (NR) $W–Cnt_{Cp}$ (NR) $W–H_{bridge}$ (2.05) $W–C_{bridge}$ (1.97, 2.05) $B–H_{bridge}$ (1.27)	B–W–W (51.7) W–W–H (83) W–H–B (94) $W–C_{bridge}$–W (82.9)	51
$[W_2(\mu\text{-}CMe)(CO)_3(\eta^5-C_2B_9H_8(CH_2C_6H_4Me\text{-}4)Me_2)$-$(\eta^5-Cp)]$	$W–C_{cage}$ (2.38) W–B (2.25, 2.41) W–W (2.65) $W–C_{CO}$ (1.98) $W–C_{bridge}$ (1.95, 2.03) $W–H_{bridge}$ (1.85) $W–Cnt_{cage}$ (NR) $W–Cnt_{Cp}$ (NR) $B–H_{bridge}$ (1.30) $B–C_{aryl}$ (1.58)	W–W–B (52.2) W–H–B (100) W–W–B (53.3)	51
$[MoW(\mu\text{-}CC_6H_4Me\text{-}4)(CO)_2(PMe_3)(\eta^6-C_2B_{10}H_{10}Me_2)$-$(\eta^5·Cp)]$	Mo–B (2.44) W–B (2.45) $W–C_{cage}$ (2.22, 2.52) W–Mo (2.70) $W–C_{CO}$ (2.00) Mo–P (2.49) $Mo–C_{Cp}$ (2.32) $W–C_{bridge}$ (2.10) $Mo–C_{bridge}$ (1.94) $Mo–H_{bridge}$ (1.80) $B–H_{bridge}$ (1.50)	B–Mo–W (53.9) $Mo–H_{bridge}$–B (96) $W–C_{bridge}$–Mo (84.0)	51
$[W(CO)_2(PPh_3)_2(\eta^5-C_2B_9H_8(CH_2C_6H_4Me\text{-}4)Me_2\}]$	$W–C_{cage}$ (2.51) W–B (2.41) W–P (2.57) $W–C_{CO}$ (1.97)	P–W–P (128) $W–C_{cage}–C_{Me}$ (111) $W–B–C_{aryl}$ (109.6)	52
$[W(CO)_3(PPh_3)\{\eta^5·C_2B_9H_8(CH_2C_6H_4OMe\text{-}2)Me_2\}]$	$W–C_{cage}$ (2.40) W–B (2.39) W–P (2.57) $W–C_{CO}$ (1.99)	C_{cage}–W–C_{cage} (40.6) B–W–B (44.4) P–W–C_{CO} (73.2–119.8) $W–B–C_{aryl}$ (114)	53
$[W_2(\mu·CC_6H_4Me\text{-}4)(CO)_3(PMe_3)(\eta^5-Cp)\{\eta^5\text{-}2,8-C_2B_9H_8$-10-$(CH_2C_6H_4Me·4)$-2,8-$Me_2\}]$	W–B (2.38) $W–C_{cage}$ (2.46) W–W (2.79) $W–C_{CO}$ (1.96)	W–W–B (125.8–157.2) $W–C_{bridge}$–W (87.1) $W–B–C_{aryl}$ (115.1)	54
$[W\{CH(C_6H_4Me\text{-}4)PPh_2CH_2PPh_2\}(CO)_2(\eta^5-C_2B_9H_9Me_2)]$	$W–C_{cage}$ (2.39) W–B (2.40) W–P (2.48) $W–C_{CO}$ (1.96) $W–C_{phos}$ (2.34)	P–W–C_{CO} (77.2, 121.8) P–W–C_{phos} (72.2)	55
$[NEt_4][closo\text{-}1,8\text{-}Me_2\text{-}11·(CH_2C_6H_4Me\text{-}4)\text{-}2\text{-}Cl\text{-}2,2,2$-$(CO)_3$-2,1,8-$WC_2B_9H_8]$	$W–C_{cage}$ (2.39) W–Cl (2.54) $W–C_{CO}$ (1.99) W–B (NR)	Cl–W–C_{CO} (75.1–134) $W–B–C_{aryl}$ (113.5)	56

Table I. (Continued)

compound	M–X (length, Å)	X–Y–X′ (angle, deg)	ref
[*closo*-1,8-Me_2-11-($CH_2C_6H_4Me$-4)-2,2-$(CO)_2$-2-(η-PhCCMe)-2,1,8-$WC_2B_9H_8$]	W–C_{cage} (2.41) W–B (2.37) W–C_{CO} (1.99) W–C_{aryl} (2.06)	W–B–C_{aryl} (114.7)	56
[$N(PPh_3)_2$][*closo*-1,7-Me_2-2-I-2,2,2-$(CO)_3$-2,1,7-$WC_2B_9H_9$]	W–C_{cage} (2.43) W–I (2.89) W–B (2.37) W–C_{CO} (1.97)	I–W–C_{CO} (74.7–131.2) W–C_{cage}–C_{Me} (108.5) I–W–C_{cage} (108.3)	56
[$WPt(\mu\text{-}CC_6H_4Me\text{-}4)(\mu\text{-}\sigma\text{:}\eta^5\text{-}C_2B_9H_8Me_2)(CO)_2(PMe_2Ph)_2$]	W–B (2.21–2.37) W–C_{cage} (2.50) Pt–B (2.17) W–Pt (2.72) W–C_{bridge} (1.89) Pt–C_{bridge} (2.14) Pt–P (2.27, 2.37) W–C_{CO} (1.99)	W–Pt–P (120.1, 142.1) W–Pt–C_{bridge} (43.9)	60
[$WPt(\mu\text{-}CC_6H_4Me\text{-}4)(\mu\text{-}\sigma\text{:}\eta^6\text{-}C_2B_{10}H_9Me_2)(CO)_2(PMe_2Ph)_2$]	W–C_{cage} (2.34) W–B (2.23–2.55) Pt–B (2.15) W–Pt (2.73) W–C_{bridge} (1.92) Pt–C_{bridge} (2.14) Pt–P (2.28, 2.36) W–C_{CO} (2.01)	W–Pt–P (121.4, 139.4) W–Pt–C_{bridge} (44.3)	60
[*exo-nido*-9,11-($CH_2C_6H_4Me$-4)$_2$-5,10-{$W(CO)_2(\eta\text{-Cp})$}-5,10-(μ-H)$_2$-7,8-$C_2B_9H_8$]	W–B (2.38, 2.50) W–C_{Cp} (2.31) W–C_{CO} (1.98) W–H_{bridge} (1.95, 2.16)	B–W–B (39.6) W–B–B (101, 153) B–W–B (39.6) C_{CO}–W–B (90.8–117.5)	50
[*exo-nido*-9,10-{$W(CO)_2(\eta\text{-Cp}^*)$}-5,10-($\mu$-H)$_2$-7,8-$C_2B_9H_8$-7,8-$Me_2$]	W–B (2.38, 2.50) W–C_{CO} (1.94) W–H (1.95, 2.16) W–C_{Cp} (2.28–2.41)	B–W–H (63, 71) W–H–B (98)	50
[$W_2Au_2(\mu\text{-CR})_2\{\mu\text{-}PPh_2(CH_2)_4PPh_2\}(CO)_4(\eta^5\text{-}C_2B_9H_9Me_2)_2$]	W–C_{cage} (2.43) W–B (2.39) W–Cnt_{cage} (1.91) W–Au (2.79) W–C_{bridge} (1.87)	W–Au–P (161.1) W–C_{bridge}–Au (86.6)	61
[*closo*-3,3,3-$(CO)_3$-3-$SnPh_3$-3,1,2-$WC_2B_9H_{11}$]$^-$	W–Sn (2.85) W–C_{cage} (2.33) W–B (2.40) W–C_{CO} (1.95)	Sn–W–Cnt_{cage} (116.4) W–Sn–C_{Ph} (114.5)	47
[Li^+(THF)][Li^+(TMEDA)]$_2$\{*commo*-Mn_3[2,3-$(SiMe_3)_2$-2,3-$C_2B_4H_4$]$_4$\}$^{3-}$	Mn–Mn (2.68) Mn–C_{cage} (2.16) Mn–B (2.19) Mn–Cnt_{cage} (1.70) Li···B (2.23–2.46)	Cnt_{cage}–Mn–Cnt_{cage} (177.6) Mn–Mn–Cnt_{cage} (90.5, 177.6)	64
[Mn(TMEDA)][*commo*-1,1′-Mn[2,3-$(SiMe_3)_2$-2,3-$C_2B_4H_4$]$_2$]	Mn–C_{cage} (2.16) Mn–B (2.24) Mn–Cnt_{cage} (1.71) Mn–Mn (2.66) Mn···B (2.32–2.48)	Cnt_{cage}–Mn–Cnt_{cage} (175.7)	67
[$(B_9C_2H_{11})ReCO)_3$]Cs	Re–C_{CO} (1.89) Re–C_{cage} (2.31) Re–B (2.34)	C_{CO}–Re–C_{CO} (41) C_{cage}–Re–B (43) B–Re–B (44.5)	68b
Middle and Late Transition Metal Complexes			
{[($Et_2C_2B_4H_4$)FeH(C_5Me_4)]$_2C_6H_4$}	Fe–C_{cage} (2.06) Fe–B (2.20) B–H_{bridge} (1.45) Fe–H_{bridge} (1.62) Fe–C_{Cp} (2.06)	B–H–Fe (93.1) B–H–B (75) B–H–Fe (93.1)	145
[$Me_2C_2B_4H_4$]$_2Fe_2(OMe)_2C_2H_4$	Fe–Fe (2.41) Fe–C_{cage} (2.06) Fe–B (2.13) Fe–O (2.08–2.23) Fe···B (2.23–2.44) Fe–Cnt_{cage} (1.64)	C_{cage}–Fe–C_{cage} (43.5) C_{cage}–Fe–B (42.4) B–Fe–B (45.1) Fe–Fe–B (53.7)	75
(η^5-C_9H_7)Fe($Et_2C_2B_4H_4$)NiCp*	Fe···Ni (3.37) Ni–B (2.02) Ni–C_{cp} (2.10) Fe–C_{cage} (1.99) Fe–B (1.91, 2.16) Fe–C_{arene} (2.03–2.18)	Fe–B–Ni (104, 122) B–B–B (86.4)	143
[*closo*-3-(η^6-C_6H_6)3,1,2-$FeC_2B_9H_{11}$]	Fe–C_{cage} (2.03) Fe–B (2.12) Fe–Cnt_{cage} (1.48)	C_{cage}–Fe–C_{cage} (46.3) C_{cage}–Fe–B (48.9–83.1) B–Fe–B (49.6–86.1)	77

Table I. (Continued)

compound	M–X (length, Å)	X–Y–X′ (angle, deg)	ref
	$Fe–Cnt_{arene}$ (1.57) $Fe–C_{arene}$ (2.10)		
$Fe(Cp)(CO)_2(CB_{11}H_{12})$	Fe···B (2.59) Fe–H (1.56) $Fe–Cnt_{cage}$ (1.70) $Fe–C_{Cp}$ (2.08)	Fe–H–B (141.1) Cnt_{cage}–Fe–H (114.3)	160
$Fe(TPP)(B_{11}CH_{12})$	Fe–H (1.82) Fe···B (NR)	Fe–H–B (NR)	162
3,1,2-(η^6-1,3,5-$Me_3C_6H_3$)$FeC_2B_9H_{11}$	$Fe–C_{cage}$ (2.06) Fe–B (2.12) $Fe–Cnt_{cage}$ (1.48) $Fe–Cnt_{arene}$ (1.60) $Fe–C_{arene}$	C_{cage}–Fe–C_{cage} (47.0) B–Fe–B (50.9) C_{cage}–Fe–B (47.5) Cnt_{cage}–Fe–Cnt_{arene} (NR)	148
1-(η-Cp)Fe-2-Me-2,3,4-$C_3B_7H_9$	$Fe–C_{cage}$ (1.95, 2.26) Fe–B (2.24) $Fe–Cnt_{Cp}$ (1.68)	Cnt_{cage}–Fe–Cnt_{Cp} (NR)	168
1-(η-Cp)Fe-4-Me-2,3,4-$C_3B_7H_9$	$Fe–C_{cage}$ (1.94, 2.28) Fe–B (2.23) $Fe–Cnt_{Cp}$ (1.68)	Cnt_{cage}–Fe–Cnt_{Cp} (NR)	168
commo-Fe-(1-Fe-2-Me-2,3,5-$C_3B_7H_9)_2$	$Fe–C_{cage}$ (1.98, 2.43) Fe–B (2.27) $Fe–Cnt_{cage}$ (NR)	Cnt_{cage}–Fe–Cnt_{cage} (NR)	169
commo-Fe-(1-Fe-5-Me-2,3,5-$C_3B_7H_9)_2$	$Fe–C_{cage}$ (1.96, 2.44) Fe–B (2.28) $Fe–Cnt_{cage}$ (NR)	Cnt_{cage}–Fe–Cnt_{cage} (NR)	169
commo-Fe-(1-Fe-5-Me-2,3,5-$C_3B_7H_9$)(1-Fe-4-Me-2,3,4-$C_3B_7H_9$)	$Fe–C_{cage}$ (1.96, 2.46) Fe–B (2.27) $Fe–Cnt_{cage}$ (NR)	Cnt_{cage}–Fe–Cnt_{cage} (NR)	169
commo-Fe-(1-Fe-10-Me-2,3,10-$C_3B_7H_9)_2$	$Fe–C_{cage}$ (1.99) Fe–B (2.24–2.36) $Fe–Cnt_{cage}$ (NR)	Cnt_{cage}–Fe–Cnt_{cage} (NR)	169
(η^6-C_9H_8)Fe^{II}($Et_2C_2B_4H_4$)	$Fe–C_{cage}$ (2.05) Fe–B (2.12) $Fe–C_{arene}$ (2.04–2.12) $Fe–Cnt_{cage}$ (NR) $Fe–Cnt_{arene}$ (NR)	Cnt_{cage}–Fe–Cnt_{arene} (177.2)	143
(η^6-C_6H_6)Fe[$Et_2C_2B_4H_4$]	$Fe–C_{cage}$ (2.02) Fe–B (2.13) $Fe–C_{arene}$ (2.04) $Fe–Cnt_{arene}$ (1.54) $Fe–Cnt_{cage}$ (1.61)	Cnt_{cage}–Fe–Cnt_{arene} (177.9)	201
(η^6-$C_6Me_3H_3$)Fe[$Et_2C_2B_4H_4$]	$Fe–C_{cage}$ (1.93, 2.06) Fe–B (2.12) $Fe–C_{arene}$ (2.08) $Fe–Cnt_{cage}$ (1.58) $Fe–Cnt_{arene}$ (1.58)	Cnt_{cage}–Fe–Cnt_{arene} (177.1)	201
(η^6-C_6Me_6)Fe[$Et_2C_2B_4H_4$]	$Fe–C_{cage}$ (2.06) Fe–B (2.13) $Fe–C_{arene}$ (2.09) $Fe–Cnt_{arene}$ (1.55) $Fe–Cnt_{cage}$ (1.62)	Cnt_{cage}–Fe–Cnt_{arene} (177.9)	201
(η^6-C_8H_{10})Fe[$Me_2C_2B_4H_4$]	$Fe–C_{cage}$ (2.09) Fe–B (2.15) $Fe–Cnt_{cage}$ (1.64) $Fe–Cnt_{arene}$ (NR) $Fe–C_{arene}$ (2.05–2.16)	Cnt_{cage}–Fe–Cnt_{arene} (168)	202
[NEt_4][FeW{μ-CH(C_6H_4Me-4)}(μ-σ:η^5-$C_2B_9H_8Me_2$)-(μ-CO)$(CO)_5$]	Fe–B (2.13) W–B (2.19) Fe–W (2.62) $W–C_{bridge}$ (2.17) $Fe–C_{bridge}$ (2.15) $Fe–C_{CO\ bridge}$ (2.02) $W–C_{CO\ bridge}$ (2.17)	W–Fe–B (53.7) Fe–W–B (51.7) W–Fe–C_{bridge} (53) W–Fe–$C_{CO\ bridge}$ (53.9)	203
[NEt_4][Fe_2W(μ-3-CPh)(μ-σ:σ',η^5-$C_2B_9H_7Me_2$)$(CO)_8$]	Fe–B (2.13) W–B (2.17) Fe–W (2.64) Fe–Fe (2.57) $W–C_{bridge}$ (2.02) $Fe–C_{bridge}$ (2.06 $Fe–C_{CO}$ (1.77)	W–B–Fe (75.6) Fe–W–Fe (58.3) W–Fe–C_{bridge} (49.2) W–Fe–Fe (60.8) Fe–Fe–C_{bridge} (51.5)	203
[CoFe($Me_4C_4B_8H_8$)($PEt_3)_2$]	$Fe–C_{cage}$ (2.06) Fe–B (2.14) Co–B (2.05) Fe–Co (2.53) Co–P (2.24) $Fe–Cnt_{cage}$ (1.63)	C_{cage}–Fe–C_{cage} (41) B–Fe–B (46.3) Co–B(cap)–Fe (78) Cnt_{cage}–Fe–Cnt_{cage} (173.1)	204

Table I. (Continued)

compound	M–X (length, Å)	X–Y–X′ (angle, deg)	ref
[*closo*-3,3-$(CO)_2$-3-$[Sn(C_6H_5)_3]$-3,1,2-$FeC_2B_9H_{11}]^-$	Fe–Sn (2.55) Fe–B (2.17) Fe–C_{cage} (2.09) Fe–Cnt_{cage} (1.55) Fe–C_{CO} (1.73)	Sn–Fe–C_{cage} (83, 143.6) C_{CO}–Fe–C_{cage} (91.4, 167.0) B–Fe–B (49.4, 84.4)	79
[*closo*-3-(CO)-3-(η^3-C_3H_5)-3,1,2-$FeC_2B_9H_{11}]^-$	Fe–C_{cage} (2.08) Fe–B (2.15) Fe–Cnt_{cage} (1.53) Fe–C_{CO} (1.72) Fe–C_{allyl} (2.03, 2.14)	C_{cage}–Fe–C_{CO} (151.2) B–Fe–B (49, 82.2) C_{cage}–Fe–C_{allyl} (90.5, 120.0)	79
[*closo*-3-(CO)-3-$COCH_3$-3-$P(CH_3)_3$-3,1,2-$FeC_2B_9H_{11}]^-$	Fe–C (2.10) Fe–B (2.18) Fe–Cnt_{cage} (1.57) Fe–P (2.18) Fe–C_{CO} (1.75) Fe–C_{acyl} (1.97)	C_{cag3}–Fe–C_{cage} (45.8) B–Fe–B (46.9, 81.7) P–Fe–C_{acyl} (85.0)	79
(η^6-$C_{10}H_8$)Fe($Et_2C_2B_4H_4$)	Fe–C_{cage} (2.05) Fe–B (2.10) Fe–Cnt_{cage} (1.60) Fe–Cnt_{arene} (1.55) Fe–C_{arene} (2.02–2.14)	Cnt_{cage}–Fe–Cnt_{arene} (176.4)	205
(η^6-$C_{14}H_{10}$)Fe($Et_2C_2B_4H_4$)	Fe–C_{cage} (2.05) Fe–B (2.17–2.33) Fe–Cnt_{cage} (1.73) Fe–C_{arene} (1.47) Fe–C_{arene} (1.92–2.14)	Cnt_{cage}–Fe–Cnt_{arene} (173.1)	205
[7,7′-μ-1,4-C_4H_8-7,8-$C_2B_9H_{10})_2Fe]^-$	Fe–Cnt_{cage} (1.54) Fe–C_{cage} (2.12) Fe–B (2.13)	C_{cage}–Fe–C′$_{cage}$ (108.5) Fe–C_{cage}–C_{bridge} (115.1)	102a
1,1-$(PPh_2CH_2)_2$-1-Cl-1,2,3-Fe($Et_2C_2B_4H_4$)	Fe–C_{cage} (2.15) Fe–B (2.14) Fe–Cl (2.27) Fe–P (2.25) Fe–Cnt_{cage} (NR)	Cl–Fe–C_{cage} (92.5) Cl–Fe–B (119–164.3) Cl–Fe–P (91.0)	92
[(η^6-C_6H_6)Fe($Et_2C_2B_4H_3$)]$_2$CH(CH_3)CH_2	Fe–C_{cage} (2.04) Fe–B (2.14) Fe–C_{arene} (2.05) Fe–Cnt_{cage} (NR) Fe–Cnt_{arene} (NR)	Cnt_{cage}–Fe–Cnt_{arene} (NR)	206
[η^6-C_6H_5($\overline{CH_2)_3}$]Fe($\overline{C_2B_4H_5}$)	Fe–C_{cage} (2.01) Fe–B (2.13) Fe–Cnt_{cage} (1.60) Fe–Cnt_{arene} (1.53) Fe–C_{arene} (2.07)	Cnt_{cage}–Fe–Cnt_{arene} (172.5)	138
[η^6-$(C_6H_5)_2$Fe($Et_2C_2B_4H_4$)]	Fe–C_{cage} (2.05) Fe–B (2.12) Fe–Cnt_{cage} (1.61) Fe–Cnt_{aryl} (1.54) Fe–C_{aryl} (2.08)	Cnt_{cage}–Fe–Cnt_{aryl} (160.7)	206
1-[η^6-$C_6(CH_3)_6$]Fe-4,5,7,8-$Me_4C_4B_3H_3$	Fe–C_{cage} (2.06) Fe–B (2.04–2.21) Fe–C_{arene} (2.11) Fe–Cnt_{cage} (1.58) Fe–Cnt_{arene} (1.58)	C_{cage}–Fe–C_{cage} (39.4) B–Fe–B (51.6) C_{cage}–Fe–B (42.6) Cnt_{cage}–Fe–Cnt_{arene} (174.1)	172
2-[η^6-$CH_3C_6H_5$]Fe-6,7,9,10-$Me_4C_4B_5H_5$	Fe–C_{cage} (2.02) Fe–B (2.09) Fe–C_{arene} (2.00–2.12) Fe–Cnt_{cage} (1.52) Fe–Cnt_{arene} (NR)	C_{cage}–Fe–C_{cage} (41.6) B–Fe–B (51.3) C_{cage}–Fe–B (41.7–81.7) Cnt_{cage}–Fe–Cnt_{arene} (NR)	172
[*commo*-3,3′-Fe{8-$N(Et)_3$-3,1,2-$FeC_2B_9H_{10}\}_2$]	Fe–C_{cage} (2.05) Fe–B (2.20) Fe–Cnt_{cage} (1.53) B–N (1.63)	C_{cage}–Fe–C_{cage} (48) B–Fe–B (49.5, 80) Cnt_{cage}–Fe–Cnt_{cage} (166)	90
[*commo*-3,3′-Fe{3,1,2-$FeC_2B_9H_{11}\}_2$][$NMe_4]_2$	Fe–C_{cage} (2.03) Fe–B (2.03) Fe–Cnt_{cage} (1.48)	C_{cage}–Fe–C_{cage} (46.9) B–Fe–B (50.2, 86.2) Cnt_{cage}–Fe–Cnt_{cage} (180)	90
2-[η^6-$Me_3C_6H_3$]Fe-1,6-$C_2B_7H_9$	Fe–C_{cage} (1.93, 2.09) Fe–B (2.12) Fe–C_{arene} (2.09) Fe–Cnt_{arene} (1.564) Fe–Cnt_{cage} (NR)	Fe–C_{cage}–B (74.9, 120.9) Cnt_{cage}–Fe–Cnt_{arene} (NR)	96
6-[η^6-$Me_3C_6H_3$]Fe(9,10-$C_2B_7H_{11}$)	Fe–B (2.12) Fe–Cnt_{cage} (1.53) Fe–Cnt_{arene} (1.56) Fe–C_{arene} (2.10)	B–Fe–B (50, 83.8) Cnt_{cage}–Fe–Cnt_{arene} (178.4)	96

Table I. (Continued)

compound	M–X (length, Å)	X–Y–X′ (angle, deg)	ref
dl-3,3′-*commo*-Fe{[$(C_2B_9H_9)N]_2(CH_2)_3$]	Fe–C_{cage} (2.08–2.15) Fe–B (2.05–2.12) Fe–Cnt_{cage} (1.52) B–N (1.51)	Cnt_{cage}–Fe–Cnt_{cage} (170.4) B–Fe–B′ (173.5)	216
3,3′-*commo*-Co{[$(C_2B_9H_9)N]_2(CH_2)_3$}	Co–C_{cage} (2.07) Co–B (2.04–2.09) Co–Cnt_{cage} (1.48) B–N (1.52)	Cnt_{cage}–Co–Cnt_{cage} (173.4) B–Co–B′ (175.4)	216
$(PC_4Me_4)Co(Et_2C_2B_3H_3)Co(NC_4Me_4)$	Co–C_{cage} (2.08) Co–B (2.08) Co–P (2.31) Co–N (2.09) Co–$C_{pyrrolyl}$ (2.05) Co–$C_{phospholyl}$ (2.08) Co–Cnt_{cage} (1.61) Co–$Cnt_{pyrrolyl}$ (1.70) Co–$Cnt_{phospholyl}$ (1.70)	Cnt_{cage}–Co–$Cnt_{pyrrolyl}$ (178.9) Cnt_{cage}–Co–$Cnt_{phospholyl}$ (178)	207
CH_2[*closo*-1-(η-C_5H_4)Co(2,3-$Et_2C_2B_4H_4$)]$_2$	Co–C_{cage} (2.01) Co–B (2.07) Co–C_{Cp} (2.05) Co–Cnt_{cage} (NR) Co–Cnt_{Cp} (NR)	Cnt_{cage}–Co–Cnt_{Cp} (NR)	144a
commo-Co(1-Co-2-Me-2,3,5-$C_3B_7H_9$)(1-Co-5-Me-2,3,5-$C_3B_7H_9$)	Co–C_{cage} (2.01, 2.60) Co–B (2.24, 2.44) Co–Cnt_{cage} (NR)	Cnt_{cage}–Co–Cnt_{cage} (NR)	169
commo-Co(1-Co-2-Me-2,3,5-$C_3B_7H_9$)$_2$	Co–C_{cage} (2.03, 2.65) Co–B (2.28, 2.54) Co–Cnt_{cage} (NR)	Cnt_{cage}–Co–Cnt_{cage} (NR)	169
[$(Et_2C_2B_4H_4)Co(C_5H_4)$]$_2$	Co–C_{cage} (2.01) Co–B (2.09) Co–Cnt_{cage} (1.56) Co–Cnt_{Cp} (1.65) Co–C_{Cp} (2.03)	Cnt_{cage}–Co–Cnt_{Cp} (176.8)	142
[$(Et_2C_2B_3H_5)Co(C_5Me_4)$]$_2C_6H_4$	Co–B (1.96, 2.05) Co–C_{cage} (2.08) Co–C_{Cp} (2.05) Co–Cnt_{cage} (NR) Co–Cnt_{Cp} (NR)	Cnt_{cage}–Co–Cnt_{Cp} (NR)	142
[$(Et)_4C_4B_8H_7$]$_2$[$OC(CH_3)_2$]$_2$CoH	Co–C_{cage} (2.07) Co–B (2.08) Co–H (NR) Co–Cnt_{cage} (NR)	B–Co–B′ (67.6–98.1) Co–B–O (95.9) B–O–B (100)	174
[$(Et)_2C_2B_4H_4$]Co[$(Et)_4C_4B_8H_7OC_4H_8$]	Co–B (2.17) Co–C_{cage} (2.23) Co–Cnt_{cage} (1.66)	B–Co–B′ (89–129.6) C_{cage}–Co–C′ (98, 115.8) Cnt_{cage}–Co–Cnt_{cage} (169.1)	173
{Cp*Co($Et_2C_2B_3H_2$)-5-C(O)Me]}$_2$Ni	Co–C_{cage} (2.09) Ni–B (2.07–2.15) Ni–C_{cage} (2.09–2.19) Co–B (2.09) Co–Cnt_{cage} (NR) Co–Cnt_{Cp} (NR) Co–C_{Cp} (NR)	Cnt_{cage}–Ni–Cnt_{cage} (NR) Cnt_{cage}–Co–Cnt_{Cp} (NR)	208
($CpCoC_4Ph_4BH$)	Co–C_{cage} (2.04) Co–B (2.14) Co–C_{Cp} (2.04)	Cnt_{cage}–Co–Cnt_{Cp} (176.7)	176
(C_5Me_5)Co[2,3-$Et_2C_2B_3H_4$-5-C(=CH_2)OC(O)Me]	Co–C_{cage} (2.06) Co–B (2.04) Co–Cnt_{cage} (NR) Co–Cnt_{Cp} (NR) Co–C_{Cp} (2.06)	Cnt_{cage}–Co–Cnt_{Cp} (NR) C_{ester}–O–C_{ester} (117.7)	98
(η^5-C_5H_5)Fe(μ-$Et_2C_3B_2H_3$)Co(η^5-C_5H_5)	Co–Cnt_{cage} (1.58) Fe–Cnt_{cage} (1.62) Fe–C_{cage} (2.07) Fe–B_{cage} (2.11) Co–C_{cage} (2.02) Co–B_{cage} (2.09) Co–Cnt_{Cp} (1.65) Fe–Cnt_{Cp} (1.65) Co–C_{Cp} (2.02) Fe–C_{Cp} (2.03)	Cnt_{cage}–Fe–Cnt_{Cp} (NR) Cnt_{cage}–Co–Cnt_{Cp} (NR)	209
2-(η^6-C_6H_5Me)-1-[$(Me_3Si)_2CH$]-2,1-$CoCB_{10}H_{10}$	Co–C_{arene} (2.14) Co–B (2.07) Co–C_{cage} (2.14) Co–Cnt_{cage} (NR) Co–Cnt_{arene} (NR)	Cnt_{cage}–Co–Cnt_{arene} (NR)	157
5:1′,2′-[1-(η-Cp)Co-2,3-$(Me_3Si)_2C_2B_4H_3$][B_2H_5]	Co–C_{cage} (2.01)	Cnt_{cage}–Co–Cnt_{Cp} (NR)	95

Table I. (Continued)

compound	M–X (length, Å)	X–Y–X′ (angle, deg)	ref
	Co–B (2.11) Co–C_{Cp} (2.00) Co–Cnt_{cage} (NR) Co–Cnt_{Cp} (NR)		
3,3′-*commo*-Co{[$(C_2B_9H_9)N(CH)]_2C(O)OH$}	Co–C_{cage} (2.07) Co–B (2.06) Co–Cnt_{cage} (NR) B–N (1.53)	Cnt_{cage}–Co–Cnt_{cage} (NR)	101
[7,7′-μ-1,3-C_3H_6-7,8-$C_2B_9H_{10})_2Co]^-$	Co–C_{cage} (2.09) Co–B (2.14) C_{cage}–C_{bridge} (1.57) Co–Cnt_{cage} (1.50)	C_{cage}–Co–C'_{cage} (101.9) Co–C_{cage}–C_{bridge} (109.8) Cnt_{cage}–Co–Cnt_{cage} (NR)	102a
[7,7′-μ-1,4-C_4H_8-7,8-$C_2B_9H_{10})_2Co]^-$	Co–C_{cage} (2.10) Co–B (2.11) Co–Cnt_{cage} (1.51) C_{cage}–C_{bridge} (1.56)	C_{cage}–Co–C'_{cage} (108) Co–C_{cage}–C_{bridge} (115.9) Cnt_{cage}–Co–Cnt_{cage} (NR)	102a
Cp*Co[$(Me_2C_2B_3Me_3)(\mu$-$H)_2$]	Co–C_{cage} (2.07) Co–Cnt_{cage} (1.54) Co–B (2.05) Co–C_{Cp} (2.06) Co–Cnt_{Cp} (1.68)	Cnt_{cage}–Co–Cnt_{Cp} (177.3)	146
[7,7′-μ-1,4-C_4H_8-7,8-$C_2B_9H_{10})_2Ni]$	Ni–C_{cage} (2.12) Ni–B (2.09) C_{cage}–C_{bridge} (1.51) Ni–Cnt_{cage} (1.48)	C_{cage}–Ni–C'_{cage} (102.9) Cnt_{cage}–Co–Cnt_{cage} (NR)	102a
1,1′-*commo*-Ni[2,4-$(SiMe_3)_2$-2,4-$C_2B_4H_4]_2$	Ni–Cnt_{cage} (1.59) Ni–B (2.09) Ni–C_{cage} (2.09)	Cnt_{cage}–Ni–Cnt_{cage} (174.4)	104
5,7,8-Me_3-11,7,8,10-[η^3-C_4Me_4H]$NiC_3B_7H_7$	Ni–B (2.17, 2.38) Ni–C_{cage} (1.94, 2.52) Ni–$Cnt_{allylic}$ (1.78) Ni–Cnt_{cage} (NR)	B–Ni–B (49.8) B–Ni–C_{cage} (42.2) C_{cage}–Ni–C_{cage} (103.9) Cnt_{cage}–Ni–$Cnt_{allylic}$ (NR)	96
(1,4,6-Me_3-2,3-Et_2-2,3,5-C_3B_3H)Ni(1,3-Me_2-4,5-Et_2-2,3-C_3B_2H)	Ni–C_{cage} (2.07) Ni–B (2.15) Ni–Cnt_{cage} (1.68) Ni–$Cnt_{borolyl}$ (1.64)	Cnt_{cage}–Ni–$Cnt_{borolyl}$ (NR)	210
[(1,4,6-Me_3-2,3-Et_2-2,3,5-C_3B_3H)Ni(COD)]$^+$[BF_4]$^-$	Ni–C_{cage} (2.11) Ni-B (2.12) Ni–Cnt_{cage} (NR) Ni–Cnt_{COD} (NR) Ni–C_{COD} (2.10)	Cnt_{cage}–Ni–Cnt_{COD} (NR)	210
[*closo*-3-(η^2-$Ph_2B(pz)_2$)-3,1,2-$NiC_2B_9H_{11}]^-$	Ni–C_{cage} (2.04, 2.26) Ni–B (2.11) Ni···$B_{pyrazolyl}$ (3.20) Ni–N (1.92) Ni–Cnt_{cage} (NR)	N–Ni–N (91.9) Ni–N–N (123.1) N–B–N (107.0)	105
1-Br-1,5-$(PPh_3)_2$-1,2,3-Ni($Et_2C_2B_4H_3$)	Ni–C_{cage} (2.12) Ni–B (2.14) Ni–Br (2.33) Ni–P (2.17) Ni–Cnt_{cage} (NR) B–P (1.88)	Br–Ni–C_{cage} (102, 136) Br–Ni–B (93–167.9) P–Ni–Br (92.7)	92
(η^5-C_5H_5)Ni(μ-$Et_2C_3B_2H_3$)Ni(η^5-C_5H_5)	Ni–Cnt_{cage} (1.69, 1.72) Ni–Cnt_{Cp} (1.74, 1.77) Ni–B (2.17) Ni–C_{cage} (2.13)	Cnt_{cage}–Ni–Cnt_{Cp} (NR)	209
(η^5-C_5H_5)Ni(μ-$Et_2C_3B_2H_3$)Co(η^5-C_5H_5)	Ni–Cnt_{cage} (1.72) Co–Cnt_{cage} (1.60) Ni–Cnt_{Cp} (1.77) Co–Cnt_{Cp} (1.66) Ni–B (2.14) Ni–C_{cage} (2.12–2.22) Co–B (2.14) Co–C_{cage} (2.02)	Cnt_{cage}–Ni–Cnt_{Cp} (NR) Cnt_{cage}–Co–Cnt_{Cp} (NR)	209
2-(η-Cp)-1-[$(Me_3Si)_2CH$]-2,1-$NiCB_{10}H_{10}$	Ni–C_{cage} (2.11) Ni–B (2.05) Ni–Cnt_{cage} (NR) Ni–C_{Cp} (2.06)	Cnt_{cage}–Ni–Cnt_{Cp} (170.5)	157
dl-3,3′-*commo*-Ni{[$(C_2B_9H_9)N]_2(CH_2)_3$]	Ni–C_{cage} (2.15) Ni–B (2.07–2.18) Ni–Cnt_{cage} (1.56) B–N (1.50)	Cnt_{cage}–Co–Cnt_{cage} (172) B–Ni–B′ (173.7)	216
meso-3,3′-*commo*-Ni{[$(C_2B_9H_9)N]_2(CH_2)_3$}	Ni–C_{cage} (2.18) Ni–B (2.09–2.14) Ni–Cnt_{cage} (1.57) B–N (1.50)	Cnt_{cage}–Co–Cnt_{cage} (169.6) B–Ni–B′ (171.9)	216

Table I. (Continued)

compound	M–X (length, Å)	X–Y–X′ (angle, deg)	ref
[2-(η^6-C_6Me_6)-*closo*-2,1,6-$RuC_2B_7H_9$]	Ru–C_{cage} (2.05, 2.19) Ru–B (2.23) Ru–Cnt_{cage} (NR) Ru–Cnt_{arene} (NR) Ru–C_{arene} (NR)	Cnt_{cage}–Ru–Cnt_{arene} (NR)	151
$(MeC_6H_4CHMe_2)_2Ru_2(Et_2C_2B_3H_3)$	Ru···Ru (3.47) Ru–C_{cage} (2.32) Ru–B (2.21) Ru–Cnt_{cage} (NR) Ru–Cnt_{arene} (NR) Ru–C_{arene} (2.15–2.25)	Ru–C_{cage}–Ru (102.8) Ru–B–Ru (103.5) Cnt_{cage}–Ru–Cnt_{arene} (174.8)	141
$(MeC_6H_4CHMe_2)_2Ru(Et_2C_2B_3H_3)CoCp$	Ru···Co (3.29) Ru–C_{cage} (2.21) Ru–B (2.21) Co–C_{cage} (2.04) Co–B (2.08) Ru–C_{arene} (2.14–2.25) Co–C_{Cp} (2.00–2.09) Co–Cnt_{cage} (NR) Co–Cnt_{Cp} (NR)	Co–C_{cage}–Ru (101.3) Co–B–Ru (100.1) Cnt_{cage}–Co–Cnt_{arene} (173.8) Cnt_{cage}–Ru–Cnt_{arene} (NR)	141
2,5,6-(η-C_6H_6)$RuC_2B_7H_{11}$	Ru–C_{cage} (2.15) Ru–B (2.19) Ru–C_{arene} (2.22) Ru–Cnt_{cage} (NR) Ru–Cnt_{arene} (NR)	C_{cage}–Ru–C_{cage} (39.8) B–Ru–B (48.9) Cnt_{cage}–Ru–Cnt_{arene} (NR)	149
[(η^6-$MeC_6H_4CHMe_2$)$Ru(Et_2C_2B_3H_3)Co(\eta^5$-$Me_4C_5)]_2$-$C_6H_4$·$2CH_2Cl_2$	Ru–C_{cage} (2.24) Ru–B (2.21) Ru–C_{arene} (2.09–2.26) Ru–Cnt_{arene} (NR) Ru–Cnt_{cage} (NR) Co–B (2.08) Co–C_{cage} (2.07) Co–$C_{Cp'}$ (2.01–2.10) Co–Cnt_{cage} (NR) Co–$Cnt_{Cp'}$ (NR)	Cnt_{cage}–Ru–Cnt_{arene} (NR) Cnt_{cage}–Co–$Cnt_{Cp'}$ (NR)	142
[1-(η^6-MeC_6H_4-*i*-Pr)-2,4-Me_2-1,2,4-$RuC_2B_8H_8$]	Ru–C_{cage} (2.12, 2.68) Ru–B (2.06–2.36) Ru–Cnt_{cage} (NR) C_{cage}–C_{cage} (1.48) Ru–C_{arene} (NR) Ru–Cnt_{arene} (NR)	Cnt_{cage}–Ru–Cnt_{arene} (172.6)	111
[5-(η^6-C_6Me_6)·7-(OMe)-*arachno*-5-RuN(Me)C(H)B_9H_{11}]	Ru–B (2.22–2.35) Ru–C_{arene} (2.18–2.25) B–N (1.48) Ru–Cnt_{cage} (NR) Ru–Cnt_{arene} (NR)	B–N–B (104.4) B–C_{cage}–B (59) Cnt_{cage}–Ru–Cnt_{arene} (NR)	159
[1-(η^5-C_5Me_5)-2-(NHEt)-7-(CNEt)-*closo*-1,2-$RhCB_9H_8$]	Rh–C_{cage} (2.16) Rh–B (2.12–2.46) Rh–C_{Cp} (2.17–2.28) Rh–Cnt_{cage} (NR) Rh–Cnt_{Cp} (NR)	C_{cage}–N–C_{cage} (117.5, 177.2) Cnt_{cage}–Rh–Cnt_{Cp} (NR)	159
[1-(η^5-C_5Me_5)-2-Me·*closo*-1,2,3-$RhC_2B_8H_9$]	Rh–C_{cage} (2.10) Rh–B (2.37) Rh–C_{Cp} (2.19) Rh–Cnt_{cage} (NR) Rh–Cnt_{Cp} (NR)	Cnt_{cage}–Rh–Cnt_{Cp} (NR)	159
(Cp*)$Rh(Et_2C_2B_3H_3)Co(Et_2MeC_3B_2Et_2)CoCp$	Rh···Co (3.32) Rh–C_{cage} (2.20) Rh–B (2.18) Rh–C_{Cp} (2.14–2.22) Rh–Cnt_{cage} (NR) Rh–Cnt_{Cp} (NR) Co···Co (3.23) Co–B (2.09) Co–C_{cage} (2.12) Co–C_{Cp} (2.05) Co–Cnt_{cage} (NR) Co–Cnt_{Cp} (NR)	Co–Co′–Rh (175) Cnt_{cage}–Rh–Cnt_{Cp} (NR) Cnt_{cage}–Co–Cnt_{Cp} (NR) Cnt_{cage}–Co–Cnt_{cage} (NR)	212
$(Et_2C_2B_4H_4)Rh(Et_2MeC_3B_2Et_2)CoCp$	Rh–C_{cage} (2.22) Rh–B (2.24) Co–B (2.05) Co–C_{cage} (2.01) Rh–Cnt_{cage} (1.76, 1.80) Rh–$Cnt_{borollyl}$ (NR) Co–C_{Cp} (2.03)	Cnt_{cage}–Rh–$Cnt_{borollyl}$ (171.4) $Cnt_{borollyl}$–Co–Cnt_{Cp} (178.1)	213

Table I. (Continued)

compound	M–X (length, Å)	X–Y–X′ (angle, deg)	ref
	$Co–Cnt_{borollyl}$ (NR) $Co–Cnt_{Cp}$ (NR)		
1,2-Ph_2-3-(η-C_5Me_5)-3,1,2-*pseudo-closo*-$RhC_2B_9H_9$	$Rh–C_{cage}$ (2.17) Rh–B (2.05–2.23) $Rh–C_{Cp}$ (2.18–2.27) $Rh–Cnt_{cage}$ (NR) $Rh–Cnt_{Cp}$ (NR)	$Cnt_{cage}–Rh–Cnt_{Cp}$ (NR)	214
[*closo*-1,2-μ-{1′,2′-$CH_2C_6H_4CH_2$–}-3,3-$(PPh_3)_2$-3-H-3,1,2-$RhC_2B_9H_9$]	$Rh–C_{cage}$ (2.30) Rh–B (2.26) Rh–P (2.33) Rh–H (1.56) $Rh–Cnt_{cage}$ (NR)	$C_{cage}–Rh–C_{aryl}$ (40.5) B–Rh–B (45.5, 77.8) H–Rh–B (168) P–Rh–P (98.7)	59
[*exo-nido*-6,10-{$(PPh_3)(PCy_3)Rh$}-6,10-μ-$(H)_2$-7,8-μ-(1′,2′-CH_2-$C_6H_4CH_2$–)-10,11-μ-(H)-7,8-$C_2B_9H_7$]	Rh–B (2.36) $Rh–H_{bridge}$ (1.83) Rh–P (2.25) $Rh–Cnt_{cage}$ (NR)	B–Rh–B (42.4) $B–Rh–H_{bridge}$ (28.2, 70.3) P–Rh–P (99.3)	59
[*closo*-1-Me-2,2-$(PEt_3)_2$-2-H-8-Ph-2,1,8-$RhC_2B_9H_9$]	Rh–B (2.38) $Rh–H_{bridge}$ (1.92) Rh–P (2.23) $Rh–Cnt_{cage}$ (NR)	B–Rh–B (43.0) $B–Rh–H_{bridge}$ (24, 64) P–Rh–P (95.6)	59
$[(PPh_3)_3Rh]^+$*nido*-7-R-7,8-$C_2B_9H_{11}]^-$	Rh–B (2.19) Rh–H (1.53) Rh–P (2.35)	B–Rh–B (48.2, 82.7) P–Rh–P (102.4) P–Rh–H (19.1)	59
[*closo*-1-Me-3,3-($CH_2CH_2C(O)OBu$)-3-PPh_3-3,1,2-$RhC_2B_9H_{10}$]	$Rh–C_{cage}$ (2.25) Rh–B (2.21) $Rh–C_{acrylate}$ (2.10) Rh–O (2.18) Rh–P (2.32)	$Cnt_{cage}–Rh–P$ (124) $Cnt_{cage}–Rh–O$ (124) $Cnt_{cage}–Rh–C_{acrylate}$ (118)	193
[*closo*-2-PPh_3-2-Cl-2,1,7-$RhC_2B_9H_{10}$-C_6H_6]	$Rh–C_{cage}$ (2.18) Rh–B (2.13) Rh–Cl (2.29) Rh–P (2.32) $Rh–Cnt_{cage}$ (NR)	P–Rh–B (96.3–128.5) $P–Rh–C_{cage}$ (96.7, 175.2) P–Rh–Cl (88.0) $Cnt_{cage}–Rh–P$ (NR) $Cnt_{cage}–Rh–Cl$ (NR)	193
[*closo*-3,3-(η^2,η^3-$C_7H_7CH_2$)-1,2-Me_2-3,1,2-$Rh(C_2B_9H_9)$]	$Rh–C_{cage}$ (2.26) Rh–B (2.19) $Rh–C_{allyl}$ (2.13–2.35) $Rh–Cnt_{cage}$ (NR)	$Cnt_{cage}–Rh–Cnt_{arene}$ (NR)	152
[3-(η^5-Cp*)-*closo*-3,1,2-$RhC_2B_9H_{11}$]	$Rh–C_{cage}$ (2.17) Rh–B (2.18) $Rh–C_{Cp*}$ (2.15–2.23) $Rh–Cnt_{cage}$ (NR) $Rh–Cnt_{Cp*}$ (NR)	C–Rh–C (44.3) B–Rh–B (49.3, 83.3) $C_{cage}–Rh–B$ (46.3–80.3) $Cnt_{cage}–Rh–Cnt_{Cp*}$ (172.9)	115
[$RhPt(\mu$-H)(μ-CO)$(PEt_3)_2(PPh_3)(\eta^5$-$C_2B_9H_{11})$]	$Rh–C_{cage}$ (2.31) Rh–B (2.26) Rh-Pt (2.73) $Rh–H_{bridge}$ (1.70) Rh–P (2.33) $Rh–C_{CO\ bridge}$ (1.99) $Rh–Cnt_{cage}$ (NR) $Pt–H_{bridge}$ (1.80) $Pt–C_{CO\ bridge}$ (1.99) Pt–P (2.33)	Rh–Pt–P (138.6) $Pt–H_{bridge}–Rh$ (102) $Cnt_{cage}–Rh–P$ (NR) $Cnt_{cage}–Rh–Pt$ (NR)	116
[RhPt{σ-C(C_6H_4Me-4)=C(C_6H_4Me-4)H}(CO)$(PEt_3)_2$-$(PPh_3)(\eta^5$-$C_2B_9H_{11})$]	Rh–B (2.25) $Rh–C_{cage}$ (2.34) Rh-Pt (2.76) Rh–P (2.29) $Rh–C_{CO}$ (1.84) $Rh–Cnt_{cage}$ (NR) Pt–B (2.29) Pt–P (2.22) $Pt–C_{aryl}$ (2.03)	Pt–B–Rh (74.9) $Pt–H_{bridge}–B$ (93) B–Pt–Rh (51.8) $Cnt_{cage}–Rh–Pt$ (NR)	116
[*closo*-3-PPh_3-3,3-{C(Ph)C(PPh_3)C(H)C(Ph)}-3,1,2-$RhC_2B_9H_{11}$]	$Rh–C_{cage}$ (2.28) Rh–B (2.28) $Rh–C_{aryl}$ (2.06) Rh–P (2.33) $Rh–Cnt_{cage}$ (NR)	$Cnt_{cage}–Rh–C_{aryl}$ (125.7) $Cnt_{cage}–Rh–P$ (130.1)	123
[{*closo*-3-PPh_3-3(μ-CN)-3,1,2-$RhC_2B_9H_{11}$}$_4$]	$Rh–C_{cage}$ (2.21) Rh–B (2.21) Rh–P (2.30) $Rh–CN_{bridge}$ (2.03) $Rh–Cnt_{cage}$ (NR)	$CN_{bridge}–Rh–CN_{bridge}$ (173.9) P–Rh–CN (85.9–95.9)	123
closo-3-(η^3-$HB(pz)_3$)-3,1,2-$RhC_2B_9H_{11}$	$Rh–C_{cage}$ (2.13) Rh–B (2.19) Rh–N (2.13) $Rh–Cnt_{cage}$ (NR)	N–Rh–N (84.6)	105

Table I. (Continued)

compound	M–X (length, Å)	X–Y–X′ (angle, deg)	ref
closo-2-(η^3-HB(pz)$_3$)-2,1,7-$RhC_2B_9H_{11}$	Rh–C_{cage} (2.16) Rh–B (2.14) Rh–N (2.10) Rh–Cnt_{cage} (NR)	N–Rh–N (83.8)	105
[PPN][*closo*-2-(PPh_3)-2-{η^2-C(*m*-FC_6H_4)NOC(=O)}-2,1,7-$RhC_2B_9H_{11}$]	Rh–C_{cage} (2.30) Rh–B (2.24) Rh–P (2.26) Rh–C_{aryl} (2.27) Rh–Cnt_{cage} (NR)	P–Rh–B (90.9, 152.6) P–Rh–C_{cage} (112) C_{aryl}–Rh–C_{aryl} (77.8)	122
[$Rh_2(\mu$-σ:η^5-$C_2B_9H_8Me_2)(CO)_3(\eta^5$-$C_2B_9H_9Me_2)$]$^-$	Rh–C_{cage} (2.21–2.44) Rh–B (2.05–2.27) Rh–Rh (2.87) Rh–C_{CO} (1.88) Rh–Cnt_{cage} (NR)	Rh–Rh–B (45.3, 48.2)	117
[RhPt(μ-H)(μ-CO)(PEt_3)$_2$(PPh_3)(η^5-7,9-$C_2B_9H_{11}$]	Rh–C_{cage} (2.33) Rh–B (2.24) Rh–Pt (2.74) Rh–$C_{CO\ bridge}$ (2.35) Rh–H_{bridge} (1.47) Rh–Cnt_{cage} (NR) Pt–P (2.30) Pt–H_{bridge} (1.75) Pt–$C_{CO\ bridge}$ (2.01)	Rh–Pt–P (119.9, 135.3) P–Pt–H_{bridge} (91.2) Pt–H_{bridge}–Rh (116.1) P–Rh–H_{bridge} (95.0) Rh–$C_{CO\ bridge}$–Pt (87.0)	118
[ReRh{μ-σ,η^5-$C_2B_9H_7(CH_2C_6H_4Me$-4)Me_2}$(CO)_4$-(η-C_5H_4Me)]	Rh–B (2.22) Rh–C_{cage} (2.25) Re–B (2.17) Rh–Re (2.88) Rh–C_{CO} (1.93) Re–C_{CO} (1.92) Re–$C_{Cp'}$ (NR) Rh–Cnt_{cage} (NR) Re–$Cnt_{Cp'}$ (NR)	Rh–Re–B (48.2) Rh–B–Re (83.4)	119
8,8-$(PPh_3)_2$-8-H-8,7,9-$RhCSB_8H_{10}$	Rh–C_{cage} (2.17) Rh–B (2.21) Rh–S (2.44) Rh–P (2.33)	Cnt_{cage}–Rh–P (NR)	165
1,1-$(PPh_3)_2$-1,1-$RhCSB_8H_9$	Rh–C_{cage} (2.11) Rh–B (2.32–2.46) Rh–S (2.34) Rh–P (2.33)	Cnt_{cage}–Rh–P (NR)	165
[(dppe)$PdC_2B_{10}H_{12}$]	Pd–C_{cage} (2.18, 2.60) Pd–B (2.25–2.45) Pd–P (2.28) Pd–Cnt_{cage} (NR)	B–Pd–P (97.4–165.1)	125
nido-[2-(η^6-C_6Me_6)-8,10-Me_2-2,8,10-$OsC_2B_8H_8$	Os–B (2.17) Os–C_{cage} (2.26) Os–C_{arene} (2.26) Os–Cnt_{cage} (NR) Os–Cnt_{arene} (NR)	Cnt_{cage}–Os–Cnt_{arene} (NR)	153
[3-(η^5-Cp*)-*closo*-3,1,2-$IrC_2B_9H_{11}$]	Ir–C_{cage} (2.16) Ir–B (2.17) Ir–C_{Cp*} (2.15–2.23) Ir–Cnt_{Cp*} (NR) Ir–Cnt_{cage} (NR)	C_{cage}–Ir–C_{cage} (44.0) B–Ir–B (47.8–85.1) C_{cage}–Ir–B (47.1–81.7) Cnt_{cage}–Ir–Cnt_{Cp*} (NR)	115
[1,1-$(PPh_3)_2$-1-H-1,2,4-$IrC_2B_8H_{10}$]	Ir–C_{cage} (2.19) Ir···C_{cage} (2.77) Ir–B (2.08, 2.34) Ir–P (2.35) Ir–H (1.62) Ir–Cnt_{cage} (NR)	B–Ir–C_{cage} (69.1) Cnt_{cage}–Ir–P (NR)	215
[(PPh_3)$HIrC_2B_{10}H_{11}$(OMe)]	Ir–C_{cage} (2.23–2.36) Ir–B (2.30–2.52) Ir–P (2.32) Ir–Cnt_{cage} (NR) Ir–H (NR)	B–Ir–P (79.5–164.3) Cnt_{cage}–Ir–P (NR)	125
[(dppe)$PtC_2B_9H_{11}$]	Pt–C_{cage} (2.50) Pt–B (2.26) Pt–P (2.26) Pt–Cnt_{cage} (NR)	B–Pt–P (97.1–171.6) Cnt_{cage}–Ir–P (NR)	125
[1,1-$(PMe_2Ph)_2$-2-Me-1,2,3-$PtC_2B_8H_9$]	Pt–C_{cage} (2.18) Pt–B (2.38) Pt–P (2.28) Pt–Cnt_{cage} (NR)	C_{cage}–Pt–C_{cage} (107.2) Cnt_{cage}–Pt–P (NR)	114
[1,1-$(PMe_2Ph)_2$-1,2,3-$PtC_2B_8H_{10}$]	Pt–C_{cage} (2.15) Pt–B (2.43, 2.57) Pt–P (2.26) Pt–Cnt_{cage} (NR)	C_{cage}–Pt–C_{cage} (98.1) Cnt_{cage}–Pt–P (NR)	114

Table I. (Continued)

compound	M–X (length, Å)	X–Y–X′ (angle, deg)	ref
[*closo*-3-(PPh_3)-3,1,2-$CuC_2B_9H_{11}$]$^-$	Cu–C_{cage} (2.31) Cu–B (2.13) Cu–P (2.14) Cu–Cnt_{cage} (1.67)	C_{cage}–Cu–C_{cage} (40) B–Cu–B (48.6, 80.2) B–Cu–P (127–155.5) Cnt_{cage}–Cu–P (NR)	89
[*closo*-3-(PPh_3)-4-{4-(C_5H_4N)CO_2CH_3}-3,1,2-$CuC_2B_9H_{10}$]	Cu–C_{cage} (2.38, 2.48) Cu–B (2.11, 2.25) Cu–P (2.16) Cu–Cnt_{cage} (1.72) B–N (NR)	C_{cage}–Cu–C_{cage} (37.4) B–Cu–B (49.5, 80.3) B–Cu–P (127.7–153.3) Cnt_{cage}–Cu–P (NR)	89
[$Cu_3(\mu$-H)$_3${$C_2B_9H_9$(4-(C_5H_4N)CO_2CH_3)}$_3$]·*n*-C_7H_{16}	Cu–Cu′ (2.51) Cu–C_{cage} (2.63) Cu–B (2.11–2.30) Cu–H_{bridge} (1.60) Cu–Cnt_{cage} (1.84) B–N (1.55)	Cu–Cu′–Cu″ (60) H_{bridge}–Cu–B (111.8–156.6) B–Cu–B (47/8, 74.3) Cu–H–B (96.4)	89
meso-3,3′-*commo*-Cu{[($C_2B_9H_9$)N]$_2$(CH_2)$_3$}	Cu–C_{cage} (2.22–2.35) Cu–B (2.15) Cu–Cnt_{cage} (1.67) B–N (1.51)	Cnt_{cage}–Cu–Cnt_{cage} (165.9) B–Cu–B′ (167.4)	216
$AgB_{11}CH_{12}$·$2C_6H_6$	Ag–H (1.97) Ag···B (2.58–2.95) Ag–C_{arene} (2.40)		164
$IrCl(CO)(PPh_3)_2$·$Ag(B_{11}CH_{12})$	Ag–H (1.06) Ag···B (2.52) Ag–Ir (2.68)		161
Li[$(HgC_2B_{10}H_{10})_4Cl$]	Hg–C_{cage} (2.09) Hg–Cl (2.94)	C_{cage}–Hg–C′$_{cage}$ (162) Hg–C_{cage}–C_{cage} (125.7)	128
f-Block Metal Complexes			
[3,3-($THF)_2$-*commo*-3,3′-Sm(3,1,2-$SmC_2B_9H_{11})_2$]$^-$[PPN]$^+$	Sm–C_{cage} (2.72) Sm–B (2.72) Sm–Cnt_{cage} (2.33) Sm–O (NR)	Cnt_{cage}–Sm–O (104–111) Cnt_{cage}–Sm–Cnt_{cage} (131.9)	179
{[η^5-1-Sm-2,3-($SiMe_3)_2$-2,3-$C_2B_4H_4$]$_3$[(μ_2-1-Li-2,3-($SiMe_3)_2$-2,3-$C_2B_4H_4$)$_3$(μ_3-OMe)][μ_2-Li(C_4H_8O)]$_3$(μ_3-O)}	Sm–Cnt_{cage} (2.40) Sm–O (2.21) Li–Cnt_{cage} (1.85) Li–O (1.83) Sm–C_{cage} (2.74) Sm–B (2.69–2.86) Li–B (2.29–2.54) Li–C_{cage} (2.16)	Cnt_{cage}–Sm–O (115.9) Sm–O–Sm (119.2) Li–O–Li (107.8) Li–O–C_{OMe} (107.4–114.1)	67
[1,1,1-(t-$C_4H_9OH)_3$-2,3-($SiMe_3)_2$-4,5-{Li(C_4H_8O)Cl}-*closo*-η^5-1-Sm-2,3-$C_2B_4H_4$]·C_4H_8O	Sm–Cnt_{cage} (2.44) Sm–O (2.10–2.31) Sm–C_{cage} (2.73) Sm–B (2.77–2.90) Li–B (2.52) Li–Cl (2.60) Li–O (1.98)	O–Sm–Cnt_{cage} (113.3) O–Sm–O (77, 113.4) Sm–O–Li (100.1) Sm–B–Li (75.3) O–Li–O (136.6) B–Li–O (92.7–106.5)	67
[*closo*-1,1,1-($MeCN)_3$-1,2,4-$EuC_2B_{10}H_{12}$]$_n$	Eu–C_{cage} (2.96, 3.12) Eu–B (2.83, 3.05) Eu–N (2.66–2.76) Eu–Cnt_{cage} (NR)	Cnt_{cage}–Eu–N (NR)	183
[1,1-($THF)_2$-*commo*-1,1′-Eu($C_2B_{10}H_{12})_2$]$^{2-}$	Eu–O (2.63) Eu–B (2.98–3.09) Eu–C_{cage} (2.89, 3.20) Eu–Cnt_{cage} (NR)	B–Eu–B (127.4) O–Eu–O (74.8) B–Eu–O (110.7) Cnt_{cage}–Eu–Cnt_{cage} (NR)	183
[{η^5-1-Gd-2,3-($SiMe_3)_2$-2,3-$C_2B_4H_4$}{μ_2-1-Li-2,3-($SiMe_3)_2$-2,3-$C_2B_4H_4$}$_3$(μ_3-OMe){μ_2-Li-C_4H_8O)}$_3$(μ_3-O)]	Gd–Cnt_{cage} (2.37) Gd–O (2.19) Gd–C_{cage} (2.70) Gd–B (2.69) Li–Cnt_{cage} (1.82–1.89) Li–C_{cage} (2.17) Li–B (2.24–2.40) Li–O (1.85)	Cnt_{cage}–Gd–O (115.9) Gd–O–Gd (119.1) Cnt_{cage}–Li–O (170) Li–O–Li (106) Li–O–C_{OMe} (113)	66
[{η^5-1-Tb-2,3-($SiMe_3)_2$-2,3-$C_2B_4H_4$}{μ_2-1-Li-2,3-($SiMe_3)_2$-2,3-$C_2B_4H_4$}$_3$(μ_3-OMe){μ_2-Li-C_4H_8O)}$_3$(μ_3-O)]	Tb–C_{cage} (2.71) Tb–B (2.72) Tb–O (2.18) Tb–Cnt_{cage} (2.36) Li–B (2.30–2.41) Li–O (1.88) Li–Cnt_{cage} (NR) Li–C_{cage} (2.13)	C_{cage}–Tb–C_{cage} (32.8) B–Tb–B (34.7) Cnt_{cage}–Tb–O (NR) Tb–O–Tb (119.0) Li–O–Li (106) Li–O–C_{OMe} (113.4)	67
[{η^5-1-Dy-2,3-($SiMe_3)_2$-2,3-$C_2B_4H_4$}{μ_2-1-Li-2,3-($SiMe_3)_2$-2,3-$C_2B_4H_4$}$_3$(μ_3-OMe){μ_2-Li-C_4H_8O)}$_3$(μ_3-O)]	Dy–C_{cage} (2.69) Dy–B (2.68) Dy–O (2.18) Dy–Cnt_{cage} (2.32)	C_{cage}–Dy–C_{cage} (32.5) B–Dy–B (34.8) Cnt_{cage}–Dy–O (NR) Dy–O–Dy (120.1)	67

Table I. (Continued)

compound	M–X (length, Å)	X–Y–X′ (angle, deg)	ref
	Li–B (2.23–2.42) Li–O (1.88–1.95) Li–Cnt_{cage} (NR) Li–C_{cage} (2.19)	Li–O–Li (105.3) Li–O–C_{OMe} (113.1)	
[{η^5-1-Ho-2,3-$(SiMe_3)_2$-2,3-$C_2B_4H_4$}{μ_2-1-Li-2,3-$(SiMe_3)_2$-2,3-$C_2B_4H_4$}$_3$(μ_3-OMe){μ_2-Li-C_4H_8O)}$_3$(μ_3-O)]	Ho–Cnt_{cage} (2.33) Ho–C_{cage} (2.70) Ho–B (2.69) Ho–O (2.15) Li–B (2.26–2.46) Li–C_{cage} (2.14) Li–Cnt_{cage} (1.86) Li–O (1.82–1.95)	Cnt_{cage}–Ho–O (117.4) Ho–O–Ho (118.8) Li–O–Li (104.1) Li–O–C_{OMe} (109.2–117.9)	67
$Yb(C_2B_9H_{11})(DMF)_4$	Yb–B/C_{cage} (2.74) Yb–O (2.37)	O–Yb–O (90)	179
$[U(C_2B_9H_{11})_2Cl_2][Li(OC_4H_8)_4]_2$	U–B (2.64–2.86) U–Cl (2.59) Li–O (1.92) U–C_{cage} (2.73) U–Cnt_{cage} (NR)	Cl–U–Cl (90.3) Cnt_{cage}–U–Cnt_{cage} (137) Cnt_{cage}–U–Cl (NR)	190

[a] Mean values are given for bond angles and bond lengths. Cnt denotes the centroid of the bonding face. NR means not reported.

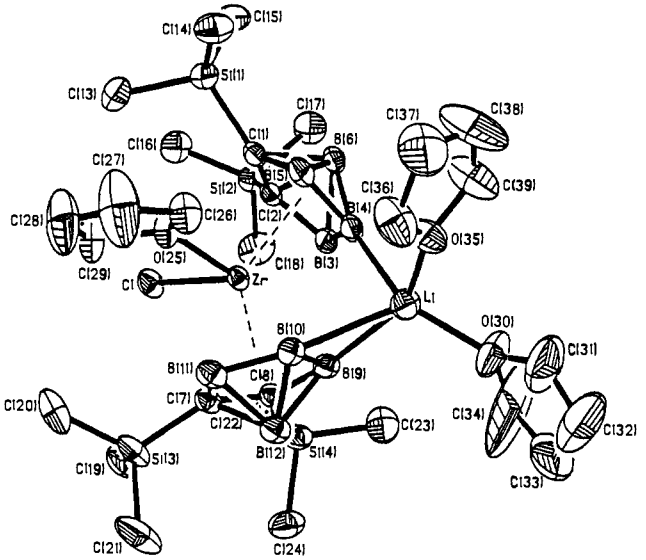

Figure 4. An ORTEP drawing of a zwitterionic zirconacarborane sandwich complex. Reprinted from ref 29. Copyright 1990 American Chemical Society.

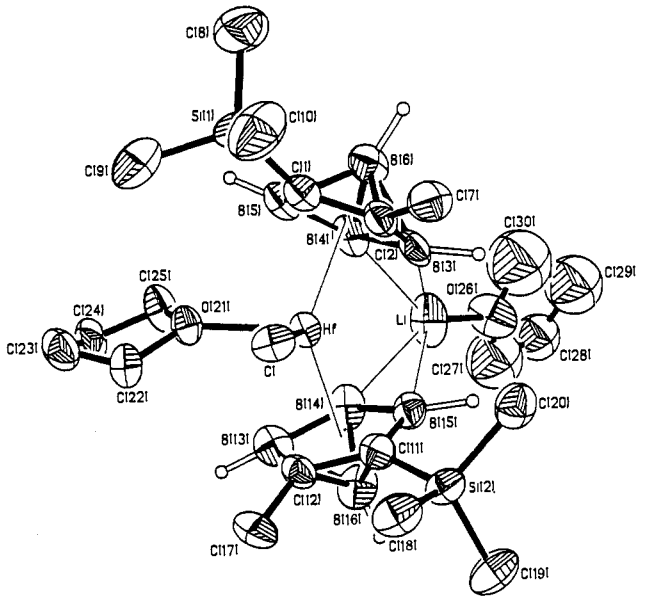

Figure 5. Crystal structure of 1-Cl-1-(THF)-2,2′-$(SiMe_3)_2$-3,3′-Me_2-4′,5,5′,6′-Li(THF)[1,1′-*commo*-Hf$(C_2B_4H_4)_2$]. Reprinted from ref 30. Copyright 1993 International Union of Crystallography.

[η^5-$(C_5H_5)_2$]$ZrCl_2$.[36] The coordination geometry of the zirconium metal was described as a distorted tetrahedron whose vertices are occupied by a Cl atom, a THF molecule, and two C_2B_4 cages. Since the Zr metal is bonded to a chlorine atom as well as the carborane cages, for charge compensation an additional $Li^+(THF)_2$ moiety is bound to the unique boron and one other boron of the carborane faces within the coordination sphere so as to form a formal "zwitterion" consisting of an anionic {Zr(Cl)(THF)[η^5-$(SiMe_3)_2C_2B_4H_4$]$_2$}$^-$ sandwich that is complexed with an exo-polyhedral [Li-$(THF)_2$]$^+$ cation. The bent-sandwich geometry of the complex has been rationalized on the basis of the location of the THF molecule and the Cl atom on the metal with the average Cl–Zr–THF angle of 90°, thus resembling those of the metallocene derivatives. With the exception of the number of Li^+-bound THF's, all of the zirconium- and hafnium-sandwiched metallacarboranes are isostructural as determined by X-ray crystallography.[29–31] For comparison, the crystal structure of a hafnacarborane of a similar ligand system, 4′,5,5′,6-Li(THF)-1,1′-*commo*-Hf(THF)Cl[2-$(SiMe_3)$-3-(Me)-2,3-$C_2B_4H_4$]$_2$, is shown in Figure 5.

The presence of a Cl atom and THF molecules on the metals provides a new dimension to the chemistry of these complexes as these could be converted to a neutral, THF-free and alkyl-substituted derivative of the type R′M[$(R_2C_2B_4H_4)_2$Li] (M = Zr, Hf) that does not possess a counterion outside the coordination sphere. Since 14-electron, d^0, alkyl-substituted and solvent-free bent metallocene [$(C_5R_5)_2$M(R′)]$^+$ with the selective counteranion such as methylaluminoxane has proven to be an effective catalyst in the Ziegler–Natta olefin polymerization, the bent-sandwich carborane complexes, described above, could be developed as better catalysts than the corresponding Cp analogues.[37] Such neutral, isoelectronic, carborane-based complexes could obviate the severe problems of devising an innocent, noncoordinating counteranion which have complicated the metallocene systems. In fact, it was demonstrated most recently by Jordan et al. that a new class of neutral, d^0, group 4 metal bent-metallocene–carborane complexes of the general formula [(Cp*)M(R)$(C_2B_9H_{11})$] (M = Zr,

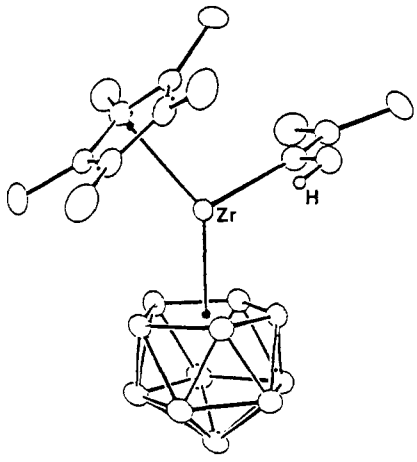

Figure 6. X-ray structure of $Cp^*(C_2B_9H_{11})Zr[C(Me)=CMe_2]$. Reprinted from ref 32. Copyright 1991 American Chemical Society.

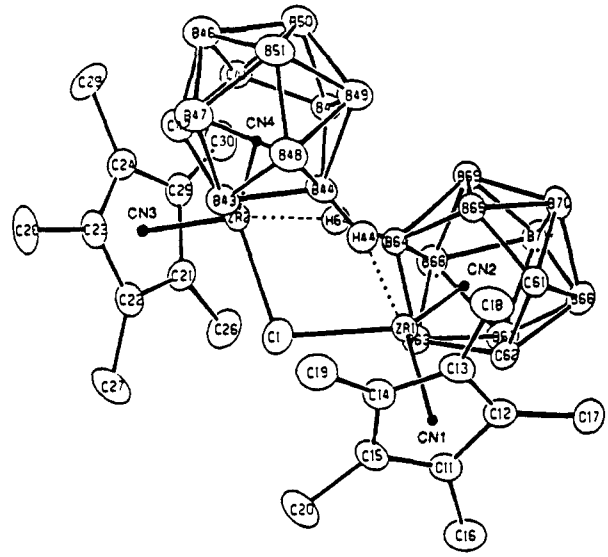

Figure 7. X-ray structure of $[(Cp^*)(C_2B_9H_{11})Zr]_2(\mu\text{-}CH_2)$. Reprinted from ref 32. Copyright 1991 American Chemical Society.

Hf) can be synthesized and structurally characterized.[32] The synthesis and reactivity of this novel class of compounds are summarized in Scheme I.

As can be seen from Scheme I, both Zr and Hf sandwich complexes react with 2-butyne via single insertion to yield the monomeric alkenyl complexes $(Cp^*)(C_2B_9H_{11})M[C(Me)=C(Me)_2]$. The crystal structure of the Zr complex (see Figure 6)[32] unambiguously shows its bent-sandwich geometry at the metal center similar to those described above.[29-31] The alkenyl group lies in the plane between the two η^5 ligands and is distorted by an agostic interaction involving one of the β-Me hydrogens. The neutral complexes, $[(Cp^*)M(R)(C_2B_9H_{11})]$ (M = Zr, Hf), are found to be moderately active catalysts in ethylene polymerization as evidenced by the room temperature oligomerization of propylene to 2-methylpentene predominantly (see Scheme I). Thermolysis of the Zr complex in toluene-d_8 at 45 °C quantitatively yields the novel methylidene-bridged complex, while the hafnium complex undergoes a slower CH_4 elimination, even at 75 °C, to yield the analogous CH_2-bridged dimeric complex. The crystal structure of the methylidene-bridged Zr complex $[(Cp^*)(C_2B_9H_{11})Zr]_2(\mu\text{-}CH_2)$, shown in Figure 7, exhibits two bent-metallocene–carborane Zr centers bridged by a CH_2 group.[32] The centroid–Zr–centroid angle is 134.9° and the Zr–centroid distances are 2.234 Å (Zr–Cp*) and 2.091 Å (Zr–$C_2B_9H_{11}$). There are close B—H···Zr contacts involving a B–H bond of each dicarbollide ligand and the Zr (Zr···H = 2.09 Å). The bond distances and angles are consistent with the increased steric crowding in the complex. Thus, the work of Jordan et al.[32] suggests that 14-electron, d^0, mixed-ligand bent-metallocene complexes are highly electrophilic as evidenced by the high olefin and acetylene insertion reactivity and by the facile reactions leading to CH_2-bridged dimeric complexes. These promising results have led Jordan et al. to synthesize a number of high-valent tantalum complexes as precursors to cationic, d^0, and mixed-ligand Ta–alkyl derivatives such as $[(Cp)$-

Scheme I. Synthesis and Reactivity of Bent-Metallocene–Carborane Complexes of Group 4 Metals (Reprinted from ref 32. Copyright 1991 American Chemical Society)

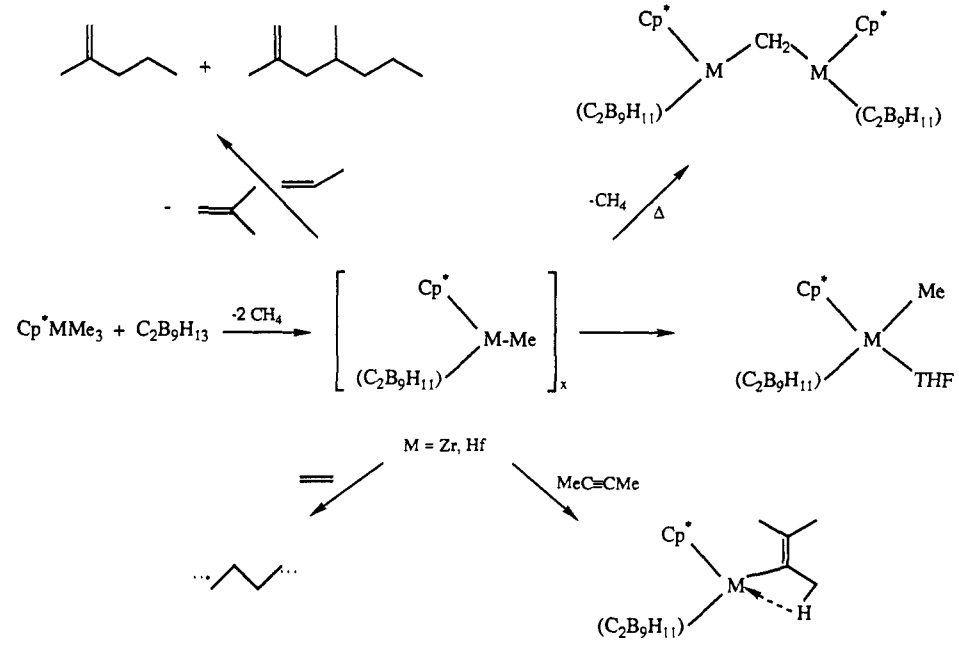

Scheme II. Syntheses of Ta(V) Dicarbollide Complexes

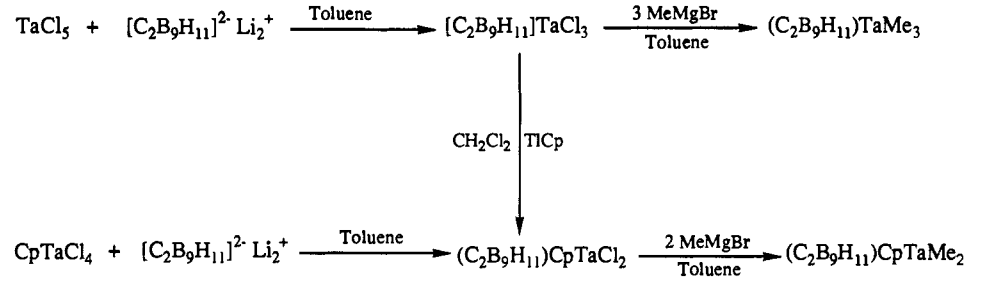

$(C_2B_9H_{11})Ta(R)(L)]^+$.[38] Since this complex is isoelectronic and isostructural with group 4 alkyl of the type $[(C_5R_5)_2M(R')]^+$,[27] a rich insertion, olefin polymerization, and C–H activation chemistry with the mixed-ligand bent-sandwiched tantalum(V) complexes could also be expected. Scheme II represents the systematic synthetic approach to these novel bent-metallocene–carborane complexes.[38] The crystal structure of one of the precursors, $(C_2B_9H_{11})TaCl_3$, shows that the complex consists of a monomeric, three-legged piano-stool geometry with the dicarbollide ligand symmetrically bonded to the apical $TaCl_3$ unit (see Figure 8), thus resembling the structure of $CpTiCl_3$.[39] As described in Scheme II, this complex reacts further with 1 equiv of TlCp′ in CH_2Cl_2 to produce a mixed-ligand bent-metallocene–carborane complex, $Cp'(C_2B_9H_{11})TaCl_2$, which could also be prepared directly from the reaction of dicarbollide dianion with $Cp'TaCl_4$ in toluene.[38] The structure of this mixed-ligand Ta precursor was also determined by X-ray crystallography. As can be seen in Figure 9, the compound adopts a monomeric bent-metallocene-type structure with the (C_2B_3 centroid)–Ta–(Cp′ centroid) angle of 133.5° and Cl–Ta–Cl angle of about 92°, which are similar to those observed for d^0 Cp_2MX_2 complexes.[36] The Ta–dicarbollide distances are almost identical to those found in the previous Ta complex with Ta–B and Ta–C distances ranging from 2.45 to 2.50 Å. However, the shorter Ta–(C_2B_3 centroid) distance (2.011 Å), 0.1 Å less than the Ta–(Cp′ centroid) distance, is in line with the general trend of stronger donor ability of the carborane ligands versus a Cp ligand.

It is clear from the recent results, described above in the area of sandwiched metallacarborane–metallocene derivatives containing Sc, Y, Zr, and Hf metals, that a fascinating and potentially useful research is emerging.[26,28–32,38]

The first anionic chromium sandwich complex, $[3,3'\text{-}Cr\{1,2\text{-}(Me)_2\text{-}1,2\text{-}C_2B_9H_9\}_2]^-$, and the corresponding mixed Cp–carborane analogue, $(\eta^5\text{-}Cp)Cr(C_2B_9H_{11})$, were synthesized nearly 25 years ago by Hawthorne and co-workers.[40] The crystal structure of the sandwich complex consisted of two icosahedral cages fused at the formal Cr(III) metal ion.[41] Unlike the chromicinium analogue and the mixed ligand complex, the *commo*-chromacarborane is stable to hydrolysis and is not affected even by hot concentrated sulfuric acid. In addition, the complex could not be reduced to the corresponding Cr(II) species when treated with sodium amalgam or oxidized to Cr(IV) species with strong oxidizing reagents, without cluster demolition.[40] However, the first anionic, formal Cr(III) sandwich complex of a C_2B_4 carborane system, that could be oxidized to the corresponding neutral Cr(IV) complex, was reported only recently.[10,42] The anionic sandwich complex of the type $[1,1'\text{-}commo\text{-}Cr\{2\text{-}(SiMe_3)\text{-}3\text{-}(R)\text{-}2,3\text{-}C_2B_4H_4\}_2]^-$

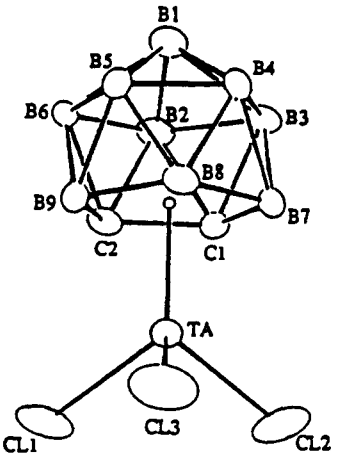

Figure 8. Structure of $(C_2B_9H_{11})TaCl_3$. Reprinted from ref 38. Copyright 1992 American Chemical Society.

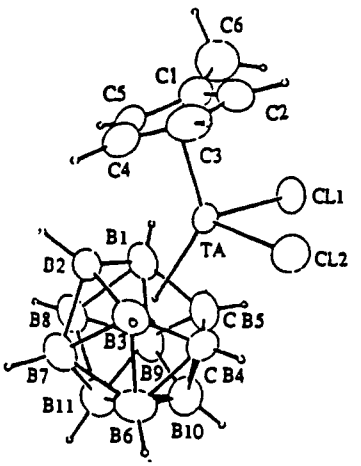

Figure 9. Structure of $Cp'(C_2B_9H_{11})TaCl_2$. Reprinted from ref 38. Copyright 1992 American Chemical Society.

(R = $SiMe_3$, Me, H), with the counterion $Li(THF)_4$ or $Li(TMEDA)_2$, was synthesized from the reaction between $CrCl_3$ and the corresponding THF-solvated lithium sodium double salt in a molar ratio of 1:2 in benzene, followed by extraction and crystallization of the product from a solution of benzene and THF or TMEDA as shown in Scheme III.[42] The structures of these complexes were determined by X-ray crystallography. The structures reveal that the chromacarborane complexes are all ionic species in which the Cr metal is parallel sandwiched by the two carborane ligands with the slight slippage of the metal toward the cage carbons (av Cr–C = 2.17 Å, av Cr–B = 2.25 Å) giving rise to a C_{2h} symmetry for the $Cr(C_2B_4)_2$ cage framework.[42] A representative structure of the complex, when R = $SiMe_3$, is shown in Figure 10.

The Cr–C(cage) bond distances are shorter than those (2.26 and 2.27 Å) found in the corresponding icosahedral

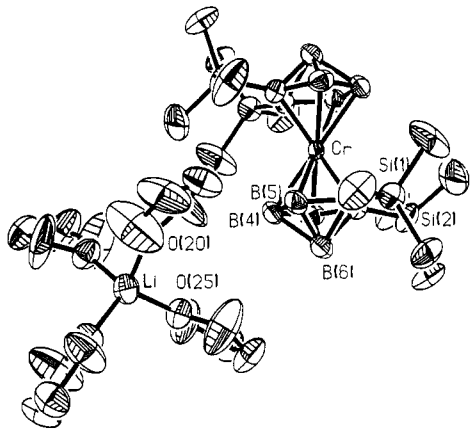

Figure 10. Molecular structure of $Li(THF)_4\{1,1'$-*commo*-$Cr[2,3\text{-}(SiMe_3)_2\text{-}2,3\text{-}C_2B_4H_4]_2\}$. Reprinted from ref 42. Copyright 1992 American Chemical Society.

Scheme III. Syntheses of Cr(III) and Cr(IV) Complexes (Reprinted from ref 42. Copyright 1992 American Chemical Society)

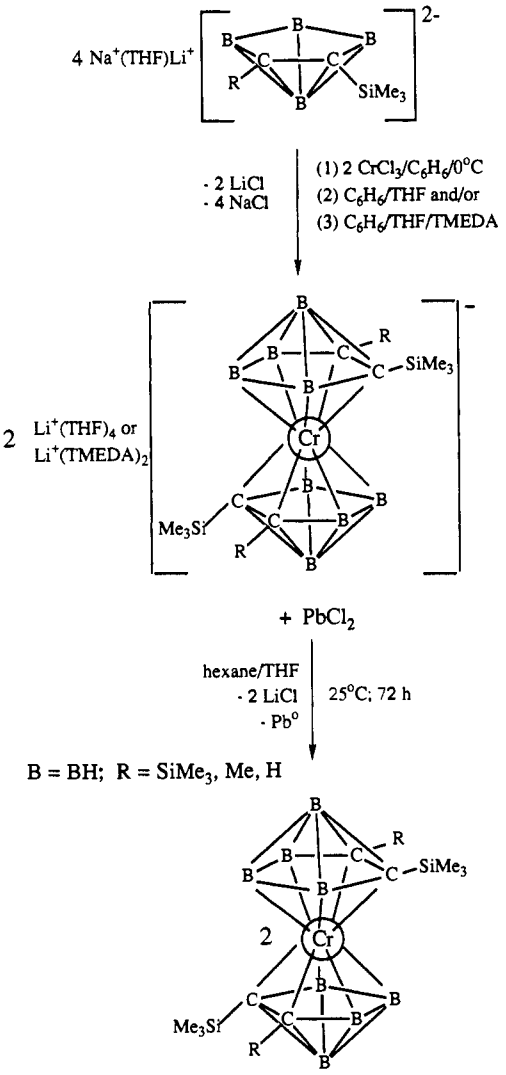

analogue[41] and about the same as those in the mixed-ligand complex, $1\text{-}Cr(\eta^7\text{-}C_7H_7)\text{-}2,3\text{-}(Et)_2\text{-}2,3\text{-}C_2B_4H_4$,[43] and in chromocene.[44] The ESR spectrum of the anionic Cr complex, $\{[(SiMe_3)_2C_2B_4H_4]_2Cr\}^-$, exhibits an unresolved ESR signal at $g = 1.989$ with a peak to peak line width of 2.2 mT. The observed signal is too broad for detection of ^{53}Cr isotope splitting which is typically in the order of 1.5 mT. However, the solid-state low-temperature ESR spectrum exhibits the characteristic features of Cr(III) (d^3) centers with large zero-field splitting D. The effective magnetic moment of 3.93 μ_B at room temperature is consistent with an $S = {}^3/_2$ paramagnetic system that follows the Curie law with a Curie constant of 1.933 and a g value of 2.03.[42]

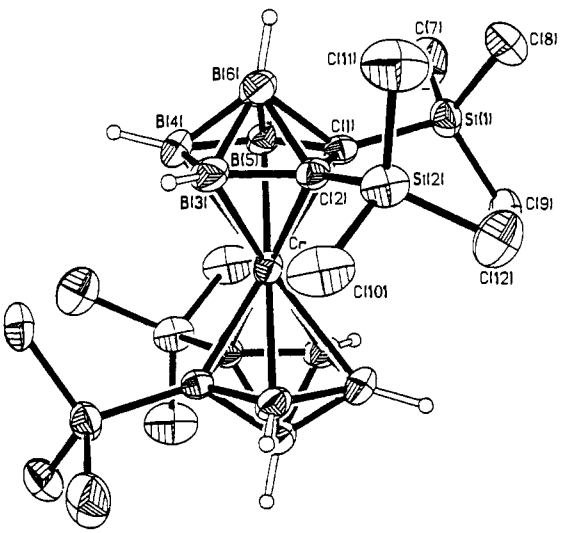

Figure 11. Perspective view of the neutral Cr(IV) complex. Reprinted from ref 10. Copyright 1992 American Chemical Society.

The chemical oxidation of the anionic Cr(III) sandwich species with $PbCl_2$ produced the novel, diamagnetic, and neutral Cr(IV) sandwich complexes as dark-red, air-sensitive, and crystalline solids in 63% yields (see Scheme III). The structure of the oxidized species, when R = $SiMe_3$, was determined by X-ray diffraction and is shown in Figure 11.[10,42] The structure shows that the Cr^{IV} metal is not symmetrically bonded to the C_2B_3 faces, but is slightly dislocated toward the cage carbons. This slippage produces Cr–C distances that are about 0.14 Å shorter than the average Cr–B distances. Although the experimental deviations tend to mask any differences in the analogous bond lengths in the Cr(III) precursor, the bond distances suggest a similar slip distortion is occurring in all complexes regardless of the difference in formal charges of the metal atoms.[10,42] The effective magnetic moment of 0.99 μ_B at 25 °C indicates the presence of some paramagnetic impurities, such as unoxidized Cr^{III} precursor or products of the reaction of Cr^{IV} complex with the sample holder. Nonetheless, the singlet state of the complex is consistent with the observation that its well-resolved ^1H, ^{11}B, and ^{13}C NMR spectra could be obtained.[10,42]

Fenske–Hall MO calculations on the model compounds, $[1,1'\text{-}commo\text{-}Cr\{2,3\text{-}C_2B_4H_6\}_2]^-$ and $1,1'\text{-}commo\text{-}Cr[2,3\text{-}C_2B_4H_6]_2$, revealed that the Cr bonds to the carborane cages mainly with its d_{xz} and d_{yz} orbitals, and the d^3 electrons of the metal are distributed in MO's $29a_g$, $30b_g$, and $31a_g$ (see Figure 12).[42] Despite the structural similarity, as one goes from the Cr(III) sandwich to the corresponding Cr(IV) species, there is an increase in the energy difference between MO's $29a_g$ and $30b_g$. However, in view of the calculated orbital energy separations in the paramagnetic Cr(III) species including the icosahedral analogue and chromocene, it is difficult to rationalize how depopulation of MO $31a_g$ could induce spin pairing in the two lower energy orbitals. Xα-scattered wave SCF MO calculations on

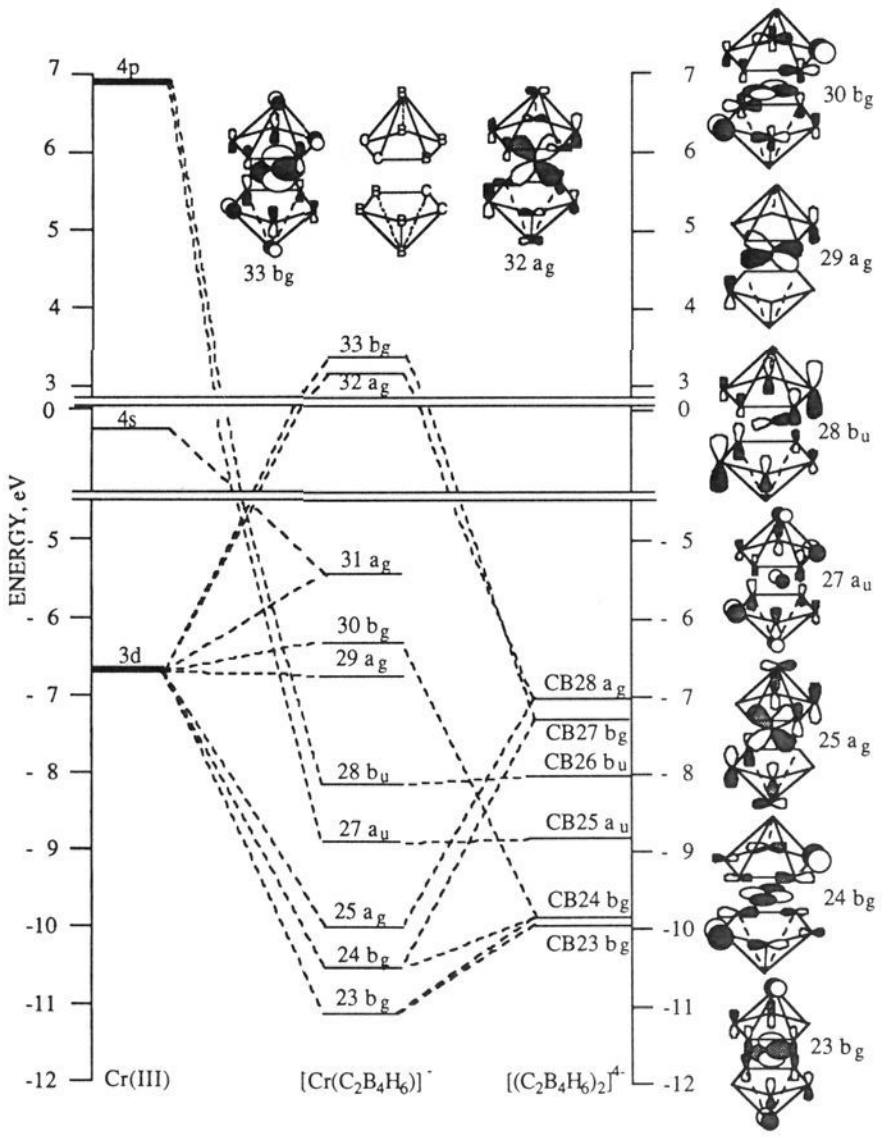

Figure 12. Molecular orbital correlation diagram for {1,1′-*commo*-Cr[2,3-$C_2B_4H_6$]$_2^-$}. Reprinted from ref 42. Copyright 1992 American Chemical Society.

both species showed essentially the same results as did the Fenske–Hall calculations, that the metal d electrons are distributed in a set of three closely spaced metal centered MO's very similar to those described above (see Figure 12).[42] One other possibility is that of a singlet···$(29a_g)^1(30b_g)^1$ configuration that could arise from unusually large zero-field splitting in the triplet state, or by some other interaction. Such a configuration would be more consistent with the MO analysis. However, it is not apparent how such interaction could arise. Since the unit cell of the structure of Cr(IV) sandwich complex consists of four molecules that are well separated with the shortest Cr–Cr distance of 9.851 Å, it seems unlikely that intermolecular interactions could be an important factor for spin pairing in the complex to yield a diamagnetic species.

The syntheses and structures of polynuclear metal clusters, so-called "clustered clusters", have dominated the chemistry of d-block elements in recent years. In addition to several interesting papers by Hawthorne and co-workers, Stone's research group has contributed significantly to this area of research.[45] The first in the series of heterotetranuclear metallacarboranes has been $[M_2Cu_2(\mu\text{-}CO)_4(CO)_2(\mu\text{-}H)_2(C_2B_9H_{10})_2]^{2-}$ (M = Mo, W), whose $(PPN)_2$ salt was synthesized, in yields of 18–61%, as shown in eq 2.[46]

$$2\mathrm{Tl}[\textit{closo}\text{-}3,1,2\text{-}\mathrm{TlC_2B_9H_{11}}] + 2(\mathrm{PPN})^+\mathrm{Cl}^- + 2[\mathrm{M(CO)_3(MeCN)_3}] \xrightarrow[25\ ^\circ\mathrm{C}]{\mathrm{MeCN}} 2(\mathrm{PPN})[\textit{closo}\text{-}3,3,3\text{-}(\mathrm{CO})_3\text{-}3\text{-}\mathrm{Tl}\text{-}3,1,2\text{-}\mathrm{MC_2B_9H_{11}}] + 2\mathrm{CuCl} \xrightarrow{\mathrm{MeCN}} (\mathrm{PPN})_2[\mathrm{M_2Cu_2}(\mu\text{-}\mathrm{CO})_4(\mathrm{CO})_2(\mu\text{-}\mathrm{H})_2(\mathrm{C_2B_9H_{10}})_2] + 2\mathrm{TlCl} \quad (2)$$

The structure of the Mo complex was determined by X-ray diffraction which displays well-separated PPN^+ cations and cluster anion consisting of a planar $MoCu_2Mo$ rhomb that is incorporated into two 12-vertex molybdacarboranes with C_{2h} symmetry (Figure 13). Two uneven $MoCu_2$ triangles share the Cu–Cu edge to form a heteronuclear "raft". The shorter of the two Mo–Cu distances, the first known bonds (2.656 and 2.834 Å) between Mo^0 and Cu^I metals, is also associated with two CO groups that bridge the metal atoms.[46]

An interesting bimetallic cluster (PPN)[*closo*-3,3,3-$(CO)_3$-3-$(SnPh_3)$-3,1,2-$M(C_2B_9H_{11})$] (M = Cr, Mo, W), that incorporates both transition and main group metals, has been synthesized in an analogous reaction, described in eq 2.[47] The crystal structure of the tungstacarborane derivative, shown in Figure 14, consists of a discrete anion of metallacarborane fragment

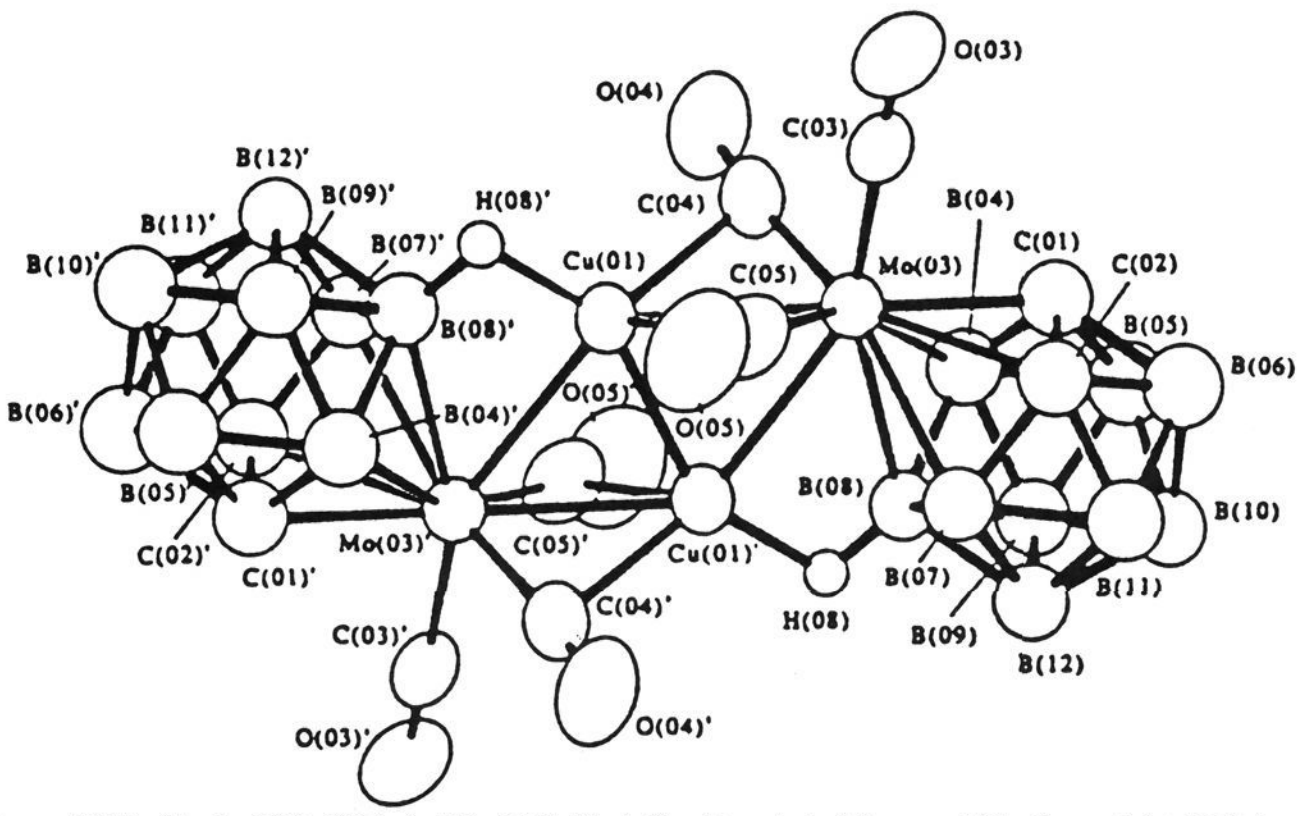

Figure 13. Structure of $[Mo_2Cu_2(\mu\text{-}CO)_4(CO)_2(\mu\text{-}H)_2(C_2B_9H_{10})_2]^{2-}$. Reprinted from ref 46. Copyright 1987 American Chemical Society.

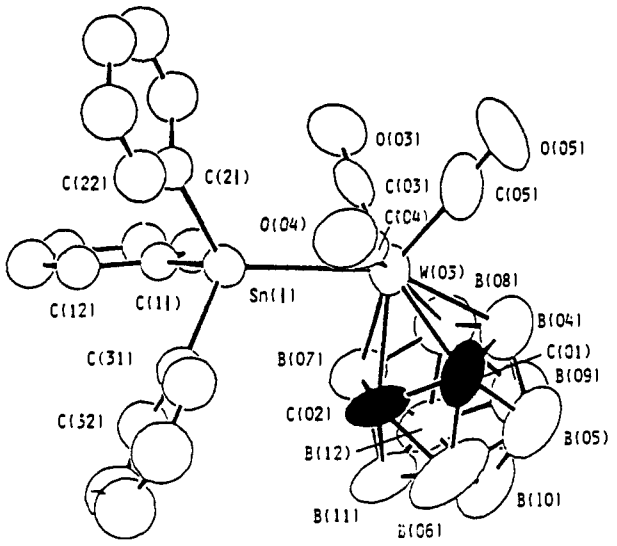

Figure 14. A view of the molecular structure of [*closo*-3,3,3-$(CO)_3$-3-$SnPh_3$-3,1,2-$WC_2B_9H_{11}$]$^-$. Reprinted from ref 47. Copyright 1991 Elsevier Sequoia.

and the PPN^+ cation (not shown). The transition metal unit, while bonding to $SnPh_3$ group, caps the pentagonal C_2B_3 plane of the *nido*-carborane dianion to form a 12-vertex *closo*-WC_2B_9 cluster. The W–Sn distance of 2.825 Å is similar to those observed in the structures of [{$W(CO)_3(C_5H_5)$}$_2SnPh_2$] (2.81 Å)[48] and [(μ-Cl)-($MeSnCl_2$)$W(CO)_3$($MeSCH_2CH_2SMe$)] (2.759 Å),[49] thus indicating dπ–dπ bonding between formal W^0 and Sn^{IV} metals, that is consistent with the ^{119}Sn NMR spectrum of the complex.[47] This work, together with the earlier study, suggests that a number of heteropolynuclear cluster complexes, including the mixed main group and transition metal species, can be synthesized. Since alkylidyne–metal cluster chemistry has been instrumental in the success of Fischer–Tropsch reactions and alkyne metathesis, a merger of chemistry between alkylidyne–metal and metallacarborane clusters has long been expected. In fact, the pioneering work of Stone and co-workers has profitably exploited the isolobal analogy between the organometallic species [$W(\equiv CR)(CO)_2(\eta^5\text{-}C_5R'_5)$] and [$W(\equiv CR)(CO)_2$-($\eta^5\text{-}C_2B_9H_9R'_2$)]$^-$ (R′ = H, Me). Since most of Stone's published work, prior to 1990, has been reviewed,[45] our discussion will be limited to the recently published work in this area of active research.

In series of papers, Stone and co-workers have studied the protonation reactions of alkylidyne(carborane) complexes of group 6 metals with HBF_4·Et_2O or HI alone or in the presence of varieties of unsaturated substrate molecules.[50–56] The protonation of the salt [NEt_4][$W(\equiv CR)(CO)_2(\eta^5\text{-}C_2B_9H_9Me_2)$] (where R = C_6H_4Me-4, Me) with HBF_4·Et_2O affords a product in which the CR group has migrated from tungsten to the C_2B_9 fragment. The migration of C_6H_4Me-4 group was confirmed by the crystal structure of [$W(CO)_2(PPh_3)_2\{\eta^5$-$C_2B_9H_8(CH_2C_6H_4Me\text{-}4)Me_2\}$].[52] The influence of the $C_{(cage)}$-substituents on the dicarbollide ligands has also been observed in most of the protonation reactions. This reactivity pattern is different from the isolobal cyclopentadienyl analogues [$W(\equiv CR)(CO)_2(\eta^5\text{-}C_5R'_5)$] (where R′ = H, Me).[57] The protonation probably proceeds via the initial formation of an alkylidene-tungsten complex [$W\{=C(H)R\}(CO)_2(\eta^5\text{-}C_2B_9H_9Me_2)$] in which the metal center is electronically unsaturated. Addition of CO molecules presumably promotes the

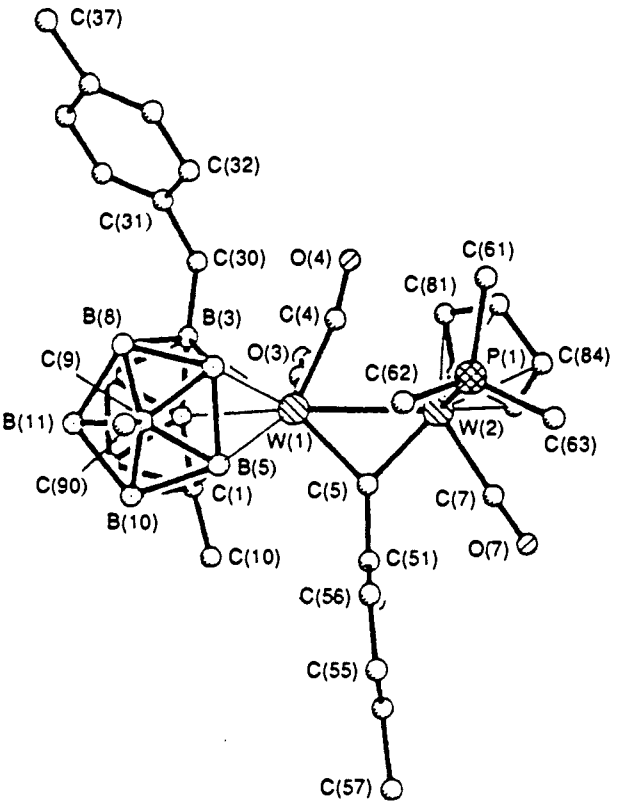

Figure 15. The molecular structure of [$W_2(\mu\text{-}CC_6H_4Me\text{-}4)(CO)_3(PMe_3)(\eta^5\text{-Cp})\{\eta^5\text{-}2,8\text{-}C_2B_9H_8\text{-}10\text{-}(CH_2C_6H_4Me\text{-}4)\text{-}2,8\text{-}Me_2\}$]. Reprinted from ref 54. Copyright 1992 Royal Society of Chemistry.

insertion of alkylidene group into an adjacent B–H bond. However, the protonation of the complex in the presence of [$M'(\equiv CR)(CO)_2(\eta^5\text{-}C_5H_5)$] produces the dinuclear cluster [$MM'(\mu\text{-R})(CO)_3\{\eta^5\text{-}C_2B_9H_8\text{-}(CH_2C_6H_4Me\text{-}4)Me_2\}(\eta^5\text{-}C_5H_5)$] (where M, M′ = Mo, W; R = C_6H_4Me-4, Me).[51] In the same report, these authors have shown the removal of a BH vertex from the C_2B_{10} cage forming a stable C_2B_9 cluster along with the migration of CR group and the formation of M=M bond. The X-ray structures, presented in Figures 15–17, unambiguously show the presence of a metal–metal double bond (W=W 2.651 Å or W=Mo 2.702 Å) in each of these complexes.[51]

It has been demonstrated that the migration of alkylidyne group takes place during the protonation in the presence of a number of substrates including CO, PPh_3, $PHPh_2$, $CNBu^t$, Ph_2C_2, dppm, and dppe.[53–55] However, the migration of a CR group to the P atom, forming a ylide of the type [$W\{CH(C_6H_4Me\text{-}4)\text{-}PPh_2(CH_2)_nPPh_2\}(CO)_2(\eta^5\text{-}C_2B_9H_9Me_2)$], was observed when the substrate was either dppm or dppe.[55] Such ylide formations have been observed previously in alkylidene chemistry.[58] Recently, the double migration of alkylidyne groups from tungsten to the borons on the C_2B_3 face of a dicarbollide ligand has been reported.[50] The crystal structures of the products confirmed these intriguing migrations of the alkylidyne moieties.[53–55] Figure 18 represents the X-ray structure that clearly shows the double migration of $CH_2C_6H_4$Me-4 groups in a dicarbollide–tungsten complex.[50]

A novel, anionic, "carbons apart" tungstacarborane derivative, [*closo*-1,8-Me_2-11-$(CH_2C_6H_4Me\text{-}4)$-2-Cl-2,2,2-$(CO)_3$-2,1,8-$WC_2B_9H_9$]$^-$, was synthesized from the corresponding "carbons adjacent" analogue in a similar reaction involving aqueous HCl.[56] The crystal structure

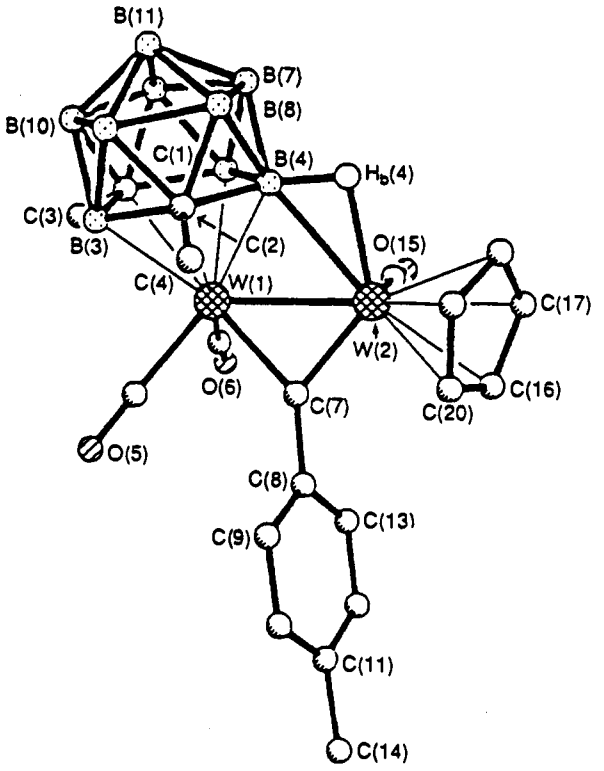

Figure 16. Molecular structure of $[W_2(\mu\text{-}CC_6H_4Me\text{-}4)(CO)_3(\eta^5\text{-}C_2B_9H_9Me_2)(\eta^5\text{-}Cp)]$. Reprinted from ref 51. Copyright 1991 Royal Society of Chemistry.

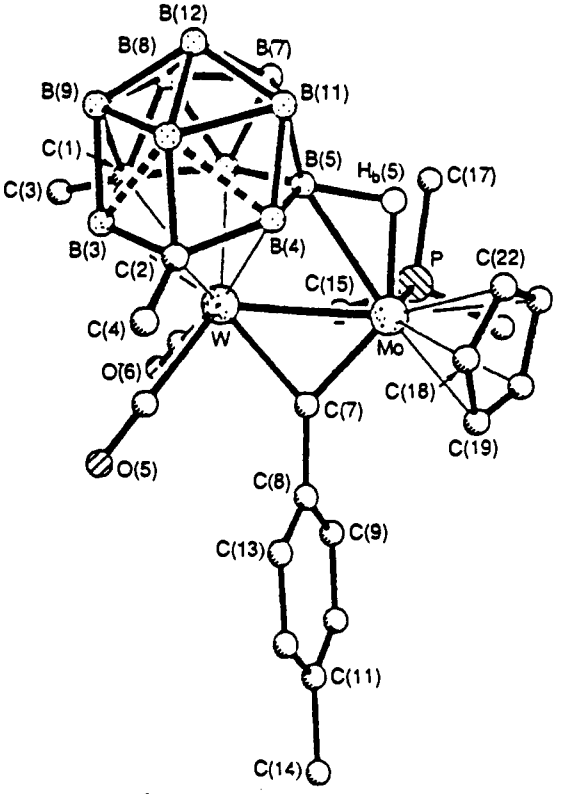

Figure 17. Molecular structure of $[MoW(\mu\text{-}CC_6H_4Me\text{-}4)(CO)_2(PMe_3)(\eta^6\text{-}C_2B_{10}H_{10}Me_2)(\eta^5\text{-}Cp)]$. Reprinted from ref 51. Copyright 1991 Royal Society of Chemistry.

(see Figure 19) unambiguously shows the "carbons apart" geometry of the complex with the tungsten metal, while capping the *nido*-icosahedral C_2B_9 cage, ligated by three CO groups and a Cl atom. Although a similar type of cage rearrangement was previously observed by Hawthorne et al. for a rhodacarborane complex,[59]

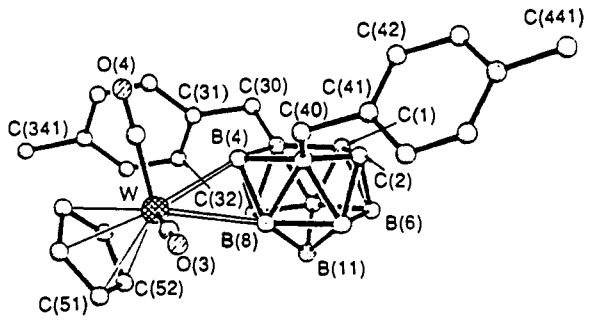

Figure 18. The molecular structure of $[exo\text{-}nido\text{-}9,11\text{-}(CH_2C_6H_4Me\text{-}4)_2\text{-}5,10\text{-}\{W(CO)_2(\eta\text{-}Cp)\}\text{-}5,10\text{-}(\mu\text{-}H)_2\text{-}7,8\text{-}C_2B_9H_8]$. Reprinted from ref 50. Copyright 1992 Royal Society of Chemistry.

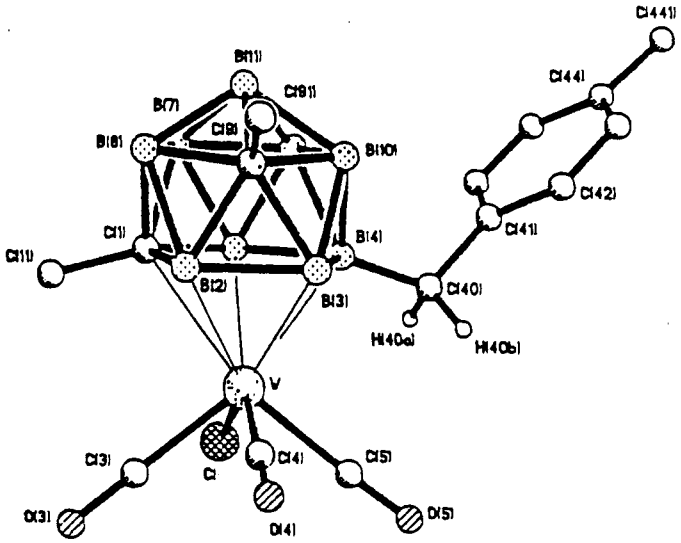

Figure 19. Structure of the anion of $[NEt_4][closo\text{-}1,8\text{-}Me_2\text{-}11\text{-}(CH_2C_6H_4Me\text{-}4)\text{-}2\text{-}Cl\text{-}2,2,2\text{-}(CO)_3\text{-}2,1,8\text{-}WC_2B_9H_8]$. Reprinted from ref 56. Copyright 1992 American Chemical Society.

this represents the first example of a *reversible* cage rearrangement in metallacarborane chemistry.

It is clear from the work of Stone and co-workers that the nature of the products, in all the cases of protonation reactions, is influenced not only by protonating agents, cage carbon substituents or the substrate molecules, but also by the reaction temperatures. As varieties of new compounds become available, the mechanistic details tend to complicate the "so-called" simple protonation reactions. Nevertheless, this area of research seems to be developing faster than ever and undoubtedly has dominated the chemistry of electronically unsaturated organometallic "clustered clusters".

The research on tungsten complexes has also been extended to mixed-metal clusters without the migration of alkylidyne moieties. The heteropolynuclear metallacarboranes of the types $[WPt(\mu\text{-}CR)(\mu\text{-}\sigma\text{:}\eta^x\text{-}C_2B_nH_{n-1}Me_2)(CO)_2(PMe_2Ph)]$ (where $x = 5$, $n = 9$; $x = 6$, $n = 10$)[60] and $[W_2Au_2(\mu\text{-}CR)_2\{\mu\text{-}Ph_2P(CH_2)_nPPh_2\}(CO)_4(\eta^5\text{-}C_2B_9H_9Me_2)]$ (where $n = 2$–6) can be synthesized from a reaction involving $[Au_2Cl_2\{\mu\text{-}Ph_2P(CH_2)_nPPh_2\}]$ or $[PtCl(Me)(PMe_2Ph)_2]$ and a mixture of $TlBF_4$ and $[NEt_4]^+[W(\equiv CR)(CO)_2(\eta^5\text{-}C_2B_9Me_2)]^-$.[61] While the crystal structures of these mixed-metal species unambiguously show the formation of metal–metal bonds (W–Pt = 2.720–2.738 Å, and W–Au = 2.798 Å), the structure of the mixed W_2Au_2 species (see Figure 20), with $n = 4$, confirms the presence

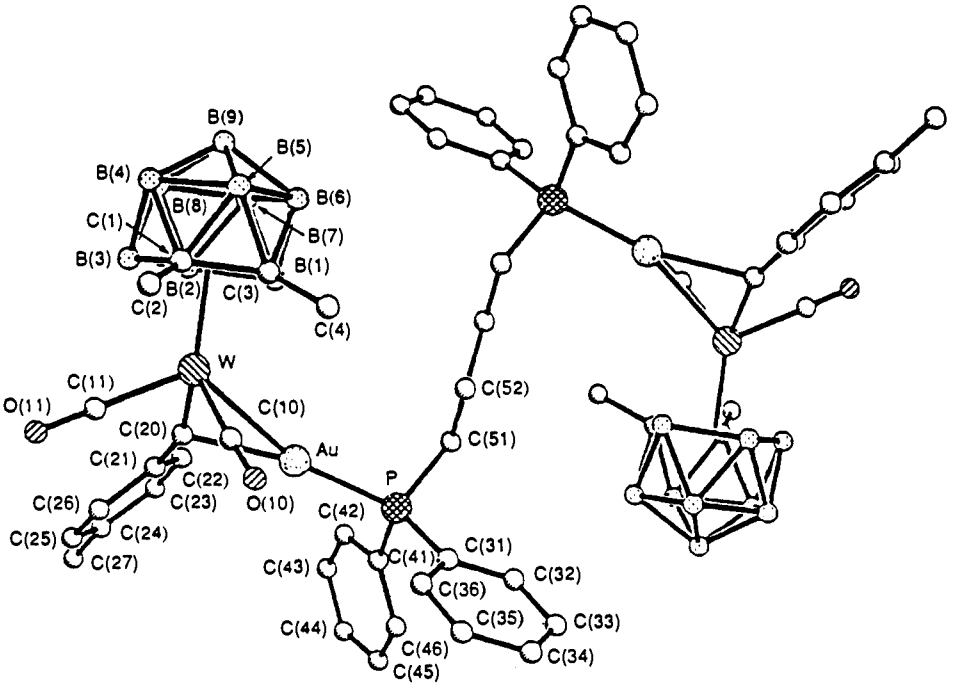

Figure 20. Molecular structure of $[W_2Au_2(\mu\text{-}CR)_2\{\mu\text{-}PPh_2(CH_2)_4PPh_2\}(CO)_4(\eta^5\text{-}C_2B_9H_9Me_2)_2]$ showing W–Au bond. Reprinted from ref 60. Copyright 1990 Royal Society of Chemistry.

of two tungstacarboranes that are bridged by $[Au\text{-}P(Ph)_2(CH_2)_2]_2$ unit, with a center of inversion at the midpoint of the chain of methylene groups. The overall geometry of the ligands at the W center can be described at best as a distorted square pyramid or a "four-legged piano stool". Despite an unsymmetrical bridging of the W–Au bond by the *p*-tolylmethylidyne ligand, the distance of tungsten from the C_2B_3 centroid (1.919 Å) of the dicarbollide ligand in each unit appears to be normal.[61]

The manganese or rhenium complexes of a number of carborane ligand systems have been known since the first report on $Cs[(C_2B_9H_{11})M(CO)_3]$ (M = Mn^I or Re^I) by Hawthorne and Andrews in 1965.[62] However, most of the reported manganacarborane complexes are half-sandwiched closo species with $Mn(R_3P)_x(CO)_{3-x}$ (R = alkyl or aryl group; x = 0, 1, or 2) unit occupying a vertex of either an icosahedron or its lower homologues.[25] Until recently, the only known manganacarborane sandwiches have been the anionic complexes of the type $[4,4'\text{-}Mn^{II}(1,6\text{-}C_2B_{10}H_{12})_2]^{2-}$ and $[Mn^{IV}(CB_{10}H_{11})_2]^{2-}$ whose geometries have not been confirmed by X-ray crystallography.[63] The synthesis and X-ray crystal structure of a novel zwitterionic and paramagnetic manganese sandwich complex, $\{[Li(THF)][Li(TMEDA)]_2\}\{commo\text{-}Mn_3[2,3\text{-}(SiMe_3)_2\text{-}2,3\text{-}C_2B_4H_4]_4\}$, was reported most recently.[64] The synthetic pathways are given in eq 3. A "butterfly" geometry for

$$9Na(THF)Li[2,3\text{-}(SiMe_3)_2C_2B_4H_4] + 6MnCl_2 \xrightarrow[\text{(2) hexane/THF/TMEDA}]{\text{(1) THF 0 °C, 1 h and 25 °C, 24 h}} 3LiCl + 9NaCl + 2\{[Li(THF)][Li(TMEDA)]_2\}\{commo\text{-}Mn_3[2,3\text{-}(SiMe_3)_2\text{-}2,3\text{-}C_2B_4H_4]_4\} + closo\text{-}1,2\text{-}(SiMe_3)_2\text{-}1,2\text{-}C_2B_4H_4 \quad (3)$$

the molecule is evident in X-ray analysis of the complex (Figure 21) that shows the three Mn atoms forming a central plane with no connectivities between the two

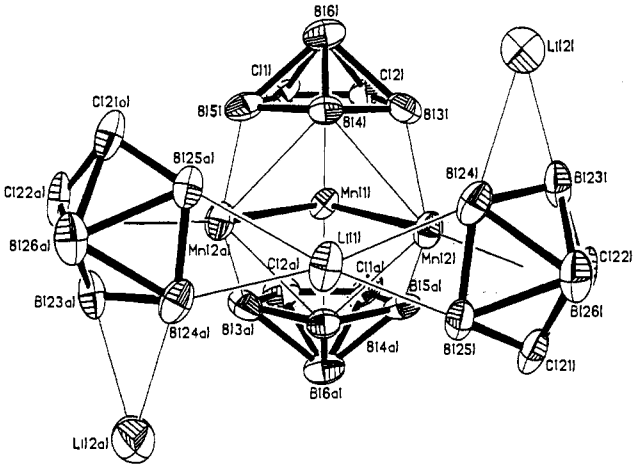

Figure 21. The crystal structure of $\{[Li^+(THF)][Li^+(TMEDA)]_2\}\{commo\text{-}Mn_3[2,3\text{-}(SiMe_3)_2\text{-}2,3\text{-}C_2B_4H_4]_4\}^{3-}$. Reprinted from ref 64. Copyright 1991 American Chemical Society.

terminal Mn's which are separated by about 3.28 Å [$Mn_{(terminal)}$–$Mn_{(central)}$–$Mn_{(terminal)}$ = 75.5°; $Mn_{(central)}$–$Mn_{(terminal)}$ = 2.68 Å].[64] The central Mn atom is essentially η^5-bonded to two C_2B_3 faces, forming a parallel sandwich species, with the metal to cage distances ranging from 2.155 to 2.249 Å, indicating a stronger bonding of the metal to ligands than in the corresponding high-spin Cp analogue (av Mn–C = 2.42 Å).[65] The "butterfly" geometry of the complex is presumably stabilized by four $Mn_{(terminal)}$–$B_{(cage)}$ bonds on either side of the central Mn atom with the carborane cages. In a formal sense, the Mn complex is a hybrid of both the sandwich (commo) and half-sandwich (closo) geometries. The presence of three loosely B-bound $[Li(solv)]^+$ units within the coordination sphere makes the complex a zwitterionic cluster.[64] The effective magnetic moment (8.3 μ_B at 298 K) of the complex decreases monotonically with decreasing temperature and reaches 6.2 μ_B at 15 K, indicating a significant antiferromagnetic coupling between the central and

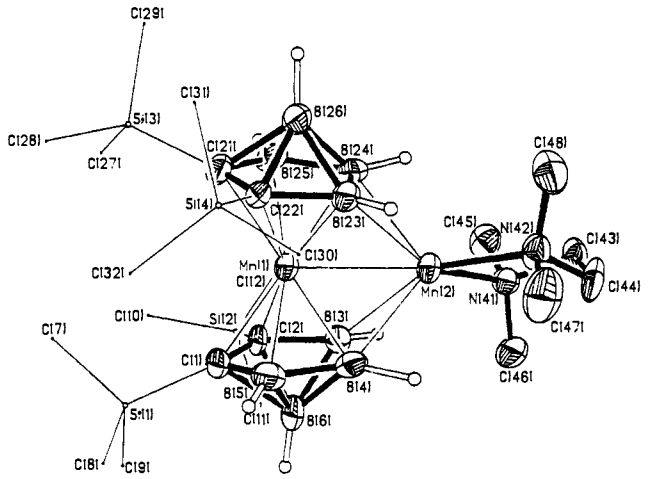

Figure 22. The crystal structure of a manganacarborane sandwich, [Mn(TMEDA)][*commo*-1,1′-Mn[2,3-$(SiMe_3)_2$-2,3-$C_2B_4H_4]_2$] showing the exo-polyhedrally wedged second Mn atom. Reprinted from ref 67.

terminal Mn atoms. The shorter central Mn–centroid distance (1.708 Å), when compared to that of terminal Mn–centroid distance of 2.125 Å, is consistent with the high-spin Mn^{I}–Mn^{III}–Mn^{I} trinuclear system. There was no signal in the X-band EPR spectrum of the complex at 25 °C.[64]

An entirely different result was obtained when a trinuclear half-sandwich gadolinacarborane cluster, {*closo*-Gd_3[2,3-$(SiMe_3)_2$-2,3-$C_2B_4H_4]_3(\mu_2$-*closo*-Li_3[2,3-$(SiMe_3)_2$-2,3-$C_2B_4H_4]_3)[\mu_2$-Li(THF)$]_3(\mu_3$-OMe)-(μ_3-O)},[66] was reacted with $MnCl_2$ as in the previous reaction. In fact, the isolated product was a less complicated Mn–cluster system, 3,3′,4,4′-Mn(TMEDA)-*commo*-1,1′-Mn[2,3-$(SiMe_3)_2$-2,3-$C_2B_4H_4]_2$, indicating that a different reaction sequence is taking place when predominantly ionic lanthanacarboranes are used solely as the source for carborane ligands. The room temperature effective magnetic moment (7.6 μ_B) of the Mn_2 complex decreases monotonically with decreasing temperature and reaches 5.6 μ_B at 80 K, indicating that a significant antiferromagnetic coupling exists between the two Mn atoms. The crystal structure of the product (Figure 22) clearly shows that the Mn atom, formally in +2 oxidation state, is somewhat parallel sandwiched by two carborane cages (Mn–C = 2.167 Å, Mn–B = 2.243 Å, and Cnt–Mn–Cnt = 175.5°).[67] For charge balance, an additional exo-polyhedral Mn^{II}(TMEDA) unit is present within the coordination sphere by bonding to two borons of each cage and to the central Mn atom (Mn–Mn = 2.665 Å). The incorporation of a second metal atom into the structure of sandwich complexes as counterion has been observed previously in carborane complexes of Sc, Y, Zr, and Hf.[26,28-31]

The study of cyclodextrin inclusion complexes with organometallic species, where they behave as the guest molecules is of current interest. Inspired by the success in forming inclusion complexes between *o*-carborane and cyclodextrins Chetcuti et al. have reported the formation of the first inclusion metallacarborane complexes of the general formula, [Cs[*closo*-3,3,3-$(CO)_3$-3,1,2-$MC_2B_9H_{11}$-α or β-(cyclodextrin)] (where M = Mn, Re).[68a] The crystal structure of the Re complex shows that the cyclodextrins are packed in a head to tail manner, forming a channel structure, while the *closo*-rhenacarborane guest anions are present in the host channels with their alternatively tilted axis. An interesting structural feature is that adjacent channels are antiparallel to one another so as to align the guests of one channel in the opposite direction of the adjacent one.[68a] The bond distances and lengths between the metal and the carborane cage are not changed from the values reported earlier for Cs[*closo*-3,3,3-$(CO)_3$-3,1,2-$MC_2B_9H_{11}$].[68b] Since inclusion compounds show increasing applications in catalysis[69] and for enzyme modeling,[70] there is a wealth of fascinating chemistry yet to be explored in this area of metallacarborane chemistry.

B. Middle and Late Transition Metal Complexes

The variety of known transition metal carborane complexes incorporating all types of carborane ligands, large or small, is very extensive since the discovery of the similarities of the dicarbollide dianions with the formally isolobal cyclopentadienide ion in the formation of the first metallocene-type sandwich complexes such as $[Fe^{II}(C_2B_9H_{11})_2]^{2-}$ and $[Fe^{III}(C_2B_9H_{11})_2]^{-}$.[8] There are a number of review articles, monographs, and chapters in books that adequately cover most of the published work in this area until 1982.[1,4,71] The transition metal complexes, based on mixed carborane and arene ligands, or incorporating purely the carborane ligands that contain one, three, or four carbons in the cage framework, and those complexes of linked cage and multidecker systems, are discussed separately in the following sections. Therefore, our discussions in this part of the review are limited to the sandwiched and half-sandwiched transition metal complexes.

In series of papers on metal-promoted face to face fusion of carborane cages, Grimes and co-workers have exemplified the formation of a single polyhedral C_4B_8 cluster involving either an iron sandwich ($R_2C_2B_4H_4)_2Fe^{II}H_2$ or its cobalt analogue ($R_2C_2B_4H_4)_2Co^{III}H$ (R = Me, Et, or *n*-propyl).[3a,42,43,46,47,72-74] Nonetheless, the mechanism of this "oxidative ligand fusion" was not reported until recently. In a systematic study of the fusion process, these authors have confirmed that the reaction is predominantly intramolecular with respect to the ligands and no evidence of ligand exchange could be found even in the mixtures containing two dissimilar FeH_2–carborane complexes. The finding of this study is the slow formation of a paramagnetic Fe_2 complex in THF from the corresponding diamagnetic mononuclear FeH_2 species known as the first intermediate, thus indicating the existence of the second intermediate in the ligand fusion process. An X-ray diffraction study confirmed the structure of this second intermediate as a dimetallic complex having one iron atom sandwiched between two C_2B_4 ligands and the second iron in a wedging position coordinated to the complex via four Fe–B bonds.[75] Since the diiron species is isostructural with the previously described dimanganese complex (see Figure 22),[67] it can also be regarded as a formal zwitterionic sandwich complex whose coordination sphere contains both the cation and the anion. Although, the two iron atoms are within the normal bonding distance (2.414 Å), the ^{57}Fe Mössbauer spectra can be interpreted, at best, as the species with no or very little direct Fe–Fe interaction. While the magnetic susceptibility and Mössbauer data suggest that both the iron atoms are formally in +2 oxidation state, the central and the outer Fe atoms are in low-spin (diamagnetic) and high-spin (paramagnetic) con-

Scheme IV. A Schematic Diagram Showing the Reactivity of Diiron Complex {[*closo*-3-CO-3,3'-(μ-CO)-3,1,2-$FeC_2B_9H_{11}]_2^{2-}$} (Reprinted from ref 80. Copyright 1991 American Chemical Society)

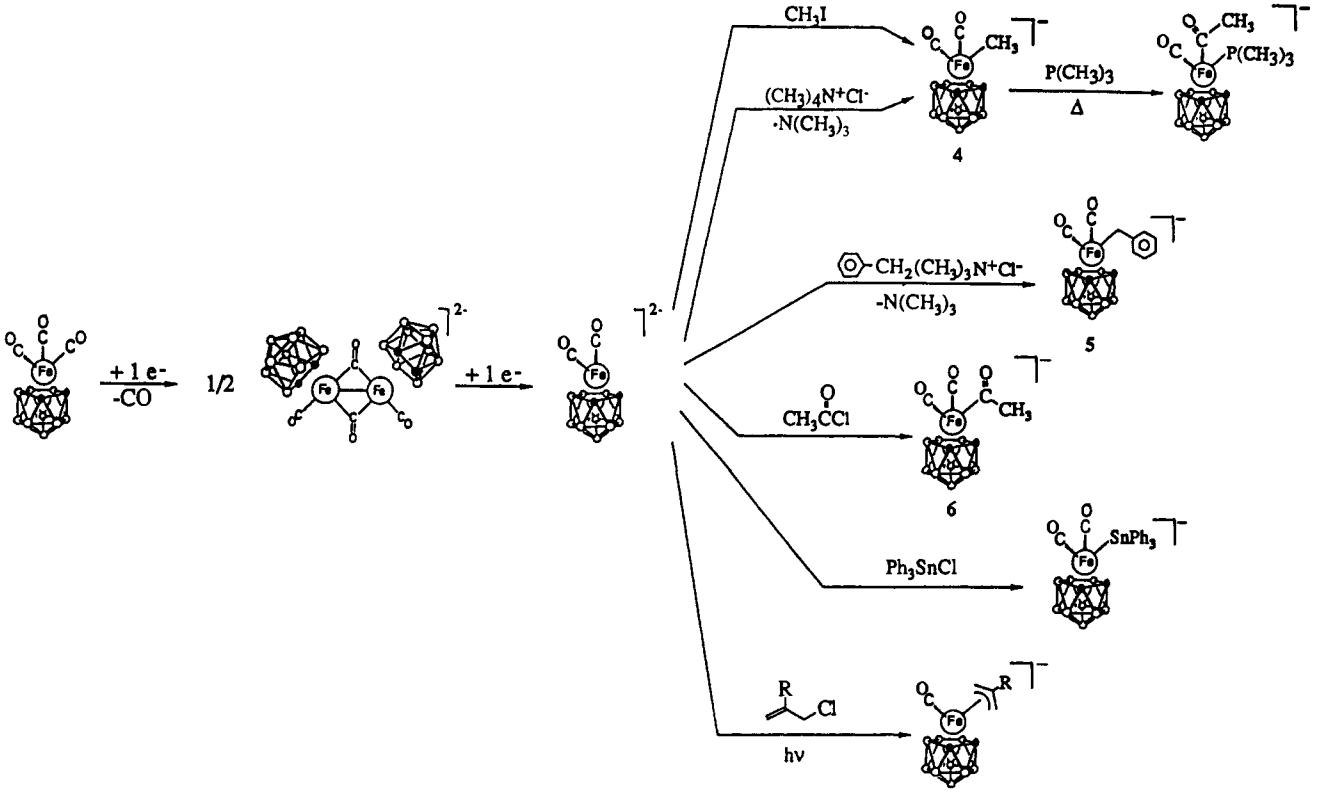

figurations, respectively. Presumably, the fusion of the two carborane faces at the B–B edges in the formation of the corresponding C_4B_8 species is induced by the presence of four outer Fe–B bonds as found in the crystal structure of the diiron complex.[75] The bonding in this "wedge"-bridged dinuclear sandwich as well as in its monoiron precursor, $(R_2C_2B_4H_4)_2Fe^{II}H_2$, has been investigated by using extended Hückel MO calculations. The results show that the electronic factors prevent the formation of stable bent-sandwich ferracarborane complexes, but prefer a wedging position for the second metal atom.[76]

Although, the dicarbollide anions have been utilized continuously since the birth of the metallacarborane chemistry, ferracarboranes have been relatively less investigated except for a few studies.[77,78] The recent reports from Hawthorne's laboratory have demonstrated the synthetic versatility of mononuclear iron(II) ferracarboranes which are the relatively unexplored metallacarborane counterparts of CpFe (Fp) derivatives.[79,80] The mononuclear iron complexes of the type [*closo*-3,3-$(CO)_2$-3-L-3,1,2-$FeC_2B_9H_{11}$] (where L = PPh_3, CH_3CN, $P(OCH_3)_3$, and CO) were prepared by the reaction of dimeric iron dicarbonyl carborane [*closo*-3-CO-3,3'-(μ-CO)-3,1,2-$FeC_2B_9H_{11}]_2^{2-}$ with anhydrous CuCl and the monodentate ligands. The ligand substitutions can also be carried out directly on the dianion [*closo*-3,3-$(CO)_2$-3,1,2-$FeC_2B_9H_{11}]_2^{2-}$ as shown in Scheme IV. The structural assignments of these complexes were supported by their X-ray crystal structures, each of which show the presence of a polyhedral FeC_2B_9 unit in which the iron adopts a pseudooctahedral coordination. The structure of the unsubstituted Fp analogue, [*closo*-3,3,3-$(CO)_3$-3,1,2-$FeC_2B_9H_{11}$], is shown in Figure 23.[80] The structure shows that the C_2B_3 bonding face is almost planar and the $Fe(CO)_3$ unit is approximately centered over this face, giving rise to a Fe–centroid

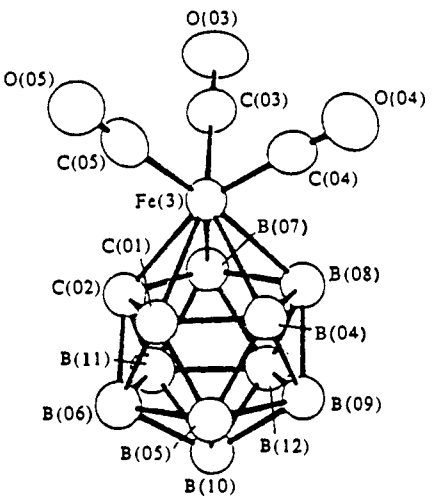

Figure 23. Molecular structure of [*closo*-3,3,3-$(CO)_3$-3,1,2-$FeC_2B_9H_{11}$]. Reprinted from ref 80. Copyright 1991 American Chemical Society.

distance of 1.562 Å. Although the C–O distances (1.131, 1.143, and 1.118 Å) are slightly greater than those of $[CpFe(CO)_3]PF_6$ (1.111, 1.112, and 1.113 Å),[81] they are similar (1.136–1.138 Å) when compared to those in $[(CO)_3Fe(C_2B_3H_7)]$.[82] With the exception of $SnPh_3$ unit occupying one of the facial coordination sites, the ferracarborane anion, [*closo*-3,3-$(CO)_2$-3-[Sn-$(C_6H_5)_3$]-3,1,2-$FeC_2B_9H_{11}$]$^-$, adopts an identical closo structure as its precursor, and as such, the iron atom is approximately centered over the C_2B_3 face (Fe–centroid = 1.557 Å) (see Figure 24).[79] The Fe–Sn distance of 2.554 Å is comparable to that in [Fp-$Sn(C_6H_5)_3$].[83] However, it has generally been observed in the crystal structures of these complexes that the metal center is slightly slipped toward the cage carbons above the C_2B_3 face while the opposite is true for the

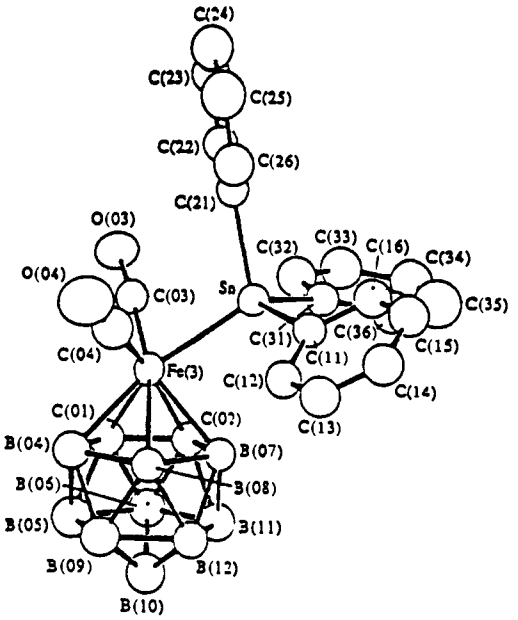

Figure 24. Structure of [*closo*-3,3-$(CO)_2$-3-[Sn$(C_6H_5)_3$]-3,1,2-$FeC_2B_9H_{11}$]$^-$. Reprinted from ref 79. Copyright 1991 American Chemical Society.

main group metallacarboranes.[84] Fehlner and coworkers have used Fenske–Hall quantum chemical technique to examine the structural distortions from an idealized closo geometry in metallacarborane clusters of the type 1,1,1-$(CO)_3$-1-Fe-2,3-$(Me)_2$-2,3-$C_2B_4H_4$. The results indicated that the greater interaction of the metal with the cage carbons is predominantly due to normal cluster-bonding effects since the antibonding interaction between the "t_{2g}" metal set and the cage carbons is negligible as opposed to that in the main group system.[85]

The dinegatively charged dicarbollide ligands promote the formation of anionic sandwich complexes with the metal when it is formally present in oxidation state less than +4.[86] The reduction of the charge by one unit on each ligand could result in the formation of neutral,[87] cationic,[88] or clustered sandwich complexes[89] in which the metals are present in accessible low oxidation states. Metallacarborane complexes incorporating charge-compensated ligands have been previously prepared by various methods including ligand rearrangement, reduction of a metal complex and addition of dialkyl sulfide.[4] A general methodology has now been developed to synthesize a number of prototype *commo*-metallacarboranes of Fe and Co and their corresponding charge-compensated dicarbollide ligands.[90] The crystal structure of the neutral and charge-compensated Fe^{II} sandwich complex [*commo*-3,3′-Fe{8-$N(C_2H_5)_3$-3,1,2-$FeC_2B_9H_{10}$}$_2$] is shown in Figure 25, and for comparison, the structure of the anionic species [*commo*-3,3′-Fe{3,1,2-$FeC_2B_9H_{11}$}$_2$][$N(CH_3)_4$]$_2$, prepared previously from the dinegatively charged dicarbollide ligand,[91] was also determined very recently and is shown in Figure 26.[90] In both structures the Fe atom is sandwiched between the two planar pentagonal faces of the dicarbollide ligands with the average metal to cage distances of 2.05–2.20 Å in the charge-compensated species and 2.03 Å in the other that make the metal–centroid distances of 1.50, 1.56, and 1.48 Å, respectively. The stronger bonding of the metal in the anionic complex, as evidenced by the shorter Fe–carborane distances, could be rationalized on the basis of the dinegatively

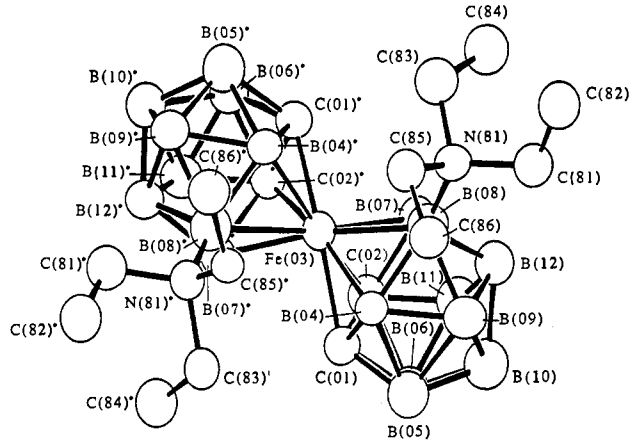

Figure 25. Structure of [*commo*-3,3′-Fe{8-$N(C_2H_5)_3$-3,1,2-$FeC_2B_9H_{10}$}$_2$]. Reprinted from ref 90. Copyright 1991 American Chemical Society.

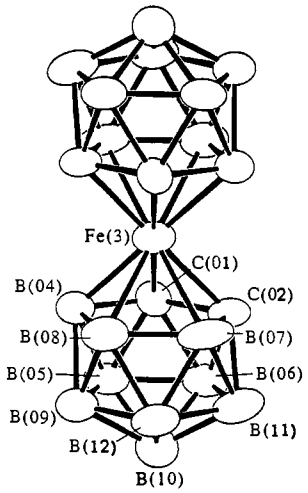

Figure 26. Structure of [*commo*-3,3′-Fe{3,1,2-$FeC_2B_9H_{11}$}$_{12}$][$N(CH_3)_4$]$_2$. Reprinted from ref 90. Copyright 1991 American Chemical Society.

charged dicarbollide ligand when compared to that in the neutral sandwich complex in which the ligands are charge-compensated monoanions.[90]

The first charge-compensated metal complex of a C_2B_4 carborane system, 1-Br-1-(PPh_3)-1-Ni^{II}[2,3-Et_2-5-(PPh_3)-2,3-$C_2B_4H_3$], was isolated unexpectedly as a purple, diamagnetic, half-sandwich species from the reaction of the [*nido*-2,3-$Et_2C_2B_4H_5$]$^-$ monoanion with $(Ph_3P)_2NiBr_2$ in THF at room temperature.[92] In the same report, the syntheses, structural characterizations and properties of neutral, diamagnetic Co complex and neutral, paramagnetic low-spin Fe^{III} complex of the general formula $(Ph_2PCH_2)_2(Cl)M(Et_2C_2B_4H_4)$ were also described. The crystal structures show the presence of a slightly distorted 7-vertex *closo*-MC_2B_4 cage in each complex. The presence of a halide ion facilitated some substitution reactions at the metal center in the presence of KCN and MeMgI, but the exchange with the H^- ion was unsuccessful unlike the analogous cyclopentadienyliron complex.[93] In addition, the reaction of the Co complex with Grignard reagent, MeMgI, proceeded quite differently, thus forming 1-Co-[$(Ph_2PCH_2)_2$(I)]-2,3-$Et_2C_2B_4H_4$ as opposed to the expected [$(Ph_2PCH_2)_2$(Me)Co($Et_2C_2B_4H_4$)].[92]

Metal atom synthesis has been used widely in organometallic chemistry. This methodology has been

profitably exploited by Sneddon and co-workers in the synthesis of a number of unusual metallacarboranes.[94-96] The reactions of thermally generated iron and cobalt atoms with *arachno*-2,6-$C_2B_7H_{13}$ and cyclopentadiene, toluene, mesitylene, or 2-butyne yielded a wide variety of unique, air- and water-stable metallacarborane clusters.[96] The resulting mixed-ligand sandwich complexes 2-(η-C_5H_5)Co-1,4-$C_2B_7H_9$, 4-(η-C_5H_5)Co-2,3-$C_2B_7H_{11}$, 2-(η^6-R)Fe-1,6-$C_2B_7H_9$, and 6-(η^6-R)Fe-9,10-$C_2B_7H_{11}$, (where R = toluene or mesitylene) were characterized by spectroscopy, and the structures of the iron species were also determined by X-ray crystallography.[96] A similar reaction involving hexaborane(10), bis(trimethylsilyl)acetylene, and cyclopentadiene gave an unusual mixed-ligand complex as a major product whose crystal structure shows a unique bridged structure consisting of a [1-(η-C_5H_5)Co-2,3-$(Me_3Si)_2C_2B_4H_3$] sandwich in which the terminal hydrogen on the unique boron is replaced by a B_2H_5 moiety via a three-center B–B–B bond. Alternatively, the complex can be viewed as a metallacarborane-bridged diborane derivative.[95] Unfortunately, the metal atom synthesis cannot be applied to the targeted metallacarborane complexes since generality does not exist in the reaction pathways of these systems.

Metallacarboranes and their derivatives, formed by the addition of organic functional groups, have been used as synthons in the preparation of multidecker sandwich complexes.[3a] The chemical reactivity of anions derived from $(C_5Me_5)Co(Et_2C_2B_3H_5)$ toward electrophilic reagents to prepare a number of functionalized metallacarborane derivatives was explored recently by Grimes and co-workers.[97-99] Consequently, the unique boron-substituted chloro, bromo, and iodo derivatives were prepared by the reactions of $[(C_5Me_5)Co(Et_2C_2B_3H_4)]^-$ with $MeSO_2Cl$, $BrCH_2CN$, and CF_3I, while the reaction with $C(O)CF_3Cl$ produced exclusively B(nonunique)–$C(O)CF_3$ derivative. Monohalo B(nonunique)–X derivatives were also obtained by the reaction of $(C_5Me_5)Co(Et_2C_2B_3H_5)$ with *N*-halosuccinimides. The reaction of $[(C_5Me_5)Co(Et_2C_2B_3H_4)]^-$ with acetyl chloride gave boron(unique)-substituted 2-vinyl acetate derivative instead of the acetyl one. The base-catalyzed cleavage of this complex produces B(unique)-substituted acetyl complex. The structure of this vinyl acetate-substituted cobaltacarborane complex was confirmed by X-ray crystallography.[97] Evidently, these B-substituents control the sandwich-stacking process.

Recently, Hawthorne et al. have synthesized systematically a variety of functionalized Venus flytrap-type metal cluster complexes of a C_2B_9 carborane system and demonstrated their utility in immunodiagnosis and radioimmunotherapy by binding radiotransition metals in the complex to tumor-associated monoclonal antibodies.[100] The structures of the pyrazole $B_{(cage)}$-bridged and alkylene carbon-bridged metallacarboranes were confirmed by X-ray diffraction studies.[101,102a] The crystal structure of an alkylene carbon-bridged complex, [7,7′-μ-1,3-C_3H_6(7,8-$C_2B_9H_{10})_2$Co][$MePh_3P$],[102a] shown in Figure 27, is similar to the one reported for a disulfide boron-bridged cobaltacarborane complex, [HCS_2-$(C_2B_9H_{10})_2$Co].[102b]

In contrast to icosahedral systems, most of the reported metallacarboranes of C_2B_4 carborane systems are those in which the cage carbons reside in adjacent

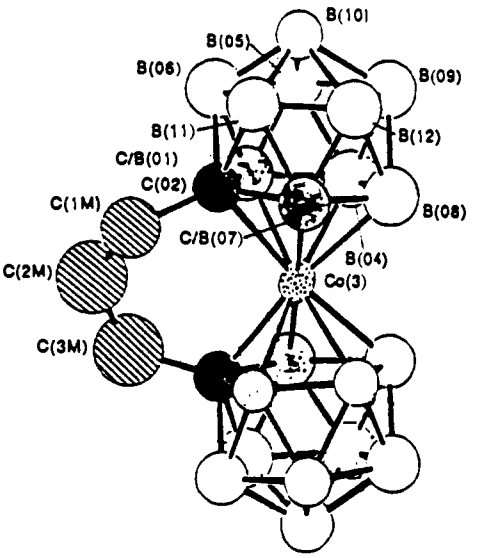

Figure 27. Molecular structure of [7,7′-μ-1,3-C_3H_6-(7,8-$C_2B_9H_{10})_2$Co]$^-$. Reprinted from ref 102a. Copyright 1992 American Chemical Society.

Scheme V. A Schematic Diagram for the Preparation of Ni(IV) Sandwich Complex Based on Carbons Apart C_2B_4 Carborane Ligands (Reprinted from ref 104)

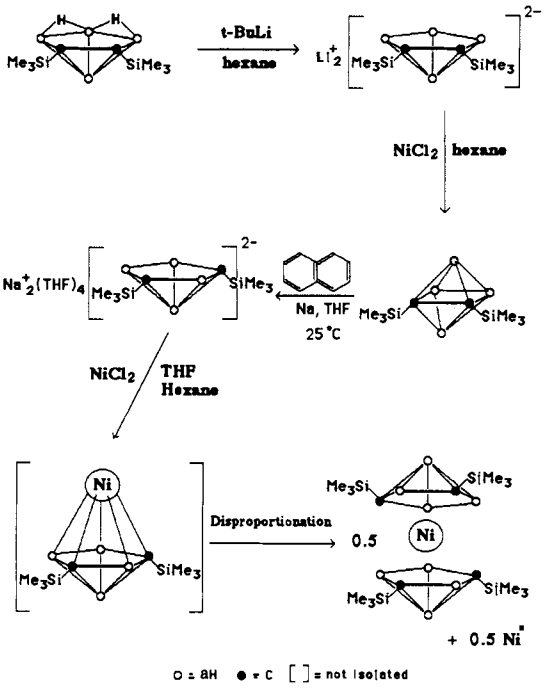

positions. Exceptions to these have been observed in some cases where cage carbons were separated when the metal complex was heated at very high temperature.[4] Until recently, neither the "carbons apart" anionic ligands nor a general methodology existed for the formation of such carbons apart metalla-C_2B_4 carboranes. Recent report on high-yield, room temperature synthesis of "carbons apart" C_2B_4 carborane dianion [2,4-$(SiMe_3)_2$-2,4-$C_2B_4H_4$]$^{2-}$ along with its structure determination has provided a much needed diversity to the chemistry of small metallacarboranes.[103] Although this dianion was produced from the corresponding "carbons adjacent" analogue as shown in Scheme V, its reactivity toward $NiCl_2$ seems to be different. For example, the reaction of the dilithium salt of the carbons adjacent dianion, [2,3-$(SiMe_3)_2$-

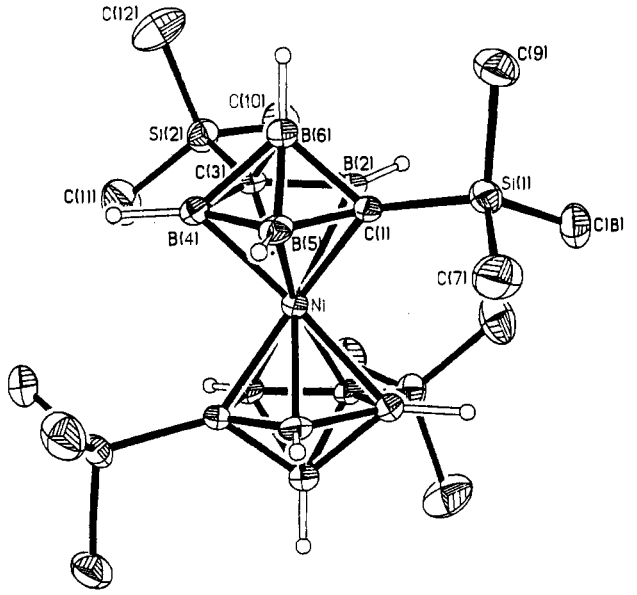

Figure 28. Molecular structure of a Ni(IV) sandwich complex showing the carbon apart geometry of carborane cages. Reprinted from ref 104.

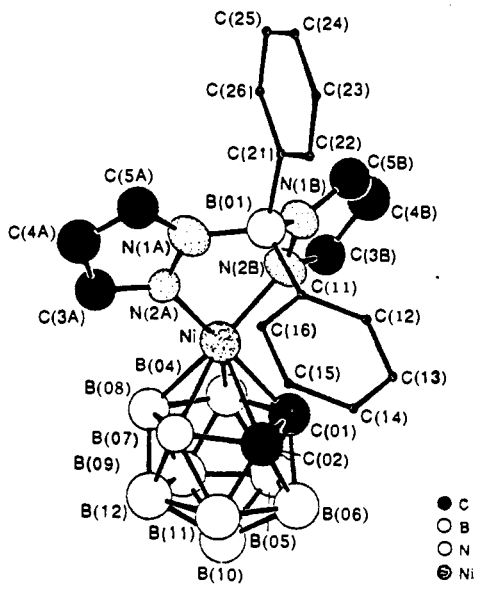

Figure 29. Structure of [*closo*-3-(η^2-$Ph_2B(pz)_2$)-3,1,2-$NiC_2B_9H_{11}$] without the hydrogen atoms. Reprinted from ref 105. Copyright 1990 American Chemical Society.

2,3-$C_2B_4H_4]^{2-}$, with anhydrous $NiCl_2$ failed to produce the expected *closo*-nickelacarborane, instead undergoes a redox reaction to yield Ni^0 and closed-cage product 1,2-$(SiMe_3)_2$-1,2-$C_2B_4H_4$ which is the precursor for the "carbons-apart" dianion. In contrast, a *commo*-nickel complex could be isolated from the reaction of the carbons apart dianion with $NiCl_2$ as shown in Scheme V.[104] The crystal structure of this Ni(IV) sandwich,[104] shown in Figure 28, unambiguously confirms its "carbons apart" geometry with the Ni atom approximately centered over the C_2B_3 face. A ligand exchange reaction between *closo*-3,3-$(PhMe_2P)_2$-3,1,2-$NiC_2B_9H_{11}$ and $[Me_4N][Ph_2B(pz)_2]$ in THF has also been studied. The crystal structure of the product [3-(η^2-$Ph_2B(pz)_2$)-3,1,2-$NiC_2B_9H_{11}$][Me_4N], shown in Figure 29,[105] reveals that the six-membered $Ni(N_2)_2B$ ring adopts a boat conformation. The anion shows no distortions from idealized closo geometry as measured by the slip parameter Δ in contrast to the metallacarborane

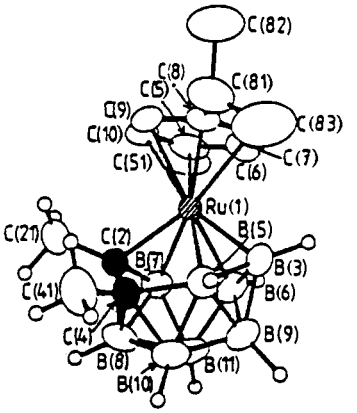

Figure 30. Molecular structure of [1-(η^6-MeC_6H_4-*i*-Pr)-2,4-Me_2-1,2,4-$RuC_2B_8H_8$]. Reprinted from ref 111. Copyright 1987 American Chemical Society.

complexes of other d^8 metals with dicarbollide ligands.[106] Nevertheless, it exhibits an unusual distortion in that the phenyl group of $[Ph_2B(pz)_2]^-$ ligand interacts with the hydrogen atom at C(2) atom of the C_2B_3 face and consequently, the Ni–C(2) interatomic distance is lengthened to 2.26 Å as compared to Ni–C(1) distance of 2.04 Å. Similarly, the isomeric products of a rhodium complex, *closo*-3-(η^3-$HB(pz)_3$)-3,1,2-$RhC_2B_9H_{11}$ were also prepared by the same authors and have been structurally characterized.[105]

The molecular geometries of some 9-, 10-, and 11-vertex metallacarboranes that contain no other heteroatoms are central to the discussion because they do not obey the electron-counting rules.[107,108] Consequently, there was an open question whether these complexes are indeed closo or so-called "isocloso" species. Without the X-ray data, it has been said that the 11-vertex metallacarboranes such as $CpCoC_2B_8H_{10}$, [$(PPh_3)_2HIrC_2B_8H_{10}$], and [$(C_6H_6)RuC_2B_8H_{10}$],[109,110] *obey* the Williams–Wade rules because their skeletal electron counts are straightforward and they are presumed to have simple closo deltahedral geometries.[6,7] However, these proposed closo deltahedral geometries have been contradicted by the X-ray structure of [1-(η^6-MeC_6H_4-*i*-Pr)-2,4-Me_2-1,2,4-$RuC_2B_8H_8$] (see Figure 30) that unambiguously exhibits a quadrilateral open face,[111] and hence it exemplifies the limitation of the skeletal electron-counting rules of Williams and Wade. This compound was prepared in 30% yield from the reaction between [$(MeC_6H_4$-*i*-Pr)$RuCl_2]_2$ and *nido*-$Me_2C_2B_8H_{10}$. The crystal structure shows that the RuC_2B_8 cluster is considerably distorted from the idealized closo geometry. The Ru(1)···C(4) distance of 2.683 Å is approaching nonbonding compared to Ru(1)–C(2) distance of 2.124 Å. As such an open face involving Ru(1), C(2), C(4), B(5) atoms is formed. The Ru(1)–B(5) bond is also longer (2.363 Å compared to 2.29 Å). This type of structure has been previously reported for isonido 10-vertex iridacarborane [$(PPh_3)(Ph_2PC_6H_4)$-$IrB_8H_7C(OH)$].[112,113] These authors have also studied an interesting rotational fluxionality in [1,1-$(PMe_2Ph)_2$-1,2,3-$PtC_2B_8H_9X$] complexes that is accompanied by a flexing of the 10-vertex η^6-{$C_2B_8H_9X$} moiety between extreme nido and arachno 10-vertex geometries.[114] The crystal structure of the 11-vertex platinacarborane (where X = H) is shown in Figure 31. The $(R_3P)_2Pt$ unit is bonded to a six-membered open face of the carborane ligand to form a closo geometry. These results demonstrate that the minor variation in cluster

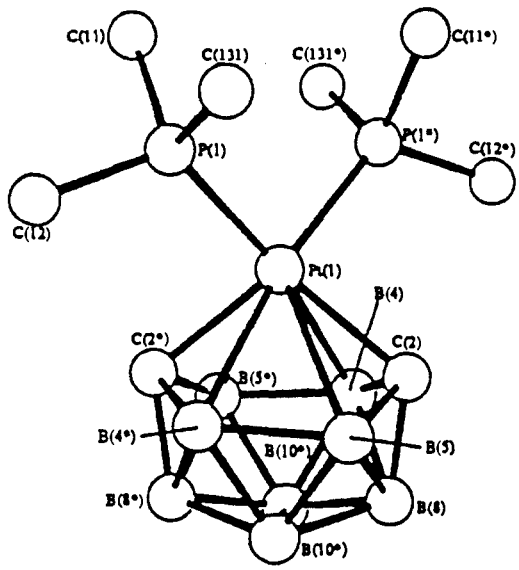

Figure 31. The structure of $[1,1\text{-}(PMe_2Ph)_2\text{-}1,2,3\text{-}PtC_2B_8H_{10}]$. Reprinted from ref 114. Copyright 1991 American Chemical Society.

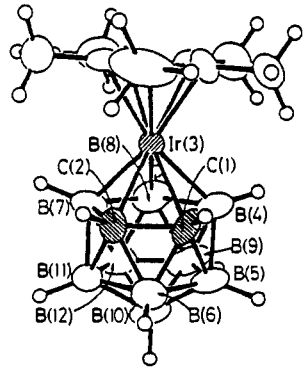

Figure 32. Molecular structure of $[3\text{-}(\eta^5\text{-}C_5Me_5)\text{-}3,1,2\text{-}IrC_2B_9H_{11}]$. Reprinted from ref 115. Copyright 1990 Royal Society of Chemistry.

substitutions can induce an overall change in the geometries of the molecules.[114] The rhodium and iridium compounds of the type $[3\text{-}(\eta^5\text{-}C_5Me_5)\text{-}3,1,2\text{-}MC_2B_9H_{11}]$ (where M = Rh, Ir) have been prepared recently according to eq 4.[115]

$$^1/_2[\{M(\eta^5\text{-}Cp^*)Cl_2\}_2] + Cs[C_2B_9H_{12}] + tmnd \rightarrow [(\eta^5\text{-}Cp^*)MC_2B_9H_{11}] + [Htmnd]Cl + CsCl$$

tmnd = *N,N,N′,N′*-tetramethylnaphthalene-1,8-diamine (4)

Since both complexes are isostructural, only the crystal structure of the iridium species, $[3\text{-}(\eta^5\text{-}C_5Me_5)\text{-}3,1,2\text{-}IrC_2B_9H_{11}]$, is shown here (see Figure 32). Despite the similarity between the two structures, the distortion of the MC_2B_9 cage is slightly greater in the rhodacarborane complex.[115] The smaller magnitude of the distortion in these complexes is particularly noteworthy when compared to the open quadrilateral face in the 11-vertex ruthenium complex $[1\text{-}(\eta^6\text{-}MeC_6H_4\text{-}i\text{-}Pr)\text{-}2,4\text{-}Me_2\text{-}1,2,4\text{-}RuC_2B_8H_8]$ described previously.[116] A comparison of the patterns in the NMR spectra of these metallacarboranes with those of *closo*-$1,2\text{-}C_2B_{10}H_{12}$, *nido*-$7,8\text{-}C_2B_9H_{13}$, and $[nido\text{-}C_2B_9H_{12}]^-$ anion suggests that shielding similarities apparently exist between the anionic $[nido\text{-}C_2B_9H_{12}]^-$ fragment and the metallacarborane rather than between the neutral species.[115]

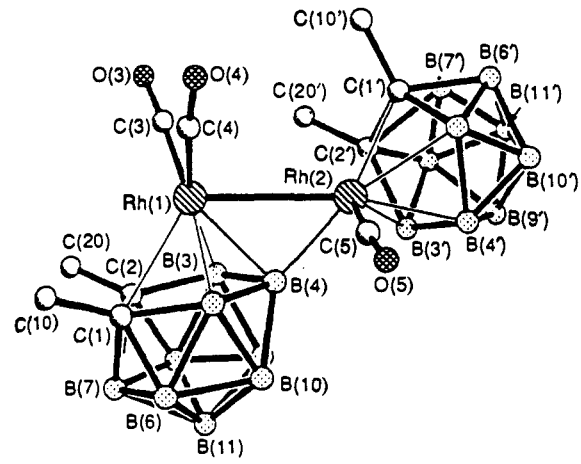

Figure 33. The structure of the anion $[Rh_2(\mu\text{-}\sigma\text{:}\eta^5\text{-}C_2B_9H_8Me_2)(CO)_3(\eta^5\text{-}C_2B_9H_9Me_2)]^-$. Reprinted from ref 117. Copyright 1991 Royal Society of Chemistry.

Nonetheless, the controversy still remains in the overall classification of these complexes with respect to closo or nido geometries.[6,7]

Stone and co-workers have explored the reactivity of anionic rhodacarboranes in the preparation of polynuclear clusters with metal–metal bonds.[116-119] The work reported prior to 1991 has been recently reviewed by Stone.[45] The rhodacarboranes of the type $[NEt_4]\text{-}[Rh(CO)_{2-x}(PPh_3)_x(\eta^5\text{-}C_2B_9H_9R_2)]$ (where $x = 0$ or 1; R = H or Me) have been used to prepare compounds with Rh–Rh, Rh–Re, Rh–Cu, Rh–Au, and Rh–Pt bonds. The crystal structures of these complexes show different roles of the carborane cages such as a spectator ion in $[RhPt\{\sigma\text{-}C(C_6H_4Me\text{-}4)\text{=}C(C_6H_4Me\text{-}4)H\}(CO)\text{-}(PEt_3)(PPh_3)(\eta^5\text{-}C_2B_9H_{11})]$ cluster,[116] a bridging ligand via B–H–M bonds in complexes $[CoRh(CO)_2(PPh_3)(\eta\text{-}C_4Me_4)(\eta^5\text{-}C_2B_9H_{11})]$ and $[Rh_2(CO)_2(PPh_3)_2(\eta^5\text{-}C_2B_9\text{-}H_{11})]$[120] or a linking group with the B–Rh σ bond as seen in $[NEt_4][Rh_2(\mu\text{-}\sigma\text{:}\eta^5\text{-}C_2B_9H_8Me_2)(CO)_3(\eta^5\text{-}C_2B_9\text{-}H_9Me_2)$.[117] The crystal structure of $[NEt_4][Rh_2(\mu\text{-}\sigma\text{:}\eta^5\text{-}C_2B_9H_8Me_2)(CO)_3(\eta^5\text{-}C_2B_9H_9Me_2)$, shown in Figure 33, reveals that the Rh–Rh distance of 2.876 Å is significantly longer than that in $[Rh_2(CO)_2(PPh_3)_2(\eta^5\text{-}C_2B_9H_{11})]$ (2.692 Å)[120] and $[Rh_2(PPh_3)_2(\eta^5\text{-}C_2B_9H_{11})_2]$ (2.763 Å).[121] While the unique boron bridges the Rh–Rh bond with the distances of about 2.05–2.15 Å, the $Rh\text{–}C_{(cage)}$ bonds seem to be longer (2.21–2.44 Å). As a result of the $B_{(unique)}$ bridge, Rh(2) carries only one CO ligand.[117]

The mononuclear rhoda and iridacarboranes have produced some interesting metallacycles. In general, these cycloaddition reactions involved alkynes or aryl nitrile *N*-oxides and the selective *closo*-metallacarborane. The resulting metallacycles were isolated in good yields, and were characterized thoroughly including single-crystal X-ray diffraction studies.[122,123] In all the structures, no change in the geometry of the MC_2B_9 (M = Rh, Ir) cluster was observed.

The *closo*-osmacarborane, $1\text{-}Os(CO)_3\text{-}2,3\text{-}(SiMe_3)_2\text{-}2,3\text{-}C_2B_4H_4$, was prepared by the reaction of $Os_3(CO)_{12}$ with *nido*-$2,3\text{-}(SiMe_3)_2C_2B_4H_6$.[124] A pentagonal-bipyramidal geometry was assigned on the basis of multinuclear NMR spectra. The same compound was also obtained by heating the metal carbonyl with *closo*-$1\text{-}Sn\text{-}2,3\text{-}(SiMe_3)_2C_2B_4H_4$.[124] Supraicosahedral metallacarboranes of Pd and Ir incorporating $[C_2B_{10}H_{12}]^{2-}$ ligand and an icosahedral platinacarborane of the C_2B_9

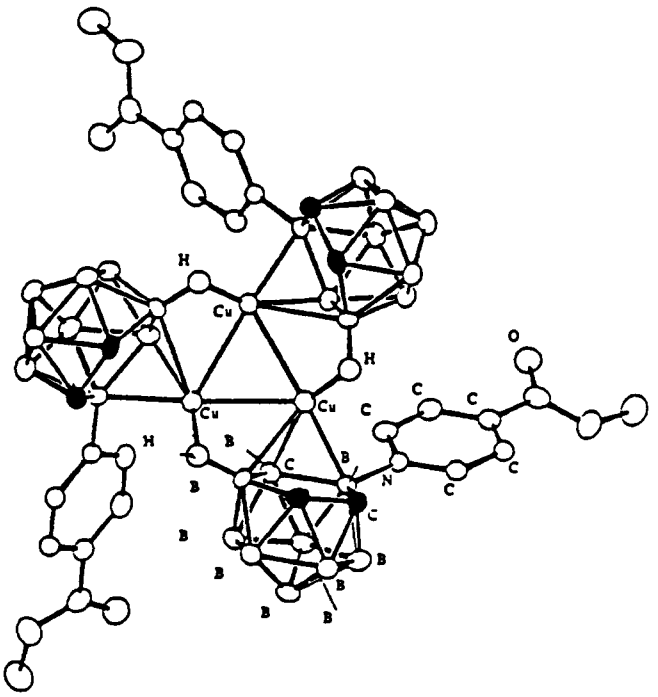

Figure 34. The crystal structure of $[Cu_3(\mu\text{-}H)_3\{C_2B_9H_9(4\text{-}(C_5H_4N)CO_2CH_3)\}_3]$. Reprinted from ref 89. Copyright 1988 American Chemical Society.

system have been reported.[125] The reaction of $[MCl_2(dppe)]$ (where M = Pd, Pt; dppe = (diphenylphosphino)ethane) with $Na_2(C_2B_{10}H_{12})$ or $Tl_3(C_2B_9H_{12})O$ gave the corresponding closo species $[(dppe)PdC_2B_{10}H_{12}]$ or $[(dppe)PtC_2B_9H_{11}]$. When petroleum ether/methanol solvent mixture was employed with the iridium reagent, the reaction yielded an unexpected product $[(PPh_3)_2HIrC_2B_{10}H_{11}(OMe)]$, whose crystal structure shows that the methoxy group is bonded to the unique boron (between the two cage carbons) of the six-membered bonding face.[125]

The mononuclear, PPN[*closo*-3-(PPh_3)-3,1,2-$CuC_2B_9H_{11}$] and dinuclear [*closo-exo*-4,8-$\{(\mu\text{-}H)_2Cu(PPh_3)\}$-3-$(PPh_3)$-3,1,2-$CuC_2B_9H_9$] copper complexes were prepared by the reaction of thallium salt of the dicarbollide ion with Cu^ICl in the presence of (PPN)Cl. On the other hand, when Cu^ICl is employed along with PPh_3, either the mononuclear [*closo*-3-(PPh_3)-4-(4-(C_5H_4N)-$CO_2CH_3)$-3,1,2-$CuC_2B_9H_{10}$] or the trinuclear [*nido*-$Cu_3(\mu\text{-}H)_3\{C_2B_9H_9$-(4-$(C_5H_4N)CO_2CH_3)\}_3$] cluster can be produced depending upon the concentration of the PPh_3 ligand.[89] The structures of these mononuclear and trinuclear cupracarborane clusters were confirmed by X-ray crystallography. The structure of [*nido*-$Cu_3(\mu\text{-}H)_3\{C_2B_9H_9(4\text{-}(C_5H_4N)CO_2CH_3)\}_3$] is shown in Figure 34. This cluster contains three $[CuC_2B_9H_{10}(4\text{-}(C_5H_4N)\text{-}CO_2CH_3)]$ units, which are linked by both Cu–H–B and Cu–Cu interactions about a crystallographic 3-fold axis that makes an interesting "pinwheel" ligand array around an equilateral Cu_3 core. The structure can also be viewed as a cluster consisting of three equilateral triangles of Cu_3, H_3, and B_3 atoms that are associated with the three Cu–H–B bridge bonds. The Cu–Cu distance of 2.52 Å is relatively short compared to that in known Cu_3 triangles (2.75–3.61 Å).[126,127]

The crystal structure of an unusual mercury complex of the $[C_2B_{10}H_{10}]^{2-}$ ligand system was reported recently by Hawthorne and co-workers.[128] Although the mercury atom in the complex is not an integral part the cage

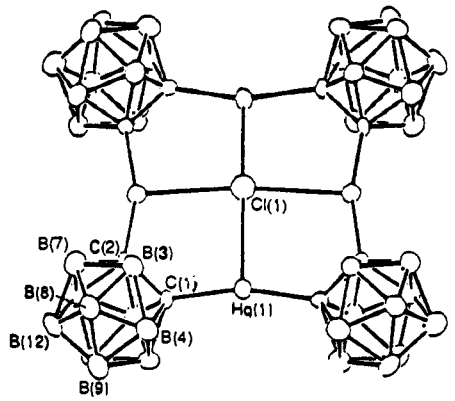

Figure 35. The crystal structure of an unusual mercury complex. Reprinted from ref 128. Copyright 1991 VCH Publishers.

framework, it has demonstrated an unusual bonding mode in the solid state so as to form a [12]crown-4-macrocycle analogue. Therefore, our discussion on this complex is limited to the structural aspect only. The crystal structure of this complex (Figure 35) consists of four divalent carborane cages linked by four Hg atoms in a cyclic tetramer with a Cl ion located in the center (Hg–Cl = 2.944 Å). The Hg–Cl bonds are shorter than the sum of their van der Waals radii. Each Hg atom links carbon atoms of two carborane cages with distances of about 2.080–2.105 Å (av C–Hg–C = 162°).

It is apparent from the above discussions that the synthetic, structural, bonding, and reactivity patterns have made the area of middle and late transition metal containing metallacarborane complexes as one of the forefrontiers of organometallic chemistry.

C. Linked-Cage and Multidecker Complexes

The synthesis of new materials having novel electronic, optical and conducting properties is of current interest. An approach to these materials is systematically linking the small sandwich units to form an extended multidecker sandwich system. Immediately following the discovery of the triple-decker structure of the type $Cp_3Ni_2^+$,[129] Grimes and co-workers were able to synthesize the first neutral triple-decker sandwich of a metallacarborane system in the early 1970's.[130] Since then, the research in this field has been dominated by the work of Grimes that has demonstrated how small metallacarboranes can be stacked and then linked systematically. Recent reviews by Grimes[3a,131-133] and Siebert[134-136] have adequately described the latest developments in this area of research. Therefore, our discussions in this section will cover only those results that need to be updated.

An effective procedure for the removal of apical BH units in metallacarboranes has been the treatment of a metallacarborane with TMEDA and H_2O or methanol at elevated temperatures.[137-140] A reaction such as the one that involved methanol and $[\eta^6\text{-}C_6H_5\text{-}(CH_2)_3FeC_2B_4H_5]$ produced the corresponding *nido*-$(\eta^6\text{-}1\text{-}[C_6H_5(CH_2)_3Fe[2\text{-}C\text{-}3\text{-}(CH)B_3H_5]$ incorporating two B–H–B bridge hydrogens to give the neutrality to the molecule.[138] As in previously developed methodology, removal of these bridge H's with appropriate reagents affords the key anionic intermediates to construct a number of desired multidecker species systematically.[131,137,139,141,142] Scheme VI illustrates the

Scheme VI. Reaction Pathways for the Formation of Multidecker Sandwich Complexes

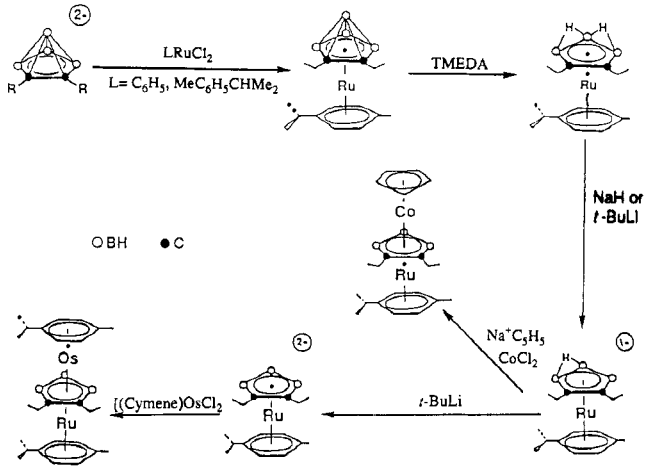

synthesis of a particular class of triple-decker sandwiches, although a more general synthetic description, that can be applied to other stacked systems as well, can be found in ref 3a. Consequently, the synthesis of a red triple-decker complex, $[(\eta^5\text{-}C_9H_7)Fe(Et_2C_2B_4H_4)NiCp^*]$, was accomplished by removing an indenyl H in the presence of BuLi from $(\eta^6\text{-}C_9H_8)Fe^{II}(Et_2C_2B_4H_4)$, followed by the addition of $NiBr_2$ and $[Cp^*]^-$ at −78 °C.[143] The crystal structure of this complex, shown in Figure 36, exhibits an 8-vertex $FeNiC_2B_4$ cluster in which the nickel atom, cage carbon atoms, and one boron atom each occupy 4-coordinate sites, while the iron and the remaining borons reside in 5-coordinate vertices. Although the geometries of $Fe(\eta^5\text{-}C_9H_7)$ and $Ni(\eta^5\text{-}Cp^*)$ units are unexceptional, the arrangement of the metal atoms with respect to the carborane ligand is such that the overall geometry of the complex can be viewed as a bent triple-decker sandwich.[143]

A linkage of two metallacarboranes can also be accomplished by using a bridging organic ligand along with the anionic carborane ligand and a metal reagent. Such an approach was employed by Sneddon and coworkers in the preparation of a linked metallacarborane complex $CH_2[closo\text{-}1\text{-}(\eta\text{-}C_5H_4)Co(2,3\text{-}Et_2C_2B_4H_4)]_2$ from $[nido\text{-}2,3\text{-}Et_2C_2B_4H_5]^-$ anion with $CoCl_2$ and $CH_2(C_5H_5)_2^{2-}$ dianion, that included an additional oxidative workup.[144a] The crystal structure of this complex, shown in Figure 37, exhibits two *closo*-1-(η-C_5H_4)Co(2,3-$Et_2C_2B_4H_4$) metallacarborane fragments joined by a cyclopentadienyl-bridging methylene group. The crystallographic parameters (see Table I) of the complex are similar to those observed in *closo*-1-(η-C_5H_5)Co(2,3-$Me_2C_2B_4H_4$).[144b] The structural features are interesting in that while both the carborane and Cp ligands eclipse one another, the *closo*-cobaltacarboranes make a 90° angle between them with the closest intermolecular H···H contacts of 2.75 Å [$H_{B(5)}$···$H_{Cp(2')}$].[144a]

A similar linked metallacarborane of the type $\{[(Et_2C_2B_4H_4)FeH(C_5Me_4)]_2C_6H_4\}$ has been synthesized from the reaction of $[nido\text{-}Et_2C_2B_4H_5]^-$ anion with the stoichiometric quantities of $[1,4\text{-}(C_5Me_4)_2C_6H_4]^{2-}$ dianion and $FeCl_2$ in THF.[145] The crystal structure of this diamagnetic complex shows the tilting of the central phenylene ring by about 55° relative to the cyclopentadienyl planes (see Figure 38). The location of the metal-bound hydrogen (1.63 Å) is such that it could be considered as bridging the central Fe atom and two

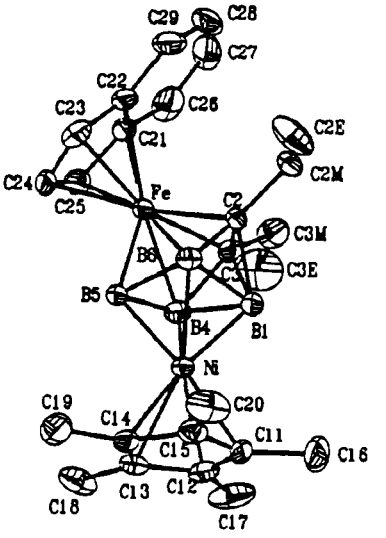

Figure 36. Molecular structure of $[(\eta^5\text{-}C_9H_7)Fe(Et_2C_2B_4H_4)NiCp^*]$ without the hydrogen atoms. Reprinted from ref 143. Copyright 1991 American Chemical Society.

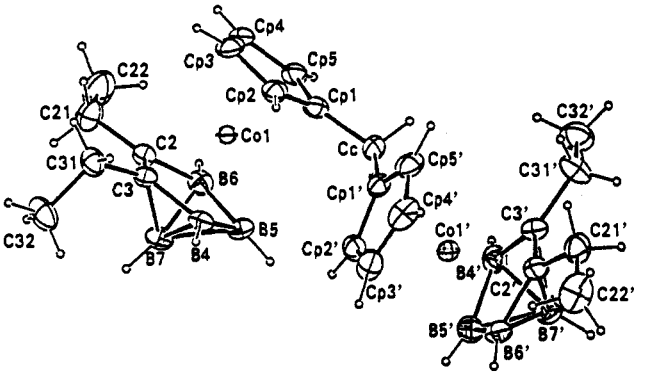

Figure 37. Molecular structure of $CH_2[closo\text{-}1\text{-}(\eta\text{-}C_5H_4)Co(2,3\text{-}Et_2C_2B_4H_4)]_2$. Reprinted from ref 144a. Copyright 1991 American Chemical Society.

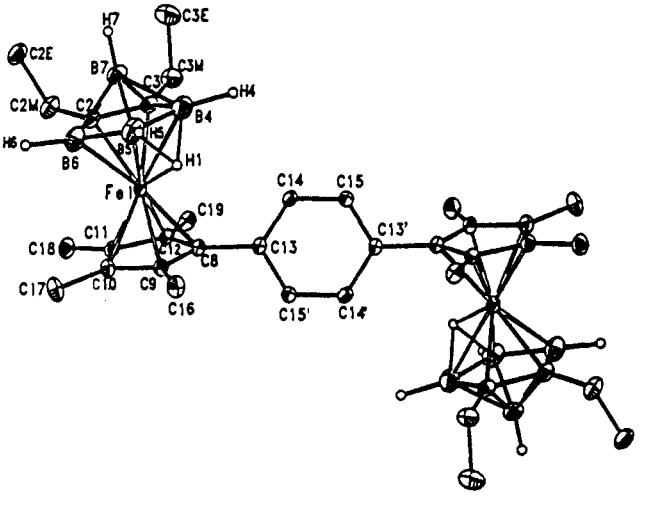

Figure 38. An ORTEP drawing of $\{[(Et_2C_2B_4H_4)FeH(C_5Me_4)]_2C_6H_4\}$. Reprinted from ref 145. Copyright 1992 American Chemical Society.

neighboring boron atoms (ca. 1.45 Å). Consequently, the distances of the metal to these boron atoms are longer than to the other (2.213–2.262 Å vs. 2.140 Å).[145] The tilting of the Cp ring (6.6°) in the complex is in the opposite direction of that observed in the analogous linked Co species, $[(Et_2C_2B_4H_4)Co(C_5Me_4)]_2C_6H_4$ (7.2°),[142] described in ref 3a. The linked diiron species also undergoes irreversible oxidation followed by a

reversible signal. However, the irreversible reduction generated a number of new and unidentified species.[145]

Most recently, a number of C- and B-substituted double- and triple-decker sandwich complexes of Co have been prepared and thoroughly characterized.[146] Initially, the precursor, $Cp^*Co(Me_2C_2B_4H_4)$, was converted to the corresponding B–Me-substituted species, $Cp^*Co(Me_2C_2B_3Me_3H_2)$, in a number of steps involving decapitation by wet TMEDA and repeated deprotonations with butyllithium, followed by the reactions with methyl iodide. The crystal structure revealed that this intermediate complex is a decapitated mixed-ligand and staggered sandwich as in $(Cp^*_2Co)^+$.[147] The shorter metal to carborane ring centroid distance, compared to that in the metallocene analogue (1.54 Å vs. 1.68 Å), demonstrates the stronger bonding capability of the carborane ligand than the cyclopentadienide as previously demonstrated.[8] The synthetic utility of this complex as well as the corresponding $C_{(cage)}$–H or –$SiMe_3$–substituted analogues has been demonstrated further in the preparation of a number of triple-decker sandwiches, $[Cp^*Co(R,R'\text{-}C_2B_3R''_3)Cp^*Co]$ (R,R',R'' = H, Me, or $SiMe_3$).[146]

The results to date indicate that the area of linked cage and multidecker sandwich complexes is still in its developing stage, and more advanced research needs to be done to find their applications, in an absolutely practical sense, as new materials in electronic industries. Nonetheless, the above results give every indication that this area of research will dominate the frontiers of organometallics for the next several decades.

D. Complexes of Arene and $C_8H_8^{2-}$ Ligands

During the last decade there has been an upsurge in the syntheses and characterizations of (π-arene)metallacarborane complexes, partly because of their utility in the preparation of multidecker clusters. Bicyclic or polycyclic arenes, coordinated to the transition metals, allow the construction of arene-bridged oligomers and polymers. Again, a recent article of Chemical Reviews described the latest developments in this area and, therefore, only the most recent results will be given here.[3a,131]

There have been some reports on unusual syntheses and structures of d-block metallacarboranes incorporating both arene and small or large carborane ligands. In reactions of small carborane ligand of the type $[Et_2C_2B_4H_5]^-$ with $C_8H_8^{2-}$ anion and MCl_3 in THF, oxidation products such as $(\eta^8\text{-}C_8H_8)M^{IV}(Et_2C_2B_4H_4)$ could be obtained in good yields when M = Ti or V. A similar reaction with chromium reagent resulted in the formation of a tropylium complex $(\eta^7\text{-}C_7H_7)\text{-}Cr^{III}(Et_2C_2B_4H_4)$ that could be the decomposition product of the expected $(\eta^8\text{-}C_8H_8)Cr^{IV}(Et_2C_2B_4H_4)$ sandwich.[43] Although all three complexes are air stable in the solid state, the V and Cr species show remarkable stability toward O_2 in solution. It has also been shown that the B-substituted mono- and diiodo derivatives of the Ti complex can be made and, therefore, these derivatives could serve as valuable precursors to multidecker sandwich complexes.[43] The crystal structures of these mixed-ligand complexes show closo 7-vertex pentagonal MC_2B_4 clusters in which the metal bonds to a planar $(C_8H_8)^{2-}$ or $(C_7H_7)^-$ ligand (Figures 39–41).[43] Although metal to arene distances do not vary signif-

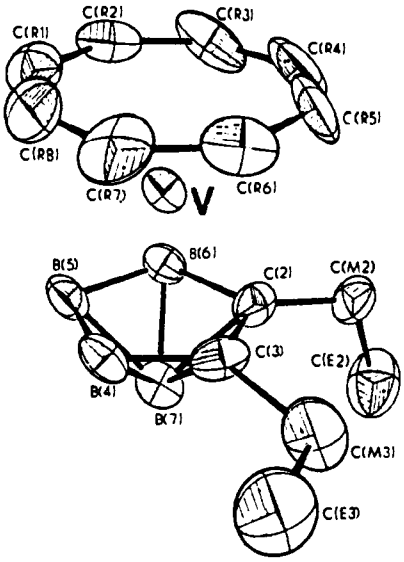

Figure 39. Molecular structure of $(\eta^8\text{-}C_8H_8)V(Et_2C_2B_4H_4)$. Reprinted from ref 43. Copyright 1984 American Chemical Society.

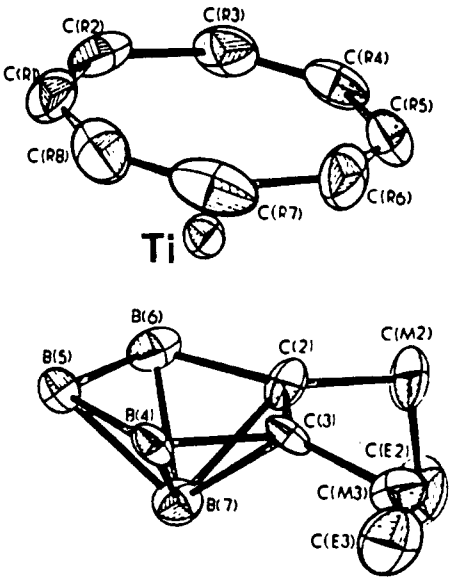

Figure 40. Molecular structure of $(\eta^8\text{-}C_8H_8)Ti(Et_2C_2B_4H_4)$. Reprinted from ref 43. Copyright 1984 American Chemical Society.

icantly, the shorter metal–(C_2B_3 centroid) distance in the structure of the vanadium complex (1.830 Å, see Figure 39), when compared to that in the titanium analogue (1.916 Å, see Figure 40) is consistent with the decrease in covalent radius of the metals going from group 4 to group 5. The magnetic susceptibility and ESR data of the paramagnetic vanadium sandwich are indicative of the formal +4 oxidation state of the metal. The room temperature solution ESR spectrum gave a g value of 1.94 with a vanadium hyperfine coupling ($\langle A \rangle$ = 155 G), but no ligand hyperfine splitting could be observed due to V–boron interactions.[43] The crystal structure of the chromium sandwich also shows essentially symmetric bonding of the metal with respect to both ligands with a dihedral angle of 2.76°.[43] Indeed, this work has demonstrated that such mixed-ligand systems can also stabilize the formal +4 oxidation state of the metals as in the purely carborane-based dianionic ligand systems.

Although the formation of [*closo*-3-(η^6-C_6H_6)-3,1,2-$FeC_2B_9H_{11}$] was reported previously in the literature,

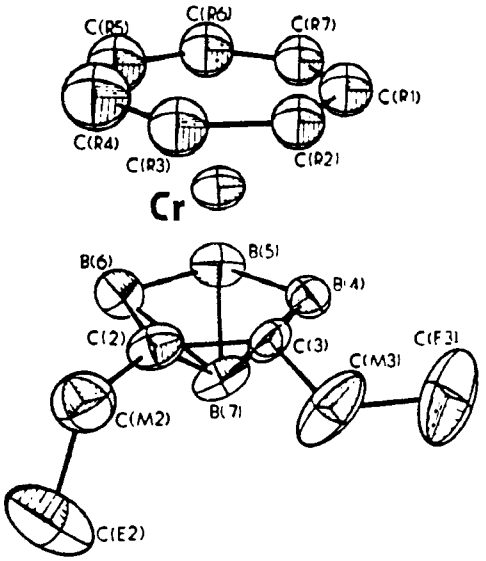

Figure 41. Molecular structure of $(\eta^7\text{-}C_7H_7)Cr(Et_2C_2B_4H_4)$. Reprinted from ref 43. Copyright 1984 American Chemical Society.

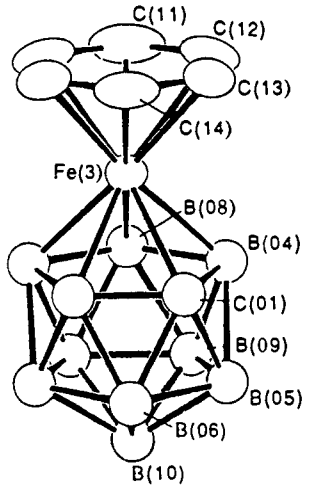

Figure 42. Molecular structure of [*closo*-3-(η^6-C_6H_6)-3,1,2-$FeC_2B_9H_{11}$]. Reprinted from ref 77. Copyright 1990 Elsevier Sequoia.

attempts to isolate this mixed-ligand species have been unsuccessful.[78,148] However, a recent report describes the high-yield synthesis and isolation of this species involving the photolysis of *closo*-3,3,3-$(CO)_3$-3,1,2-$FeC_2B_9H_{11}$ in benzene.[77]

The crystal structure, shown in Figure 42, exhibits a parallel sandwich geometry in which the Fe atom coordinates essentially the planar η^6-benzene ring and the C_2B_3 face of a dicarbollide cage symmetrically with a dihedral angle of 2.1°. The metal to C_2B_3 and C_6H_6 centroid distances (1.487 and 1.571 Å) are unexceptional. Nonetheless, an interesting structural feature of the complex can be seen in the staggered conformations of the two ligands at the metal center.[77]

The Ru and Os sandwich complexes of mixed subicosahedral carborane and π-arene ligands can also be prepared by the controlled cage degradation of the corresponding icosahedral analogue. Such a reaction involving *closo*-3,1,2-(η^6-C_6H_6)$RuC_2B_9H_{11}$ gave the subicosahedral species, 1,2,4-(η^6-C_6H_6)$RuC_2B_8H_{10}$ and 2,5,6-(η^6-C_6H_6)$RuC_2B_7H_{11}$ in low yields.[149] A potential icosahedral osmium precursor, *closo*-3,1,2-(η^6-C_6H_6)$OsC_2B_9H_{11}$], was synthesized by the reaction of (η^6-C_6H_6)$OsCl_2$·$NCCH_3$ with Tl[3,1,2-$TlC_2B_9H_{11}$].[149] Although the structures of this Os complex and the RuC_2B_8 species have not been determined in the solid state, the crystal structure of 2,5,6-(η^6-C_6H_6)$RuC_2B_7H_{11}$ (see Figure 43) shows that the metal is not located on the six-membered open face, but occupies one of the lower ring vertices adjacent to the cage carbons. The average Ru–$C_{(cage)}$, Ru–$C_{(arene)}$, and Ru–B distances (2.15, 2.22, and 2.19 Å) are well within the range of those observed for (η^6-C_6H_6)Ru^{II} complexes[111]. Thus, the structure represents a 24-electron, 10-membered *nido*-ruthenacarborane, similar to that of decaborane, and provides important information on the mechanism of the cluster degradation in metallacarborane systems.[149]

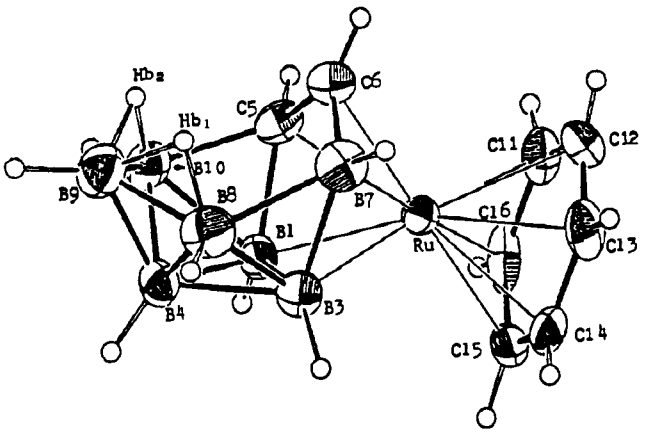

Figure 43. The crystal structure of 2,5,6-(η^6-C_6H_6)$RuC_2B_7H_{11}$. Reprinted from ref 149. Copyright 1985 American Chemical Society.

The electrochemical properties of a number of mixed-ligand metal complexes of the type (η^6-arene)M(η^5-$Et_2C_2B_4H_4$) (where M = Fe, Ru) have been reported recently by Grimes and co-workers.[150] The η^6-arene–Fe^{II} species undergoes one oxidation and one reduction process, resulting in corresponding Fe^{III} and Fe^{I} complexes (eq 5). The electrolytic oxidation of (C_6Me_6)-

$$[(\eta^6\text{-}C_6H_6)Fe(Et_2C_2B_4H_4)]^+ \leftrightarrow [(\eta^6\text{-}C_6H_6)Fe(Et_2C_2B_4H_4)] \leftrightarrow [(\eta^6\text{-}C_6H_6)Fe(Et_2C_2B_4H_4)]^- \quad (5)$$

$Fe(Et_2C_2B_4H_4)$ resulted in a green-brown solution displaying a strong ESR signal with g values 2.486 and 2.002 which are assigned to d^5, Fe^{III} complex $[(C_6Me_6)\cdot Fe(Et_2C_2B_4H_4)]^+$.[150] The Ru complex also undergoes one-electron oxidation, but, unlike Fe, the oxidation product is unstable and no reduction was observed. Overall, this study clearly indicates that a carborane ligand such as $[R_2C_2B_4H_4]^{2-}$ dianion imparts a significant thermodynamic and kinetic stabilization to Fe^{III} and Ru^{III} complexes unlike the Cp analogues.[150]

The fluxional cluster isomerization in 10-vertex *closo*-2,1,6-ruthena- and -rhodacarboranes was studied in detail and the crystal structure of [2-(η^6-C_6Me_6)-*closo*-2,1,6-$RuC_2B_7H_9$] was determined by Greenwood and co-workers.[151] The Ru–C(1) distance of 2.05 Å is significantly shorter than the Ru–C(6) distance of 2.19 Å, while the Ru–B distances are in the normal range. A number of 18-electron rhodacarboranes of the type [*closo*-3,3-(η^2,η^3-$C_7H_7CH_2$)-1,2-R^1R^2-3,1,2-$RhC_2B_9H_9$] and [*closo*-2,2-(η^2,η^3-$C_7H_7CH_2$)-2,1,7-$RhC_2B_9H_9$] (where R^1

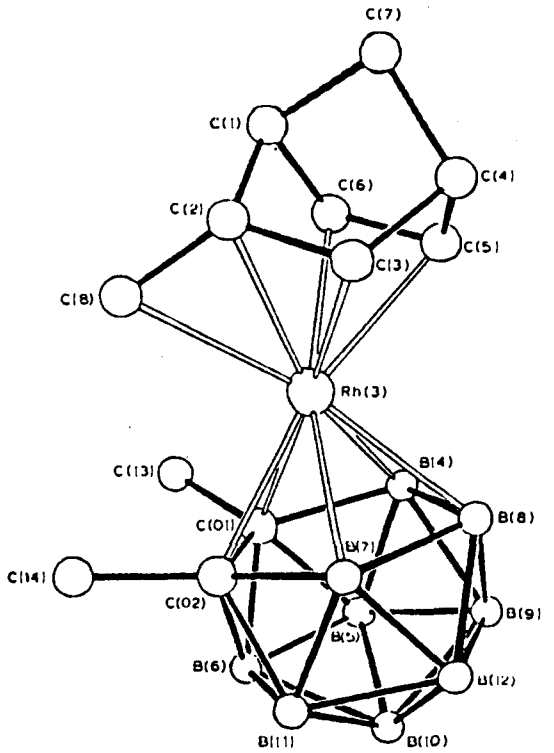

Figure 44. The molecular structure of the 18-electron rhodacarborane, *closo*-3,3-(η^2,η^3-$C_7H_7CH_2$)-1,2-Me_2-3,1,2-$RhC_2B_9H_9$. Reprinted from ref 152. Copyright 1988 Elsevier Sequoia.

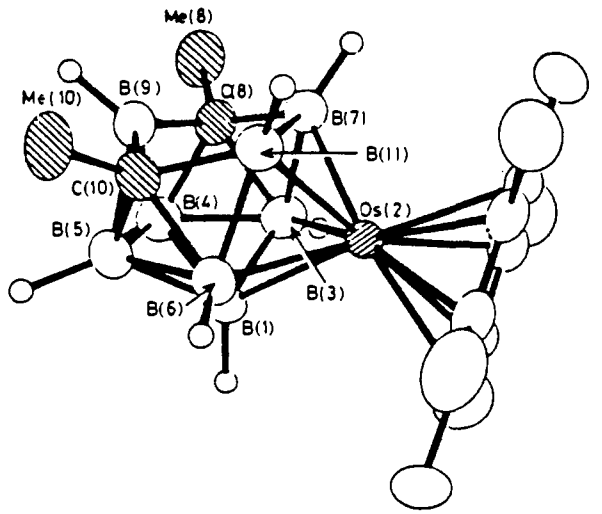

Figure 45. Molecular structure of the osmacarborane [2-(η^6-C_6Me_6)-8,10-$(Me)_2$-*nido*-2,8,10-$OsC_2B_8H_8$]. Reprinted from ref 153. Copyright 1987 Royal Society of Chemistry.

= R^2 = H, Me or Ph) have been prepared by the reaction of {2-(hydroxymethyl)norbornadiene}(acetylacetonato)-rhodium with mono- and disubstituted dicarbollide anions, followed by the acidification of the product with HPF_6.[152] The crystal structure of one of the mixed-ligand species, [*closo*-3,3-(η^2,η^3-$C_7H_7CH_2$)-1,2-Me_2-3,1,2-$RhC_2B_9H_9$], shown in Figure 44, reveals that the Rh–C^+(8) distance (2.354 Å) is considerably longer than the other Rh–C(norbornadienyl ligand) bonds (2.139–2.247 Å).[152]

An orange, air-stable, mixed-ligand species of the Os metal, [2-(η^6-C_6Me_6)-8,10-$(Me)_2$-*nido*-2,8,10-$OsC_2B_8H_8$] has been prepared quantitatively by thermal rearrangement of its so-called closo precursor, [1-(η^6-C_6Me_6)-2,4-$(Me)_2$-1,2,4-$OsC_2B_8H_8$] at 400 °C for 14 min.[153] Unlike the "slipped" platinacarboranes, the crystal structure (see Figure 45) of the complex unambiguously shows a five-membered open face without the Os metal (BCBCB), resembling that of the "26-electron" [*nido*-$B_{11}H_{14}$]$^-$ anion.[154] The average Os–B and Os–C(arene*) distances are 2.175 and 2.26 Å, respectively. This work clearly demonstrates that the electron-counting rules should be supported by the crystallographically determined structures before predictions on the geometries of such complexes are made.[6,7]

Clearly, the advances in this area have already reached a stage beyond the structural and bonding curiosities. The practical applications of monomeric species are being developed. Indeed, Grimes' elegant discovery of the utility of π-arene–metallacarboranes as basic building blocks in the construction of multidecker species (discussed in the previous section and elsewhere[3a]) has given a new dimension to this area of metalla-C_2B_4 carborane chemistry, and as such a major breakthrough could be envisioned in these and other π-arene–metallacarborane systems.

E. Complexes of Mono-, Tri-, and Tetracarbon Carborane Ligands

In contrast to the vast number of metal complexes based on dicarbon–carborane ligand systems, the mono-, tri-, and tetracarbon containing metallacarboranes are relatively less explored area of organometallic chemistry. This is partly due to unavailability of their ligand precursors readily, and in many instances the carbon and other heteroatoms, such as N, P, S, Se, etc., are inserted along with the metal substrates simultaneously into polyhedral borane clusters.[3a,71,84] Exceptions are the tetracarbametallaboranes which are prepared directly from the reaction of metal reagents with the dianionic $[R_4C_4B_8H_8]^{2-}$ ligand, produced from the corresponding neutral nido precursor, $R_4C_4B_8H_8$.[74] Nevertheless, the metal complexes of these systems represent a relatively young class of metallacarborane chemistry that has been developing slowly over the past 20 years or so, and the literature up to 1987 has been reviewed previously.[155] Therefore, we will discuss only those reports that appeared after 1987.

The C-substituted monocarba carborane ligand 9-$(CH_3)_2S$-7-[$(Me_3Si)_2CH$]-7-$CB_{10}H_{11}$, prepared from decaborane and $Me_3SiC{\equiv}CSiMe_3$ in the presence of Me_2S,[156] was reacted with [(η-Cp)Ni(CO)]$_2$ or [(η-Cp)$Co(CO)_2$] in refluxing toluene or mesitylene to synthesize {2-(η-Cp)-1-[$(Me_3Si)_2CH$]-2,1-$NiCB_{10}H_{10}$} or 7-Me_2S-2-(η-Cp)-1-[$(Me_3Si)_2CH$]-2,1-$CoCB_{10}H_{10}$} in very low yields.[157] On the other hand, the metal atom synthesis involving this monocarbaborane with Co and toluene produced, in poor yields, the corresponding *closo*-monocarbacobaltaborane {2-(η^6-$C_6H_5CH_3$)-1-[$(Me_3Si)_2CH$]-2,1-$CoCB_{10}H_{10}$} as an air-stable solid. The crystal structures of the Ni and Co mixed-ligand sandwich species have been determined, and only that of the Co complex is shown in Figure 46.[157] The Co–C distance of 2.14 Å, although similar to that in the structure of (η^6-$C_6H_5CH_3$)$Co(C_6F_5)_2$,[158] is slightly longer than the average Co–B distance of 2.07 Å, thus showing a distorted MCB_{10} cage. Consequently, the planes of the carborane and toluene ligands are tilted with respect to each other by about 7.6°. Perhaps, this tilting may purely be the result of steric crowding caused by the

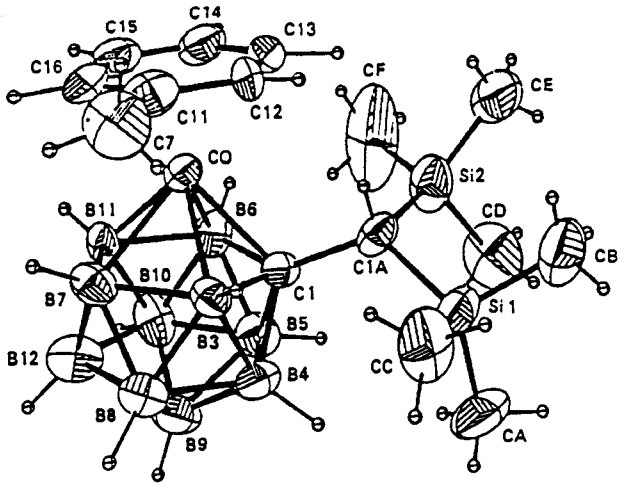

Figure 46. Crystal structure of {2-(η^6-$C_6H_5CH_3$)-1-[$(Me_3Si)_2CH$]-2,1-$CoCB_{10}H_{10}$}. Reprinted from ref 157. Copyright 1988 American Chemical Society.

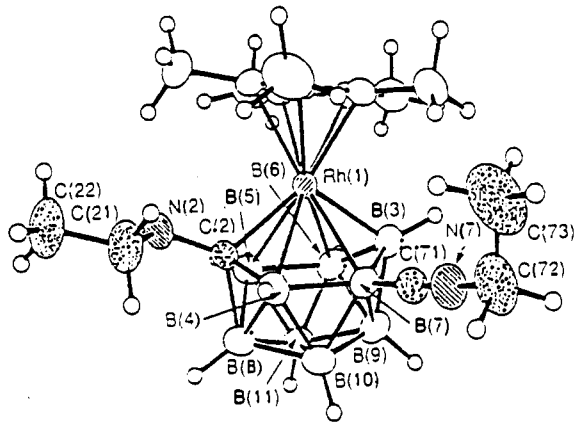

Figure 47. Molecular structure of the rhodacarborane 1-(η^5-C_5Me_5)-2-(NHEt)-7-(CNEt)-*closo*-1,2-$RhCB_9H_9$. Reprinted from ref 159. Copyright 1990 Royal Society of Chemistry.

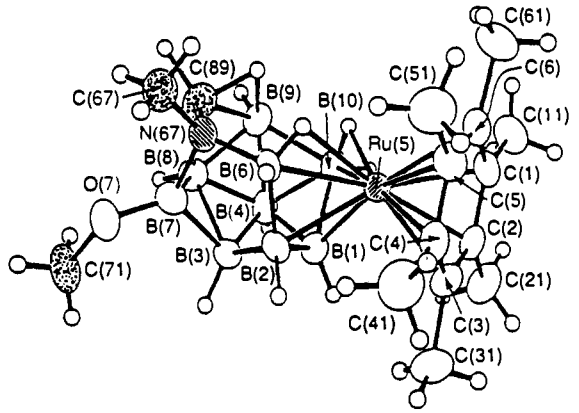

Figure 48. Molecular structure of the ruthenacarborane 5-(η^5-C_6Me_6)-7-(OMe)-*arachno*-5-RuN(Me)C(H)B_9H_{11}. Reprinted from ref 159. Copyright 1990 Royal Society of Chemistry.

$(Me_3Si)_2CH$ and the η^6-toluene units near the metal center.[157]

An insertion of C-atom into a metallaborane cluster could be accomplished as in the reaction involving 6-(η^5-C_5Me_5)-*nido*-6-RhB_9H_{13} or 6-(η^6-C_6Me_6)-8-(OMe)-*nido*-6-RuB_9H_{12} and RNC (R = Et, Me) that produced the corresponding C-inserted and both C- and B-substituted metallaborane derivative 1-(η^5-C_5Me_5)-2-(NHR)-7-(CNR)-*closo*-1,2-$RhCB_9H_9$ or both CN-inserted and B-substituted unusual and unpredicted 5-(η^6-C_6Me_6)-

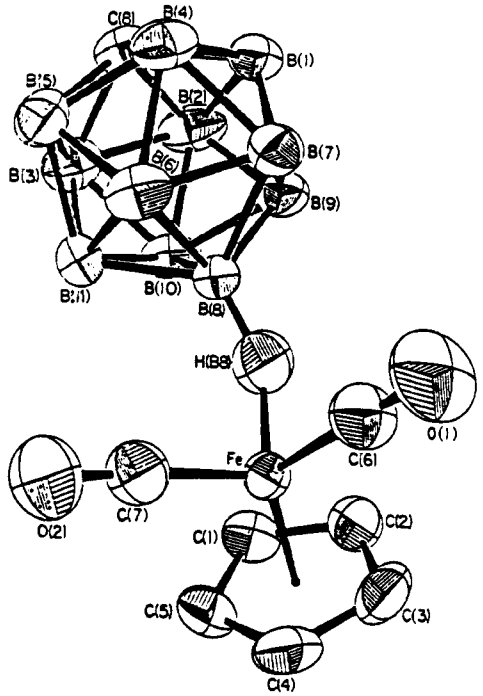

Figure 49. Molecular structure of $Fe(Cp)(CO)_2(B_{11}CH_{12})$. Reprinted from ref 160. Copyright 1989 American Chemical Society.

7-(OMe)-*arachno*-5-RuN(R)C(H)B_9H_{11} in low yields.[159] The crystal structures of these complexes are shown in Figures 47 and 48. The rhodacarborane adopts an 11-vertex closo geometry, whereas the ruthenacarborane exhibits a unique 12-vertex $RuNCB_9$ cluster that has four-membered BBCN, five-membered BBBCN, and six-membered RuBBBCN open faces. The bond angles and lengths are unexceptional (Rh–B 2.121–2.461 Å and Ru–B 2.221–2.352 Å).[159] This is one of the prime examples of serendipity that exists in such insertion reactions.

The role of monocarbaborane anion $[CB_{11}H_{12}]^-$ as the least coordinating ligand to the metal substrates has been explored by Reed and co-workers in recent years. This property of the ligand has been further demonstrated by preparing exopolyhedrally linked Fe and Ir complexes from the reaction of argentacarboranes with the corresponding Fe or Ir salt as in eq 6.[160–162] The

$$Fe(Cp)(CO)_2I + Ag(CB_{11}H_{12}) \rightarrow Fe(Cp)(CO)_2IAg(CB_{11}H_{12}) \rightarrow Fe(Cp)(CO)_2(CB_{11}H_{12}) + AgI \quad (6)$$

crystal structure of $Fe(Cp)(CO)_2(B_{11}CH_{12})$ (Figure 49) shows that the monocarbaborane anion is coordinated to iron via an Fe–H–B bridge with an angle of 141°.[160] The Fe–H distance of 1.56 Å is significantly shorter than 1.82 Å found in iron(III) porphyrinate complex, $[Fe(TPP)(B_{11}CH_{12})]$,[162] but is similar to those of "soft" ferracarboranes (1.56–1.61 Å).[163] The crystal structure of the argentacarborane precursor, $AgB_{11}CH_{12}\cdot 2C_6H_6$, shows that the silver is η^1-coordinated to a benzene molecule (2.400 Å), while the second benzene molecule is present outside the coordination sphere even though identical C–C distances could be found in both rings (see Figure 50).[164] The two Ag-H distances (1.97 Å) arise from the interaction of the silver with one $B–H_{(terminal)}$ bond of each cage resulting in a dimer in

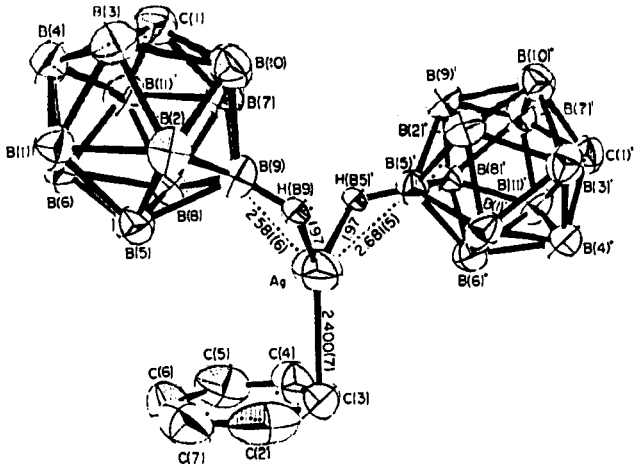

Figure 50. An ORTEP diagram of an argentamonocarbaborane. Reprinted from ref 164. Copyright 1986 American Chemical Society.

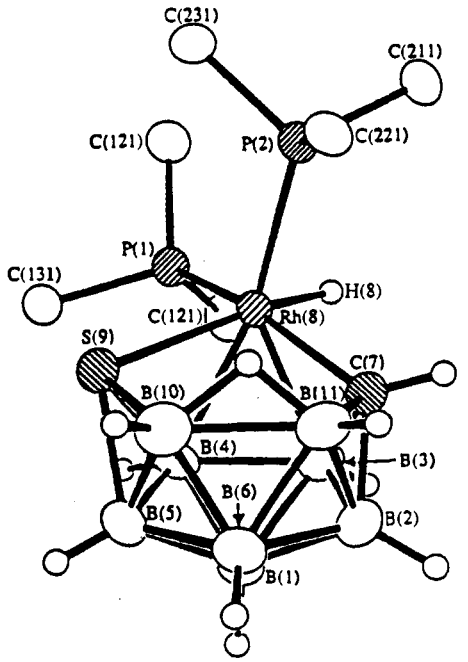

Figure 51. Molecular structure of *nido*-8,8-(PPh$_3$)-8-H-8,7,9-RhCSB$_8$H$_{10}$. Reprinted from ref 165. Copyright 1992 American Chemical Society.

which the monocarbaborane cage acts as a bridging ligand to give an alternating cation–anion chain. The bonding of Ag to two monoanionic polyhedral cages and to one arene ligand make the formal coordination number three for the metal. Although this structure represented the first example of a silver–hydrogen bonding, since then, more structures exhibiting such bonds have emerged from the same research group.[161]

A polyhedral metal complex that incorporates S, C, and Rh atoms as cluster vertices and simultaneously obeying the Williams and Wade's electron-counting rules, *nido*-8,8-(PPh$_3$)$_2$-8-H-8,7,9-RhCSB$_6$H$_{10}$, has been synthesized, in high-yield, from the reaction between *arachno*-6,9-CSB$_8$H$_{12}$ and RhCl(PPh$_3$)$_3$ in basic ethanol.[165] The X-ray diffraction analysis revealed the complex to be an open nido 11-vertex RhCSB$_8$ cluster (see Figure 51) with the Rh–S, Rh–C, and Rh–B distances of 2.447, 2.175, and 2.212 Å, respectively.[165] The thermolysis of this rhodathiamonocarbaborane species results in the formation of *closo*-1,1-(PPh$_3$)$_2$-1,1-RhCSB$_8$H$_9$ quantitatively, whose crystal structure

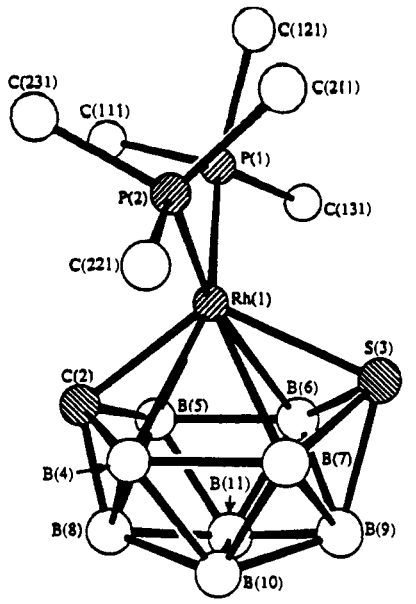

Figure 52. The crystal structure of a rhodathiamonocarbaborane. Reprinted from ref 165. Copyright 1992 American Chemical Society.

exhibits a closo deltahedral 11-vertex RhCSB$_8$ cluster (Rh–C = 2.11 Å, Rh–S = 2.34 Å, and Rh–B = 2.32–2.46 Å) that also follows the Wadian skeletal-electron counts (see Figure 52).[165]

Metallacarboranes derived from tricarbon carboranes have not been explored in great detail with the exception of Siebert's work on diborolene.[134–136] The low-yield syntheses of the tricarbaboranes restricted their synthetic utility in the production of the corresponding metallatricarbaborane complexes.[166,167] The most recent report from Sneddon's group on the improved and high-yield (ca. 80%) synthesis of the monoanionic ligand [6-CH$_3$-5,6,8-C$_3$B$_7$H$_9$]$^-$ and its subsequent conversion to a neutral precursor, *nido*-6-CH$_3$-5,6,9-C$_3$B$_7$H$_{10}$, has given hope for the rapid development of this area of metallacarborane chemistry.[168] The improved method has facilitated the high-yield syntheses of tricarbametallaborane complexes of Mn, Fe, Co, and Ni metals such as [*commo*-M(1-M-2-CH$_3$-2,3,5-C$_3$B$_7$H$_9$)$_2$] (where M = Fe or Co), [1-M′-2-CH$_3$-2,3,4-C$_3$B$_7$H$_9$] (where M′ = (Cp)Fe or Mn(CO)$_3$) and [9-(Cp)Ni-8-CH$_3$-7,8,10-C$_3$B$_7$H$_9$].[168–170] The complexes were isolated by chromatography and were fully characterized including the X-ray diffraction studies. The crystal structures of the representative tricarbaborane complexes of iron and cobalt, [*closo*-1-(η^5-C$_5$H$_5$)Fe-4-CH$_3$-2,3,4-C$_3$B$_7$H$_9$], [*commo*-Fe(1-Fe-5-CH$_3$-2,3,5-C$_3$B$_7$H$_9$)(1-Fe-4-CH$_3$-2,3,4-C$_3$B$_7$H$_9$], and [*commo*-Co(1-Co-2-CH$_3$-2,3,5-C$_3$B$_7$H$_9$)$_2$], are shown in Figures 53–55. In the former complex, the iron atom is sandwiched between cyclopentadienyl and tricarbaborane monoanions, while in the other two species, the metal is sandwiched by the two tricarbaborane ligands. In these structures, the metal atom bonds more strongly to the two 4-coordinate C atoms than to the third one as evident in the M–C distances [Fe-C(2,3) = 1.977 Å vs Fe–C(4) = 2.265 Å; Co–C(2,3) = 2.029 Å vs Co–C(5) = 2.655 Å]. Consequently, the metallatricarbaborane clusters are significantly distorted and create open four-membered MCCB and five-membered MCCBC puckered faces, in Fe and Co complexes, respectively.[168,169] In the same report, the cluster rearrangements in 11-vertex ferra- and cobaltatricarbaborane complexes resulted in methyl group

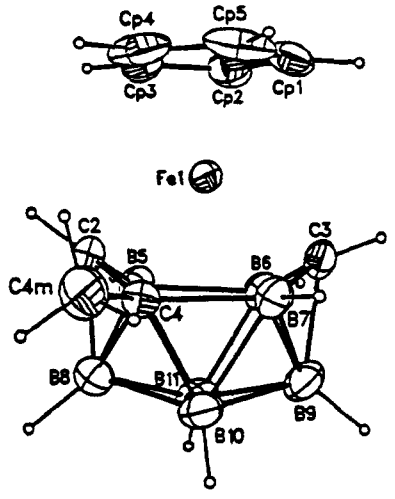

Figure 53. Molecular structure of 1-(η^5-C_5H_5)Fe-4-CH_3-2,3,4-$C_3B_7H_9$. Reprinted from ref 168. Copyright 1992 American Chemical Society.

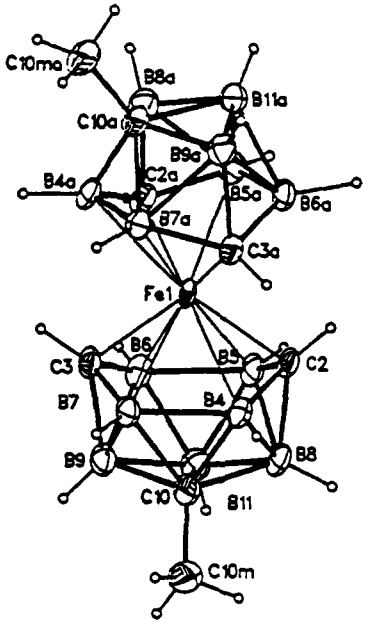

Figure 54. Molecular structure of *commo*-Fe(1-Fe-1-CH_3-2,3,10-$C_3B_7H_9)_2$. Reprinted from ref 169. Copyright 1992 American Chemical Society.

migrations from the four-coordinate carbon to the adjacent five-coordinate carbon at elevated temperatures. Isotope labeling studies[170] show that these reactions occur by means of cage-carbon skeletal rearrangements, rather than direct methyl migrations, thus resembling the mechanism observed in a metallocene (Cp_2Mo) system.[171]

Metal atom synthesis has also been employed in the preparation of four-carbon-containing mixed-ligand metal sandwich species 1-(η^6-C_6Me_6)Fe-4,5,7,8-Me_4-$C_4B_3H_3$ and 2-(η^6-MeC_6H_5)Fe-6,7,9,10-$Me_4C_4B_5H_5$ which were prepared from the reactions involving thermally generated iron atoms with pentaborane, toluene, and 2-butyne.[172] The crystal structures show open arachno and nido geometries with Fe atoms occupying the five-coordinate apical and basal vertices, respectively.[172] On the other hand, the conventional method involving the mixed dicarba- and tetracarbaborane anions, or just the tetracarbaborane anion such as $[Et_4C_4B_8H_8]^-$, with MCl_2 has produced more or less the corresponding targeted metal derivatives. Evidently, a number of Fe

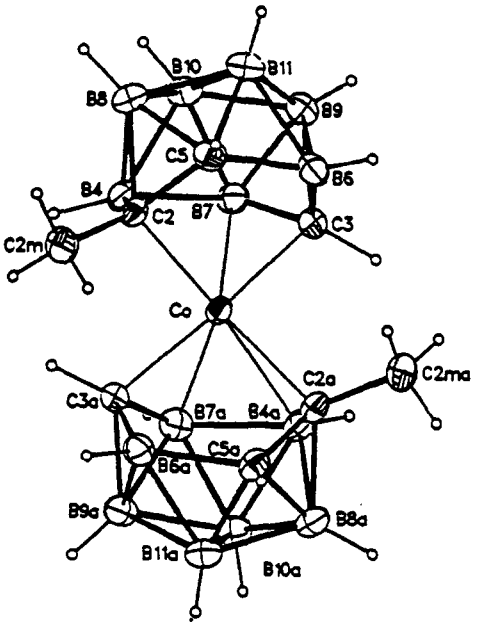

Figure 55. Molecular structure of *commo*-Co(1-Co-2-CH_3-2,3,5-$C_3B_7H_9)_2$. Reprinted from ref 169. Copyright 1992 American Chemical Society.

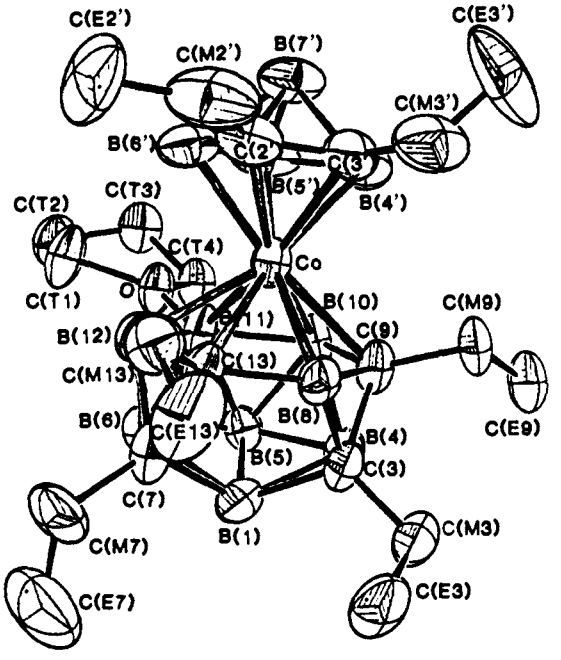

Figure 56. The crystal structure of an iron sandwich complex based on C_2B_4 and C_4B_8 carborane ligand systems. Reprinted from ref 173. Copyright 1985 American Chemical Society.

and Co complexes of a C_4B_8 ligand system has been synthesized.[173,174] The crystal structure of (Et_2-$C_2B_4H_4$)Co($Et_4C_4B_8H_7OC_4H_8$), shows the fusion between slightly distorted 7-vertex CoC_2B_4 cage (Co–C = 2.15 Å, Co–B = 2.11 Å) and the 13-vertex CoC_4B_8 cluster (Co–C = 2.23 Å, Co–B = 2.17 Å) with a pentagonal BCCBC open face away from the central metal atom (see Figure 56).[173] The 13-vertex *nido*-CoC_4B_8 cluster is formally derived from a closo 14-vertex cage (bicapped hexagonal antiprism) by removal of an equatorial vertex that makes the carbon atoms on the five-membered open face as low-coordinate ones as in the analogous Ni complex, $(Ph_2PCH_2)_2NiMe_4C_4B_8H_8$.[175] Nevertheless, the skeletal electron count in the molecule is consistent with the Williams–Wade rules.[6,7]

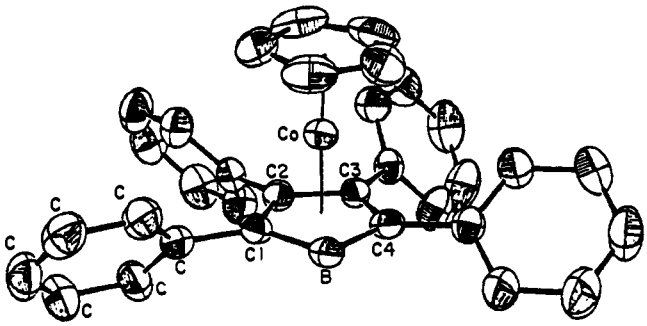

Figure 57. The solid-state structure of ($CpCoC_4Ph_4BH$). Reprinted from ref 176. Copyright 1989 American Chemical Society.

Scheme VII. Proposed Mechanism for the Insertion of a BH Unit into $Cp(PPh_3)Co(CPh)_4$ (Reprinted from ref 176. Copyright 1989 American Chemical Society)

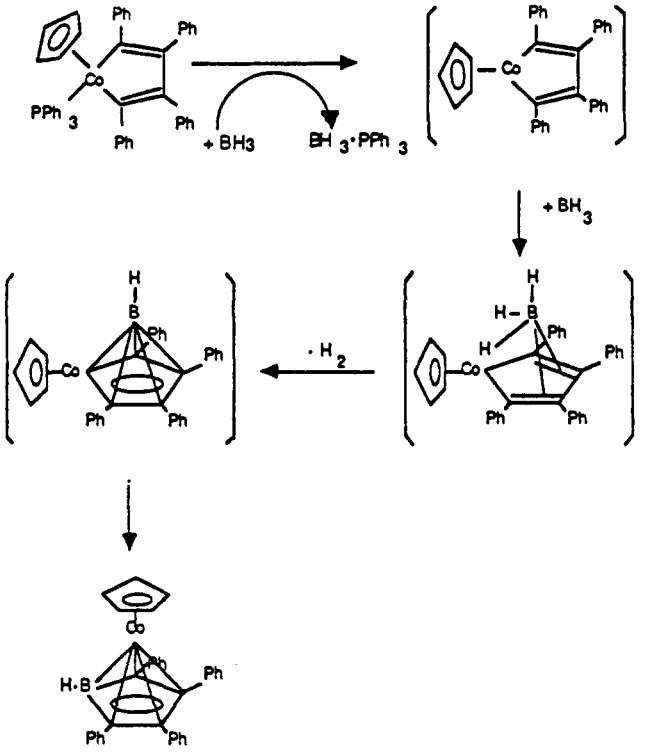

Preparation of several borabenzene complexes have been accomplished via insertion of a BH unit in an organometallic π-complex.[136] The methodology has now been extended to the metallacarborane chemistry. A cobalt sandwich compound, ($CpCoC_4Ph_4BH$) was prepared by reacting $Cp(PPh_3)Co[CPh]_4$ with BH_3·THF as shown in Scheme VII.[176] The crystal structure of this complex (Figure 57) reveals that the CpCo fragment is in the apical position, and the B–H fragment is in a basal position of the CoC_4B nido cluster core. The Co–B distance of 2.147 Å is significantly longer than the average cobalt distances to the C_4B ring carbons (2.045 Å). The Cp and BC_4 rings are coplanar and the boron atom is slightly below the plane defined by the cage carbons.[176]

The results to date indicate that the patterns of reactivity are slowly emerging in the tricarbametallaborane systems and, to some extent, in the species containing four-carbon atoms as well. Nevertheless, the future investigations in this area hold the promise of being every bit as fascinating as the previous ones.

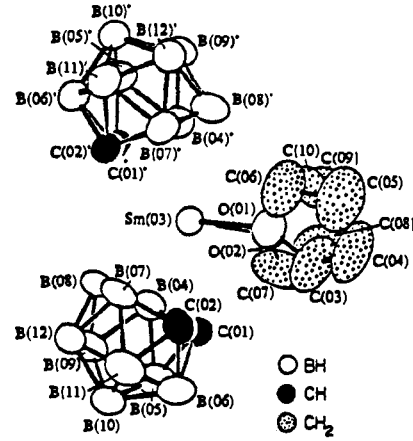

Figure 58. Molecular structure of [3,3-$(THF)_2$-*commo*-3,3′-$Sm(3,1,2\text{-}SmC_2B_9H_{11})_2$. Reprinted from ref 180. Copyright 1988 American Chemical Society.

III. Metallacarboranes of f-Block Elements

During the last decade or so, the chemistry of lanthanide elements has taken a new direction since it is no longer limited to the formation of purely ionic compounds. In fact, new classes of complexes, unusual structures, and novel reactivity patterns have emerged with the elements of lanthanides and a lanthanide congener, yttrium.[25,28,177] Although a variety of ligands has been established in organolanthanide systems, the cyclopentadienide anion and its C-substituted derivatives have been widely utilized.[178] The chemistry of lanthanide complexes of C_2B_{10}, C_2B_9, and C_2B_4 carborane ligand systems have just begun to be explored.

Consequently, Hawthorne and co-workers have prepared a number of lanthanacarboranes during the past four years or so from the reaction of Na salt of the dicarbollide dianion with LnI_2 (Ln = Yb or Sm) in THF and further oxidation of the immediate closo species with the thallacarborane salt [PPN][*closo*-3,1,2-$TlC_2B_9H_{11}$)]. The resulting half-sandwich and sandwich complexes of the general formulas [*closo*-$Ln^{II}(C_2B_9H_{11})\cdot(THF)_4$] and [PPN][*commo*-$Ln^{III}(C_2B_9H_{11})_2\cdot(THF)_2$], respectively, were obtained in good yields.[179,180]

The weak coordination of the THF solvent to the metal was demonstrated by the substitution reactions with stronger bases such as MeCN and DMF. These novel lanthanacarboranes were fully characterized including NMR spectra, magnetic susceptibility, and X-ray diffraction. The crystal structures of the [PPN] salt of sandwich samaracarborane, [3,3-$(THF)_2$-*commo*-3,3′-$Sm(3,1,2\text{-}SmC_2B_9H_{11})_2$], and the half-sandwich ytterbacarborane, [$Yb(C_2B_9H_{11})(DMF)_4$], are shown in Figures 58 and 59.[179,180] The structures reveal that the metal is essentially centered over the planar pentagonal C_2B_3 face(s). The coordination sphere of the Yb metal is completed by bonding to four DMF molecules and one dicarbollide ligand with the average Yb–B distances of 2.74 Å. On the other hand, the geometry of the Sm sandwich can be described as a distorted tetrahedron with two carborane cages and two THF molecules. While the centroid–Sm–centroid angle of 131.9° is similar to that reported for Cp^*_2LnL derivatives (L = other ligand),[181] the Sm–centroid distances of 2.33 Å in the complex are significantly shorter than those (av 2.45 Å) of $Cp^*_2Sm(Cl)(THF)$ and [$Cp^*_2Sm(I)(THF)$],[182] thus confirming the tighter bonding of the lanthanide to the dicarbollide ligands than to the Cp* anions.

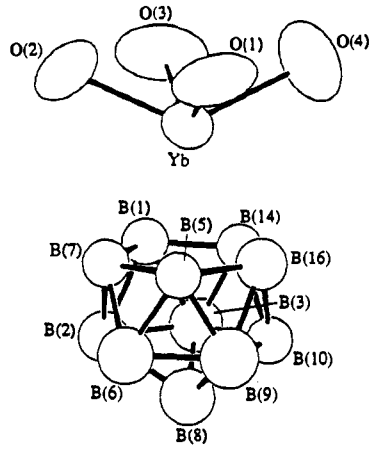

Figure 59. Molecular structure of $[Yb(C_2B_9H_{11})(DMF)_4]$. Reprinted from ref 180. Copyright 1988 American Chemical Society.

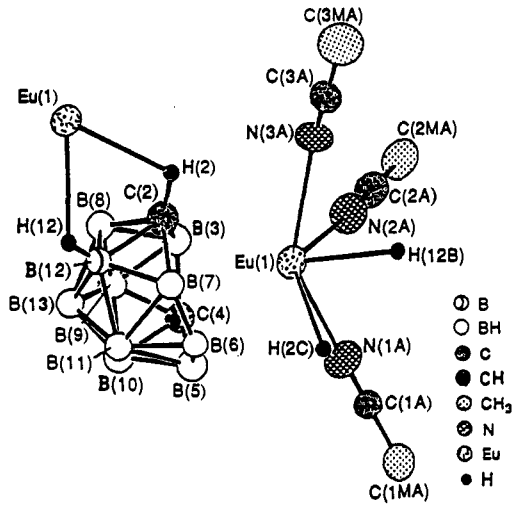

Figure 60. Structure of a polymeric Eu complex, [*closo*-1,1,1-$(MeCN)_3$-1,2,4-$EuC_2B_{10}H_{12}$]. Reprinted from ref 183. Copyright 1992 American Chemical Society.

The utility of $[C_2B_{10}H_{12}]^{2-}$ dianion in lanthanide chemistry has also been demonstrated in the synthesis of polymeric lanthanacarboranes of general formula, [*closo*·1,1,1·$(THF)_3$-1,2,4-Ln·$C_2B_{10}H_{12}]_\infty$, from the reaction of $LnI_2(THF)_2$ (where Ln = Sm, Eu) in THF.[183] When Ln = Eu, the reaction can be carried out further with 1 equiv of $Na_2[C_2B_{10}H_{12}]$ to produce the corresponding Eu sandwich, [1,1-$(THF)_2$·*commo*·1,1′-Eu(1,2,4-$EuC_2B_{10}H_{12})_2]^{2-}$ in 65% yield. Interestingly, this species can also be generated directly by the reaction of $EuCl_3$ with $Na_2[C_2B_{10}H_{12}]$.[183,184] The molecular structures of polymeric half-sandwich complex [*closo*·1,1,1-$(MeCN)_3$·1,2,4-$EuC_2B_{10}H_{12}]_\infty$ and the anionic sandwich [1,1·$(THF)_2$·*commo*-1,1′-Eu(1,2,4-Eu-$C_2B_{10}H_{12})_2]^{2-}$ are shown in Figures 60 and 61.[183,184] The crystal structure of the *closo*·europacarborane is composed of two crystallographically independent spiral chains with the carborane moieties serving each as a ligand for two europium atoms while bonding to one via both upper and lower belt so as to form Eu–H–E (where E = B or C) agostic structural arrangement (Eu–C = 3.04, Eu–B = 2.96, Eu–N = 2.678 Å).[183,184] The coordination sphere about each europium atom is completed by three acetonitrile ligands and the repeat of this arrangement gave a polymeric structure as in the strontium analogue.[185] The commo complex $[Et_4N]_2$[1,1·$(THF)_2$·*commo*-1,1′·Eu(1,2,4-EuC_2B_{10}·

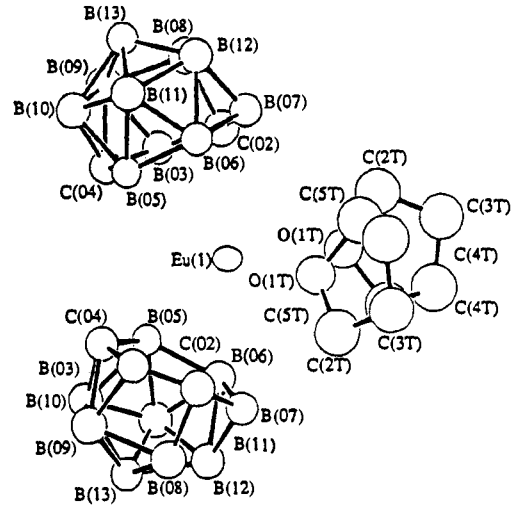

Figure 61. Molecular structure of an anionic europium sandwich complex [1,1-$(THF)_2$-*commo*-1,1′-Eu(1,2,4-$EuC_2B_{10}H_{12})_2]^{2-}$. Reprinted from ref 183. Copyright 1992 American Chemical Society.

$H_{12})_2$] (see Figure 61; Eu–C = 2.89 and 3.20 Å, Eu–B = 2.98, 2.99, 3.09 and >3.09 Å, Eu–O(THF) = 2.63 Å; centroid–Eu–centroid = 127.4°, centroid–Eu–O(THF) = 109.9 and 111.3°, O(THF)–Eu–O(THF) = 74.8°)[183,184] is isostructural with the Sm species shown in Figure 58.[179,180]

Despite the success in syntheses and structural characterizations of a number of half-sandwiched and sandwiched Sm^{II}, Sm^{III}, Yb^{II}, and Eu^{II} complexes of both C_2B_9 and C_2B_{10} carborane ligand systems, there have been no reports on the analogous species incorporating other lanthanide metals. The preliminary report on a gadolinacarborane failed to confirm its molecular geometry in the solid state.[186] The most recent report on the synthesis and crystal structure of a *closo*·gadolinium(III)–carborane cluster of the type {[η^5-1-Gd-2,3·$(SiMe_3)_2$-2,3-$C_2B_4H_4$]$_3$[$(\mu_2$-1-Li·2,3-$(SiMe_3)_2$-2,3-$C_2B_4H_4)_3(\mu_3$-OMe)][μ_2-Li-$(C_4H_8O)]_3(\mu_3$-O)} demonstrates that the Gd metal can also be incorporated as cluster vertices into carborane cages.[66] Since this complex is the first lanthanacarborane based on C_2B_4 carborane ligands, comparative reactivity and structural patterns are unavailable. In a reaction involving the THF-solvated Li_2[2,3-$(SiMe_3)_2C_2B_4H_4$] salt and anhydrous $GdCl_3$ in a molar ratio of 2:1 in dry benzene (C_6H_6), an unusual, trinuclear gadolinacarborane was produced in 58% yield. The crystal structure (Figure 62) shows that the molecule is constructed from six carborane cages, three solvated·THF molecules, three Gd atoms, and six Li atoms to form a tricapped trigonal prism with Gd atoms in the capping positions. The gadolinium metal in each *closo*-gadolinacarborane unit is η^5-bonded to the carborane face with Gd–cage atoms and Gd–centroid distances ranging from 2.71 to 2.80 Å and 2.38 to 2.4 Å, respectively. As expected, the metal–centroid distances in the complex are shorter than those in $(\eta^5$-$C_5H_5)_3Gd(THF)$,[187] [$(\eta^5$-$C_5H_5)_2$-Gd(Br)]$_2$,[188] {[$(\eta^5$-$C_5H_5)Gd]_5(\mu_2$-OMe)$_4(\mu_3$-OMe)$_4(\mu_5$-O)},[189] and in the polymeric complex [$(\eta^5$-$C_5H_5)_2$-Gd(Br)]$_\infty$.[188] While *closo*·gadolinacarboranes are bridged by both Li^+(THF) and *closo*·lithiacarborane moieties, in opposite directions, an O atom triply bridges the three Gd metals (av $Gd–O_{(central)}$ = 2.193 Å; $Gd–O_{(central)}$–Gd = 119.1°) slightly out of the Gd_3 triangular plane (0.22 Å). Since each of the six carborane ligands bears

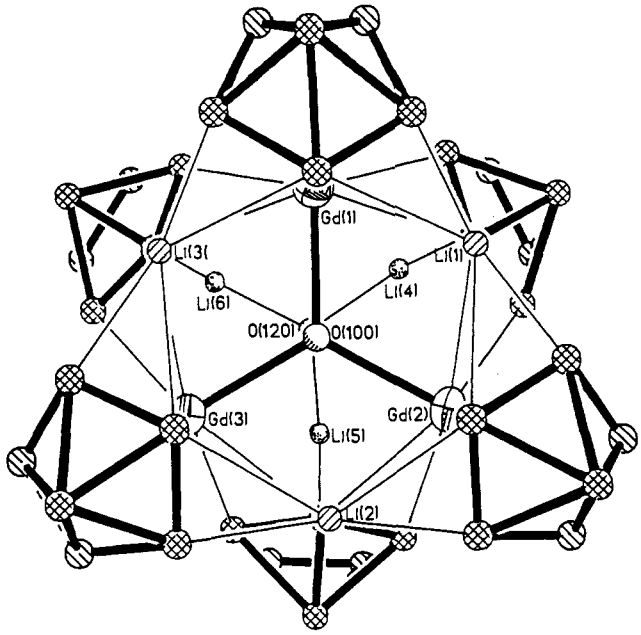

Figure 62. A perspective view (from above) showing the C_2B_4 cages and equilateral triangles of Gd and Li atoms in a trinuclear Gd complex. Reprinted from ref 66. Copyright 1992 VCH Publishers.

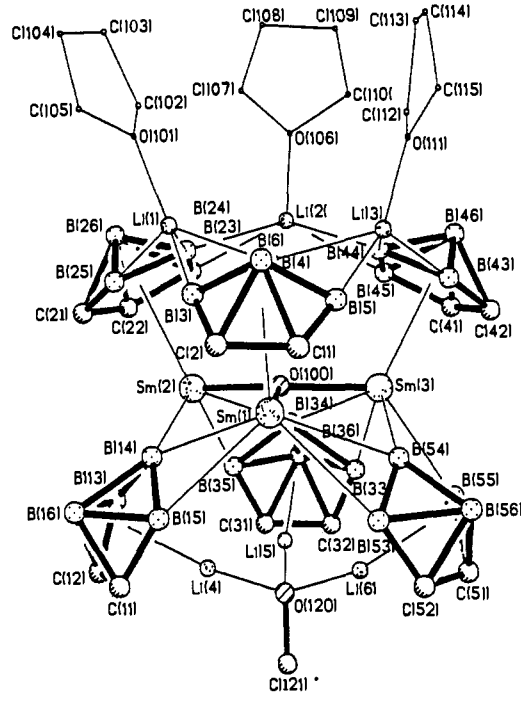

Figure 63. A perspective view of the isostructural trinuclear Sm(III) complex. Reprinted from ref 67.

a −2 charge and three Gd^{III} and six Li^{I} metals are present, for charge compensation an additional $(MeO)^-$ moiety is bound to the apical lithium atoms of the lower triangle of *closo*-lithiacarboranes in a tetrahedral fashion (av Li–O–Li = 106° and Li–O–C = 113°). The source of the methoxide ion was discovered during the syntheses of a number of isostructural lanthanacarborane complexes incorporating Sm^{III}, Tb^{III}, Dy^{III}, and Ho^{III} metals. The representative structures, when Ln = Sm and Ho, are shown in Figures 63 and 64.[67]

It is commonly known that the Sm^{II} complexes tend to undergo oxidation with oxygen-containing substrates to form the corresponding Sm^{III} species because of their high reactivity and great oxophilicity.[178] This was tested

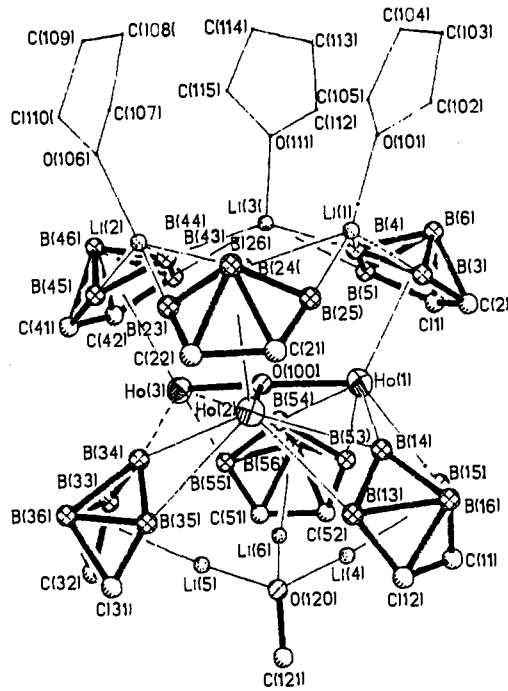

Figure 64. A perspective view of the isostructural trinuclear Ho(III) complex. Reprinted from ref 67.

by reacting $SmCl_3$ with 1 equiv of THF-solvated $Li_2[2,3\text{-}(SiMe_3)_2C_2B_4H_4]$ salt in dry benzene at 0 °C for 24 h and then treating the product with *tert*-butyl alcohol in order to isolate a Sm^{II} complex.[67] Since the complex was a pale yellow solid and most of the reported Sm^{II} species were found to be red solids,[178] formulation of the product as Sm^{II}–carborane was questionable although it was supported by its magnetic susceptibility data (μ_{eff} = 3.5 μ_B). This ambiguity was resolved by determining the crystal structure of the pale yellow solid that showed the complex to be a Sm^{II}–carborane species of the formula $[1,1,1\text{-}(t\text{-}C_4H_9OH)_3\text{-}2,3\text{-}(SiMe_3)_2\text{-}4,5\text{-}(Li(C_4H_8O)Cl)\text{-}closo\text{-}\eta^5\text{-}1\text{-}Sm\text{-}2,3\text{-}C_2B_4H_4]\cdot C_4H_8O$ (see Figure 65).[67] The C_2B_4 carborane ligand is essentially η^5 bonded to the Sm metal (Sm–centroid = 2.445 Å), and three *tert*-butyl alcohol molecules are coordinated to Sm through oxygen. The three Sm–O distances range from 2.10 to 2.31 Å, while O(13)–Sm–O(23) angle (77.3°) is severely contracted by about 36° when compared to the average value of 113.4° in other two O–Sm–O angles. This is presumably due to second coordination of O(13) atom to the THF-solvated Li metal with the distance of 1.98 Å. Perhaps, the steric repulsion between the silyl and *tert*-butyl groups could be responsible for the unusual linear arrangement of Sm, O(18), and C(19) atoms (177.7°). Nonetheless, the average O–Sm–Cnt angles of 113.3° constitute a distorted-tetrahedral geometry of the metal center in the complex. The incorporation of LiCl salt within the coordination sphere of the complex is unusual and interesting. Since the complex can be converted to the corresponding trinuclear system in the absence of *tert*-butyl alcohol, it could be considered as an intermediate species in these systems.

These recent results clearly suggest that a number of novel mono-, tri-, and polynuclear lanthanide complexes of carborane systems could be synthesized and their reactivity patterns established.

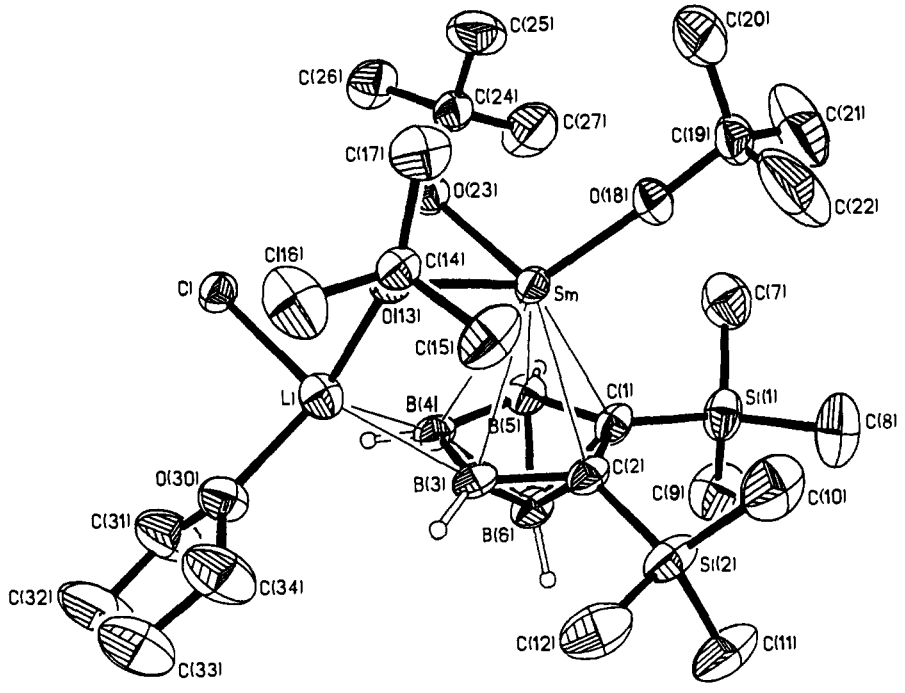

Figure 65. Molecular structure of a *closo*-samaracarborane showing the coordination of LiCl salt and *t*-BuOH molecules. Reprinted from ref 67.

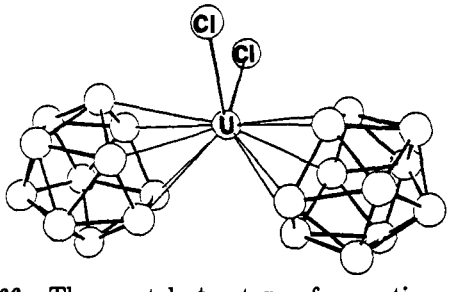

Figure 66. The crystal structure of an actinacarborane $[Li(THF)_4]_2[U(C_2B_9H_{11})_2Cl_2]$. Reprinted from ref 190. Copyright 1976 American Chemical Society.

Except for one report, in 1977, there has been no activity at all in the area of actinacarborane chemistry.[190] Since this work has been cited continuously and none of the reviews described the synthesis and crystal structure of the uranium complex in the paper, we chose to discuss this particular and *the only known actinacarborane*. As per this report, the uranium sandwich compound $[Li(OC_4H_8)_4]_2[U(C_2B_9H_{11})_2Cl_2]$ was prepared, in excess of 75% yield, by the reaction of UCl_4 with $Na_2(C_2B_9H_{11})$ in THF. The crystal structure (Figure 66) shows the coordination geometry of the uranium as a distorted tetrahedron consisting of two η^5-dicarbollide ligands and two σ-bonded Cl atoms. The average U to dicarbollide distances of 2.73 Å is comparable to those found in an uranocene derivative.[267] The centroids of the dicarbollide bonding faces form an angle of 137° about the uranium atom. The bent-sandwich geometry of the complex is very similar to those of bent metallocenes and analogous [3,3-$(THF)_2$-*commo*-3,3′-Sm(3,1,2-$SmC_2B_9H_{11})_2]^-$ and [1,1-$(THF)_2$-*commo*-1,1′-Eu(1,2,4-$EuC_2B_{10}H_{12})_2]^{2-}$ anionic complexes shown in Figures 58 and 61.[179,180,183,184]

It is obvious that a lot more synthetic, mechanistic, structural, and theoretical research has yet to be done before this area of f-block metal–carborane chemistry becomes "predictably uninteresting".

IV. Metallacarboranes In Catalysis

Impetus for the study of metallacarboranes of d-block metals has been their potential as catalysts in olefin polymerization, hydrogenation, hydrosilylation, and isomerization of unsaturated organic substrates. The most studied species are the half-sandwich rhodacarboranes with the pioneering work by Hawthorne and co-workers in the early 1970s.[17,59,191-197] Recently, Hawthorne[13] and Grimes[198] have reviewed this aspect of the metallacarboranes adequately including the work published in 1989. Therefore, we will attempt here to summarize the most salient features of these findings.

A series of closo icosahedral rhodacarboranes bearing substituents at carbon has been synthesized by the reaction of $[(PPh_3)_3RhCl]$ with the corresponding C-substituted *nido*-7-R-8-R′-7,8-$C_2B_9H_{10}]^-$ (where R = H or D and R′ = H, D, Ph, Me, and *n*-Bu). These rhodacarboranes were fully characterized by spectroscopic techniques and, in many cases, by X-ray crystallography.[59,194] While *closo*-1-R-2-R′-3,3-$(Ph_3P)_2$-3-H-3,1,2-$RhC_2B_9H_9$ (where R = R′ = μ-*o*-xylenyl) and *exo-nido*-[$(PPh_3)_2$Rh]-μ-4,9-$(H)_2$-[7-R-8-R′-7,8-$C_2B_9H_8$] (where R = R′ = Me) exist as rapidly interconverting equilibrium mixture of closo and exo-nido isomers in solution, the derivatives of the latter (R = Me, R′ = Ph and R = R′ = μ-$(CH_2)_3$–) exist solely as the exo-nido isomer. The two isomeric forms of [*closo*-3,1,2-$(Ph_3P)_2(H)RhC_2B_9H_{11}$] are shown in Figure 67.[13] In a formal sense, the exo-nido species may be viewed as a complex consisting of a $[L_2Rh]^+$ cation complexed with the [*nido*-7-R-8-R′-7,8-$C_2B_9H_{10}]^-$ anion via two Rh–H–B bridge bonds. A simplified and the most up to date mechanism, based on kinetic and deuterium-labeling studies on the exo-nido isomer, has been proposed by Hawthorne et al. for the hydrogenolysis of alkenyl acetate, alkene isomerization, and alkene hydrogenation as shown in Scheme VIII.[192]

The mechanism involves the slow formation of rhodium monohydride species, containing $B–Rh^{III}–H$ arrays, by the regioselective oxidative addition of

Scheme VIII. A *Revised* Mechanism for the Catalytic Processes Involving an *exo-nido*-Rhodacarborane Complex Based on Kinetic and Deuterium-Labeling Studies (Reprinted from ref 192. Copyright 1989 American Chemical Society)

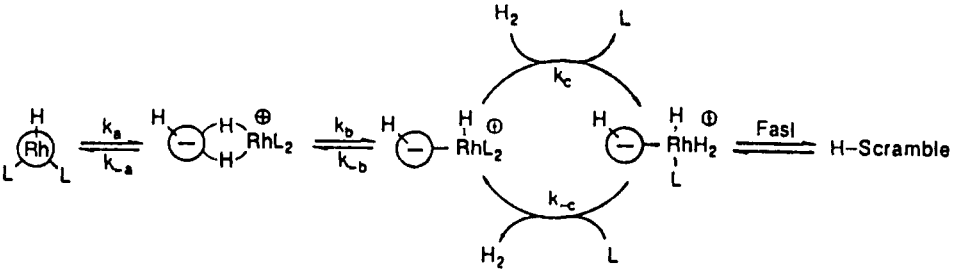

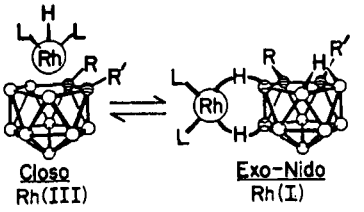

Figure 67. A schematic representation of the two isomeric forms of a rhodacarborane in solution. Reprinted from ref 13. Copyright 1988 VCH Publishers.

terminal B–H bonds to Rh^I centers. These highly reactive metal centers rapidly catalyze the addition of hydrogen to the substrates. Similarly, hydrosilanolyses of alkenyl acetates ($CH_3CO_2CR{=}CH_2$, R = CH_3, C_6H_5) with Et_3SiH in the presence of *exo-nido*-$(PPh_3)_2Rh$·7,8-(μ-$(CH_2)_3$)·7,8-$RhC_2B_9H_{11}$ or *closo*·3,3-$(PPh_3)_2$-3-H-3,1,2-$RhC_2B_9H_{11}$ were demonstrated by the same group in 1990. The mechanistic studies revealed that hydrosilanolysis predominates over hydrosilylation in a ratio of 20:1.[197] These recent findings clearly demonstrate the absence of previously proposed "cluster catalysis" mechanism involving the *closo*-rhodacarborane catalyst precursors.[196,197]

A C-substituted Ir complex, 1-[Ir(CO)(PhCN)(PPh_3)]-7-Ph-σ-1,7-$C_2B_{10}H_{10}$, was found to be an effective catalyst for homogeneous hydrogenation of terminal olefins and acetylenes at room temperature and atmospheric or subatmospheric H_2 pressure. The hydrogenation takes place by a "hydride route". Thus the dihydro complex, formed initially by fast oxidative addition of H_2 to the iridacarborane, accommodates an unsaturated substrate in the coordination sphere by dissociating the nitrile ligand on the metal.[199] A similar study involving an unusual *C*-diphos-substituted rhodacarborane, 1,2-[$(Ph_2P)_2Rh^ICO(Cl)$]-σ-1,2-$C_2B_{10}H_{10}$ in hydrogenation and hydroformylation reactions at elevated temperatures and high H_2 pressures has also been carried out.[200]

The preliminary reports on the reactivity studies, described in an earlier section, indicate that the early transition metal sandwiched carborane complexes[26,28-32,38] have the potential to be active catalysts and/or catalyst precursors in Ziegler–Natta olefin polymerization, and as such more research in this area needs to be done in 1990s before their practical applications are developed.

V. Current and Future Directions

Our discussion summarizes the most promising research published during the past 10 years or so in the area of metallacarboranes of d- and f-block elements. Although the fundamental themes have varied greatly from one research area to the other, they are all aimed at either finding their applications in electronics, ceramics, catalysis, medicine, etc., or simply providing numerous examples of violations of the traditional skeletal electron-counting rules through solid-state structure determinations. Nevertheless, this fascinating and potentially useful research is leading this unique area of organometallic chemistry toward the 21st century. As d^0, 14-electron bent metallocene complexes of Ti, Zr, Hf, and Ta, found to be effective catalysts in Ziegler–Natta olefin polymerization, the metalla species based on purely carborane ligands,[28,29-31] and those of the mixed Cp–carborane ligands[26,32,38] hold great promise. The preliminary reports on metallacarboranes of early transition metals,[28,29-31] with the speculation that these could be developed as better catalysts than the Cp analogues, have evidently inspired the researchers outside the traditional carborane chemistry (Jordan et al. and Bercaw et al., for example) who have found a "goldmine" in the area of catalysis that combines the well-established systems of Cp and carboranes. Since the structural and reactivity patterns in the lanthanide systems are similar to those of the organometallics of scandium and titanium groups, their useful applications in the field of catalysis are inevitable. The ionic nature of the lanthanacarboranes is an added advantage over the early transition metal species in terms of their further synthetic utility in other systems. This has been exemplified in the synthesis of a dinuclear "wedged" manganacarborane sandwich that could not be prepared by the conventional method involving dianionic carborane ligand and the metal reagent, thus demonstrating a superior directing ability of a lanthanide metal than the ligand itself in the formation of targeted species.[66,67] These recent findings show that there is a wealth of fascinating and useful chemistry that needs to be explored in the near future.

The success of Fischer–Tropsch reactions and alkyne metathesis is largely due to alkylidyne–metal cluster chemistry and the work of Stone undoubtedly merged the metallacarborane with alkylidyne chemistry.[45] The mechanistic aspects of the protonation reactions, especially the ligand migrations and cage isomerizations, will be the guiding points for future research in this area. Nonetheless, this area of research has yet to demonstrate its true potential to be the forefrontiers of organometallics.

Although the chemistry of middle and late transition metal–carboranes has traditionally focused on the synthetic, structural, and bonding curiosities, a potentially useful chemistry has emerged in the area of mixed-ligand (carborane and Cp or arene) metalla-C_2B_4 carboranes.[3a] In addition to Grimes' pioneering work

on multidecker sandwich complexes via the "decapitation" sequence, Hawthorne's unique way of making metallacarborane–metallacycles among other discoveries, Sneddon's high-yield route to tricarbametallaborane sandwiches, Chetcuti's method of preparing inclusion compounds, and eventual applications of all these species in variety of disciplines including BNCT, radioimmunotherapy, immunodiagnosis, electronics, ceramics, catalysis, polymers, and solvent extraction of radionuclides, etc., show every indication that this area of research will remain active for many years to come.

VI. Acknowledgment

This work was supported by grants from the National Science Foundation (CHE-9100048), the Robert A. Welch Foundation (N-1016), and the donors of the Petroleum Research Fund, administered by the American Chemical Society. The authors are indebted to Dr. Aderemi R. Oki, for helpful suggestions, and thankful to Professor John E. Bercaw of Caltech, for communicating his results prior to publication, and to Miss Komel Grover and Miss Kim Dawson, for their help in preparing the manuscript.

VII. References

(1) Grimes, R. N., Ed. *Metal interactions with Boron clusters*; Plenum: New York, 1982.
(2) Various authors. In *Electron-Deficient Boron and Carbon clusters*; Olah, G. A., Wade, K., Williams, R. E., Eds.; John Wiley and Sons: New York, 1991; *Pure Appl. Chem.* **1991**, *63*.
(3) (a) Grimes, R. N. *Chem. Rev.* **1992**, *92*, 251. (b) Bregadze, V. I. *Chem. Rev.* **1992**, *92*, 209. (c) Morris, J. H.; Gysling, H. J.; Reed, D. *Chem. Rev.* **1985**, *85*, 51. (d) Hermanek, S. *Chem. Rev.* **1992**, *92*, 325. (e) Kennedy, J. D. In *Multinuclear NMR (NMR in Inorganic and Organometallic Chemistry)*; Mason, J., Ed.; Plenum Press: New York, 1987; Chapter 8, p 221. (f) Wrackmeyer, B. *Annu. Rep. NMR Spectrosc.* **1988**, *20*, 61.
(4) Grimes, R. N. In *Comprehensive Organometallic Chemistry*; Wilkinson, G., Stone, F. G. A., Abel, E. W., Eds.; Pergamon Press: New York, 1982; Chapter 5.5, p 459.
(5) Schubert, D. M.; Manning, M. J.; Hawthorne, M. F. *Phosphorus, Sulphur, Silicon and Rel. Elem.* **1989**, *41*, 253.
(6) Wade, K. *Adv. Inorg. Chem. Radiochem.* **1976**, *18*, 1.
(7) Williams, R. E. *Adv. Inorg. Chem. Radiochem.* **1976**, *18*, 67; *Chem. Rev.* **1992**, *92*, 177.
(8) Hawthorne, M. F.; Young, D. C.; Wagner, P. A. *J. Am. Chem. Soc.* **1965**, *87*, 1818.
(9) Hanusa, T. P. *Polyhedron* **1982**, *1*, 663.
(10) Oki, R. A.; Zhang, H.; Maguire, J. A.; Hosmane, N. S.; Ro, H.; Hatfield, W. E. *Organometallics* **1991**, *10*, 2996.
(11) Jia, L.; Zhang, H.; Hosmane, N. S. *Organometallics* **1992**, *11*, 2957.
(12) Plešek, J. *Chem. Rev.* **1992**, *92*, 269.
(13) Hawthorne, M. F. In *Advances in Boron and the boranes*; Liebman, J. F., Greenberg, A., Williams, R. E., Eds.; VCH: New York, 1988; Chapter 10.
(14) Kalinin, V. N.; Mel'nik, V. A.; Sakharova, A. A.; Frunze, T. M.; Zakharkin, L. I.; Borunova, N. V.; Sharf, V. Z. *Izv. Akad. Nauk SSSR, Ser. Khim.* **1985**, 2442.
(15) Hart, F. A.; Owen, D. W. *Inorg. Chim. Acta* **1985**, *103*, L1.
(16) (a) Anon. *Res. Discl.* **1988**, *292*, 588. (b) Noyori, R.; Kitamura, M. *Modern Synth. Meth.* **1989**, *5*, 115.
(17) Long, J. A.; Marder, T. B.; Behnken, P. E.; Hawthorne, M. F. *J. Am. Chem. Soc.* **1984**, *106*, 2979.
(18) King, R. E., III; Busby, D. C.; Hawthorne, M. F. *J. Organomet. Chem.* **1985**, *279*, 103.
(19) Hatanaka, H. *Borax Rev.* **1991**, *9*, 5.
(20) Barth, R. F.; Soloway, A. H.; Fairchild, R. G. *Cancer Res.* **1990**, *50*, 1061.
(21) Peters, E. N. *J. Macromol. Sci., Rev. Macromol. Chem. C* **1979**, *17*, 173.
(22) Rees, W. S., Jr.; Seyferth, D. *J. Am. Ceram. Soc.* **1988**, *71C*, 194.
(23) Sneddon, L. G.; Mirabelli, M. G. L.; Lynch, A. T.; Fazer, P. J.; Su, K.; Beck, J. S. *Pure Appl. Chem.* **1991**, *63*, 407.
(24) Wilczynski, R.; Sneddon, L. G. *Inorg. Chem.* **1991**, *20*, 3955.
(25) Various authors. In *Comprehensive Organometallic Chemistry*; Wilkinson, G., Stone, F. G. A., Abel, E. W., Eds.; Pergamon Press: New York, 1982.
(26) (a) Marsh, R. E.; Schaefer, W. P.; Bazan, G. C.; Bercaw, J. E. *Acta Crystallogr.* **1992**, *C48*, 1416. (b) Bazan, G. C.; Schaefer, W. P.; Bercaw, J. E. *Organometallics* **1993**, in press.
(27) Shapiro, P. J.; Henling, L. M.; Marsh, R. E.; Bercaw, J. E. *Inorg. Chem.* **1990**, *29*, 4560.
(28) Oki, A. R.; Zhang, H.; Hosmane, N. S. *Organometallics* **1991**, *10*, 3964.
(29) Siriwardane, U.; Zhang, H.; Hosmane, N. S. *J. Am. Chem. Soc.* **1990**, *112*, 9635.
(30) Jia, L.; Zhang, H.; Hosmane, N. S. *Acta Crystallogr.* **1993**, *C49*, 453.
(31) Jia, L.; Wang, Y.; Saxena, A. K.; Oki, A. R.; Zhang, H.; Maguire, J. A.; Hosmane, N. S. Paper Presented at BUSA III, Pulman, WA, 1992.
(32) Crowther, D. J.; Baenziger, N. C.; Jordan, R. F. *J. Am. Chem. Soc.* **1991**, *113*, 1455.
(33) Salentine, C. B.; Hawthorne, M. F. *J. Am. Chem. Soc.* **1975**, *97*, 426.
(34) Salentine, C. B.; Hawthorne, M. F. *Inorg. Chem.* **1976**, *15*, 2872.
(35) Lo, F. Y.; Strouse, C. E.; Callahan, K. P.; Knobler, C. B.; Hawthorne, M. F. *J. Am. Chem. Soc.* **1975**, *97*, 428.
(36) Prout, K.; Cameron, T. S.; Forder, R. A.; Critchley, S. R.; Denton, B.; Rees, G. V. *Acta Crystallogr.* **1974**, *B30*, 2290.
(37) Jordan, R. F. *Adv. Organomet. Chem.* **1991**, *32*, 325.
(38) Uhrhammer, R.; Crowther, D. J.; Olson, J. D.; Swenson, D. C.; Jordan, R. F. *Organometallics* **1992**, *11*, 3098.
(39) Engelhardt, L. M.; Papasergio, R. I.; Raston, C. L.; White, A. H. *Organometallics* **1984**, *3*, 18.
(40) Ruhle, H. W.; Hawthorne, M. F. *Inorg. Chem.* **1968**, *7*, 2279.
(41) St. Clair, D.; Zalkin, A.; Templeton, D. H. *Inorg. Chem.* **1971**, *10*, 2587.
(42) Oki, A. R.; Zhang, H.; Maguire, J. A.; Hosmane, N. S.; Ro, H.; Hatfield, W. E.; Moscherosch, M.; Kaim, W. *Organometallics* **1992**, *11*, 4202.
(43) Swisher, R. G.; Sinn, E.; Grimes, R. N. *Organometallics* **1984**, *3*, 599.
(44) Gard, E.; Haaland, A. *J. Organomet. Chem.* **1975**, *88*, 181.
(45) Stone, F. G. A. *Adv. Organomet. Chem.* **1990**, *31*, 53.
(46) Do, Y.; Knobler, C. B.; Hawthorne, M. F. *J. Am. Chem. Soc.* **1987**, *109*, 1853.
(47) Kim, J.; Do, Y.; Sohn, Y. S.; Knobler, C. B.; Hawthorne, M. F. *J. Organomet. Chem.* **1991**, *418*, C1.
(48) Davis, R.; Kane-Maguire, L. A. P. In *Comprehensive Organometallic Chemistry*; Wilkinson, G., Stone, F. G. A., Abel, E. W., Eds.; Pergamon: New York, 1982; Vol. 3, p 1188.
(49) Elder, M.; Hall, D. *Inorg. Chem.* **1969**, *8*, 1273.
(50) Brew, S. A.; Jeffery, J. C.; Mortimer, M. D.; Stone, F. G. A. *J. Chem. Soc., Dalton Trans.* **1992**, 131.
(51) Brew, S. A.; Carr, N.; Mortimer, M. D.; Stone, F. G. A. *J. Chem. Soc., Dalton Trans.* **1991**, 811.
(52) Brew, S. A.; Devore, D. D.; Jenkins, P. D.; Pilotti, M. U.; Stone, F. G. A. *J. Chem. Soc., Dalton Trans.* **1992**, 393.
(53) Jeffery, J. C.; Li, S.; Sams, D. W. I.; Stone, F. G. A. *J. Chem. Soc., Dalton Trans.* **1992**, 877.
(54) Brew, S. A.; Stone, F. G. A. *J. Chem. Soc., Dalton Trans.* **1992**, 867.
(55) Brew, S. A.; Jenkins, P. D.; Jeffery, J. C.; Stone, F. G. A. *J. Chem. Soc., Dalton Trans.* **1992**, 401.
(56) Brew, S. A.; Carr, N.; Jeffery, J. C.; Pilotti, M. U.; Stone, F. G. A. *J. Am. Chem. Soc.* **1992**, *114*, 393.
(57) Fischer, E. O.; Lindner, T. L.; Huttner, G.; Friedrich, P.; Kreissl, F. R.; Besenhard, J. O. *Chem. Ber.* **1977**, *110*, 3397.
(58) Fischer, E. O. *Adv. Organomet. Chem.* **1990**, *31*, 53.
(59) Knobler, C. B.; Marder, T. B.; Mizusawa, E. A.; Teller, R. G.; Long, J. A.; Behnken, P. E.; Hawthorne, M. F. *J. Am. Chem. Soc.* **1984**, *106*, 2990.
(60) Carr, N.; Gimeno, M. C.; Stone, F. G. A. *J. Chem. Soc., Dalton Trans.* **1990**, 2617.
(61) Goldberg, J. E.; Mullica, D. F.; Sappenfield, E. L.; Stone, F. G. A. *J. Chem. Soc., Dalton Trans.* **1992**, 2495.
(62) Hawthorne, M. F.; Andrews, T. D. *J. Am. Chem. Soc.* **1965**, *87*, 2496.
(63) (a) Salentine, C. G.; Hawthorne, M. F. *Inorg. Chem.* **1976**, *15*, 2872. (b) Knoth, W. H. *Inorg. Chem.* **1971**, *10*, 598.
(64) Oki, A. R.; Zhang, H.; Hosmane, N. S.; Ro, H.; Hatfield, W. *J. Am. Chem. Soc.* **1991**, *113*, 8531.
(65) Haaland, A. *Inorg. Nucl. Chem. Lett.* **1979**, *15*, 267.
(66) Oki, A. R.; Zhang, H.; Hosmane, N. S. *Angew. Chem., Int. Ed. Engl.* **1992**, *31*, 432.
(67) Oki, A. R.; Zhang, H.; Hosmane, N. S. Papers presented at the BUSA III meeting, Pullman, WA, 1992.
(68) (a) Chetcuti, P. A.; Moser, P.; Rihs, G. *Organometallics* **1991**, *10*, 2895. (b) Zalkin, A.; Hopkins, T. E.; Templeton, D. H. *Inorg. Chem.* **1966**, *5*, 1189.
(69) Komiyama, M. *Chem. Lett.* **1988**, 689.
(70) Breslow, R.; Anslyn, E. *J. Am. Chem. Soc.* **1989**, *111*, 5972.
(71) Grimes, R. N. In *Organometallic Reactions and Syntheses*; Becker, E. I., Tsutsui, M., Eds.; Plenum Press: New York, 1977; Vol. 6, Chapter 2, p 63.
(72) Maynard, R. B.; Grimes, R. N. *J. Am. Chem. Soc.* **1982**, *104*, 5983.
(73) Boyter, H. A., Jr.; Grimes, R. N. *Inorg. Chem.* **1988**, *27*, 3075.
(74) Grimes, R. N. *Adv. Inorg. Radio. Chem.* **1983**, *26*, 55.

(75) Grimes, R. N.; Maynard, R. B.; Sinn, E.; Brewer, G. A.; Long, G. J. *J. Am. Chem. Soc.* **1982**, *104*, 5987.
(76) Calhorda, M. J.; Mingos, D. M. P. *J. Organomet. Chem.* **1982**, *229*, 229.
(77) Lee, S. S.; Knobler, C. B.; Hawthorne, M. F. *J. Organomet. Chem.* **1990**, *394*, 29.
(78) Kang, H. C.; Knobler, C. B.; Hawthorne, M. F. *Inorg. Chem.* **1987**, *26*, 3409.
(79) Lee, S. S.; Knobler, C. B.; Hawthorne, M. F. *Organometallics* **1991**, *10*, 1054.
(80) Lee, S. S.; Knobler, C. B.; Hawthorne, M. F. *Organometallics* **1991**, *10*, 1054.
(81) Gress, M. E.; Jacobson, R. A. *Inorg. Chem.* **1973**, *12*, 1746.
(82) Brennan, J. P.; Grimes, R. N.; Schaeffer, R.; Sneddon, L. G. *Inorg. Chem.* **1973**, *12*, 2266.
(83) Bryan, R. F. *J. Chem. Soc., A* **1967**, 192.
(84) Hosmane, N. S.; Maguire, J. A. *Adv. Organomet. Chem.* **1990**, *30*, 99.
(85) Barreto, R. D.; Fehlner, T. P.; Hosmane, N. S. *Inorg. Chem.* **1988**, *27*, 453.
(86) Warren, L. F., Jr.; Hawthorne, M. F. *J. Am. Chem. Soc.* **1968**, *90*, 4823.
(87) Churchill, M. R.; Gold, K.; Francis, J. N.; Hawthorne, M. F. *J. Am. Chem. Soc.* **1969**, *91*, 1222.
(88) Jones, C. J.; Francis, J. N.; Hawthorne, M. F. *J. Am. Chem. Soc.* **1973**, *95*, 7633.
(89) Kang, C. H.; Do, Y.; Knobler, C. B.; Hawthorne, M. F. *Inorg. Chem.* **1988**, *27*, 1716.
(90) Kang, H. C.; Lee, S. S.; Knobler, C. B.; Hawthorne, M. F. *Inorg. Chem.* **1991**, *30*, 2024.
(91) Hawthorne, M. F.; Young, D. C.; Andrews, T. M.; Howe, D. V.; Pilling, R. L.; Pitts, A. D.; Reintjes, M.; Warren, L. F., Jr.; Wegner, P. A. *J. Am. Chem. Soc.* **1968**, *90*, 879.
(92) Boyter, H. A., Jr.; Swisher, R. G.; Sinn, E.; Grimes, R. N. *Inorg. Chem.* **1985**, *24*, 3810.
(93) Davies, S. G.; Scott, F. *J. Organomet. Chem.* **1980**, *188*, C41.
(94) Zimmerman, G. J.; Hall, L. W.; Sneddon, L. G. *Inorg. Chem.* **1980**, *19*, 3643.
(95) Briguglio, J. J.; Sneddon, L. G. *Organometallics* **1985**, *4*, 721.
(96) Briguglio, J. J.; Sneddon, L. G. *Organometallics* **1986**, *5*, 327.
(97) Piepgrass, K. W.; Davis, J. H., Jr.; Sabat, M.; Grimes, R. N. *J. Am. Chem. Soc.* **1991**, *113*, 680.
(98) Piepgrass, K. W.; Stockman, K. E.; Sabat, M.; Grimes, R. N. *Organometallics* **1992**, *11*, 2404.
(99) Piepgrass, K. W.; Grimes, R. N. *Organometallics* **1992**, *11*, 2397.
(100) Paxton, R. J.; Beatty, B. G.; Hawthorne, M. F.; Varadarajan, A.; Williams, L. E.; Curtis, F. L.; Knobler, C. B.; Beatty, J. D.; Shively, J. E. *Proc. Natl. Acad. Sci. U.S.A.* **1991**, *88*, 3387.
(101) Hawthorne, M. F.; Varadarajan, A.; Knobler, C. B.; Chakrabarti, S.; Paxton, R. J.; Beatty, B. G.; Curtis, F. L. *J. Am. Chem. Soc.* **1990**, *112*, 5365.
(102) (a) Gomez, F. A.; Johnson, S. E.; Knobler, C. B.; Hawthorne, M. F. *Inorg. Chem.* **1992**, *31*, 3558. (b) Churchill, M. R.; Gold, K.; Francis, J. N.; Hawthorne, M. F. *J. Am. Chem. Soc.* **1969**, *91*, 1222.
(103) Hosmane, N. S.; Jia, L.; Zhang, H.; Bausch, J. W.; Prakash, G. K. S.; Williams, R. E. *Inorg. Chem.* **1991**, *30*, 3793.
(104) Jia, L.; Wang, Y.; Saxena, A. K.; Oki, A. R.; Zhang, H.; Maguire, J. A.; Hosmane, N. S. Papers presented at the BUSA III meeting, Pullman, WA, 1992; *Organometallics*, submitted for publication.
(105) Schubert, D. M.; Knobler, C. B.; Trofimenko, S.; Hawthorne, M. F. *Inorg. Chem.* **1990**, *29*, 2364.
(106) Colquhoun, H. M.; Greenhongh, T. J.; Wallbridge, M. G. H. *J. Chem. Soc., Chem. Commun.* **1978**, 322.
(107) Bould, J.; Crook, J. E.; Greenwood, N. N.; Kennedy, J. D.; McDonald, W. S. *J. Chem. Soc., Chem. Commun.* **1982**, 346.
(108) Bould, J.; Greenwood, N. N.; Kennedy, J. D.; McDonald, W. S. *J. Chem. Soc., Chem. Commun.* **1982**, 465.
(109) Evans, W. J.; Hawthorne, M. F. *J. Am. Chem. Soc.* **1971**, *93*, 3063.
(110) Jung, C. W.; Hawthorne, M. F. *J. Am. Chem. Soc.* **1980**, *102*, 3024.
(111) Bown, M.; Fontaine, X. L. R.; Greenwood, N. N.; Kennedy, J. D.; Thornton-Pett, M. *Organometallics* **1987**, *6*, 2254.
(112) Crook, J. E.; Greenwood, N. N.; Kennedy, J. D.; McDonald, W. S. *J. Chem. Soc., Chem. Commun.* **1981**, 933.
(113) Greenwood, N. N. In *Electron-Deficient Boron and Carbon Clusters*; Olah, G. A., Wade, K., Williams, R. E., Eds.; John Wiley and Sons: New York, 1991; Chapter 6, p 165.
(114) Kennedy, J. D.; Thornton-Pett, M.; Stibr, B.; Jelinek, T. *Inorg. Chem.* **1991**, *30*, 4481.
(115) Fontaine, X. L. R.; Greenwood, N. N.; Kennedy, J. D.; Nestor, K.; Thornton-Pett, M.; Hermanek, S.; Jelinek, T.; Stibr, B. *J. Chem. Soc., Dalton Trans.* **1990**, 681.
(116) Goldberg, J. E.; Howard, J. A. K.; Muller, H.; Pilotti, M. U.; Stone, F. G. A. *J. Chem. Soc., Dalton Trans.* **1990**, 3055.
(117) Pilotti, M. U.; Topaloglu, I.; Stone, F. G. A. *J. Chem. Soc., Dalton Trans.* **1991**, 1355.
(118) Goldberg, J. E.; Mullica, D. F.; Sappenfield, E. L.; Stone, F. G. A. *J. Chem. Soc., Dalton Trans.* **1992**, 2693.
(119) Pilotti, M. U.; Stone, F. G. A.; Topaloglu, I. *J. Chem. Soc., Dalton Trans.* **1991**, 1621.
(120) Carr, N.; Gimeno, M. C.; Goldberg, J. E.; Pilotti, M. U.; Stone, F. G. A.; Topaloglu, I. *J. Chem. Soc., Dalton Trans.* **1990**, 2253.
(121) Baker, R. T.; King, R. E.; Knobler, C.; O'con, C. A.; Hawthorne, M. F. *J. Am. Chem. Soc.* **1978**, *100*, 8266.
(122) Chetcuti, P. A.; Walker, J. A.; Knobler, C. B.; Hawthorne, M. F. *Organometallics* **1988**, *7*, 641.
(123) Kalb, W. C.; Demidowicz, Z.; Speckman, D. M.; Knobler, C. B.; Teller, R. G.; Hawthorne, M. F. *Inorg. Chem.* **1982**, *21*, 4027.
(124) Hosmane, N. S.; Sirmokadam, N. N. *Organometallics* **1984**, *3*, 1119.
(125) Alcock, N. W.; Taylor, J. G.; Wallbridge, M. G. H. *J. Chem. Soc., Dalton Trans.* **1987**, 1805.
(126) Bresciani, N.; Marsich, N.; Nardin, G.; Randaccio, L. *Inorg. Chim. Acta* **1974**, *10*, L5.
(127) Hartl, H.; Maldjour-Hassan-Abadi, F. *Z. Naturforsch. B: Anorg. Chem., Org. Chem.* **1984**, *39B*, 149.
(128) Yang, X.; Knobler, C. B.; Hawthorne, M. F. *Angew. Chem., Int. Ed. Engl.* **1991**, *30*, 1507.
(129) Salzer, A.; Werner, H. *Angew. Chem.* **1972**, *84*, 949.
(130) Beer, D. C.; Miller, V. R.; Sneddon, L. G.; Grimes, R. N.; Mathew, M.; Palenik, G. J. *J. Am. Chem. Soc.* **1973**, *95*, 3046.
(131) Grimes, R. N. *Pure Appl. Chem.* **1987**, *59*, 847.
(132) Grimes, R. N. In *Advances in Boron and the Boranes*; Liebman, J. F., Greenberg, A., Williams, R. E., Eds.; VCH: New York, 1988; Chapter 11, p 235.
(133) Grimes, R. N. In *Electron-Deficient Boron and Carbon Clusters*; Olah, G. A., Wade, K., Williams, R. E., Eds.; Wiley: New York, 1991; Chapter 11, p 261.
(134) Siebert, W. *Angew. Chem., Int. Ed. Engl.* **1985**, *24*, 943.
(135) Siebert, W. *Pure Appl. Chem.* **1987**, *59*, 947.
(136) Siebert, W. *Adv. Organomet. Chem.* **1980**, *18*, 301.
(137) Spencer, J. T.; Grimes, R. N. *Organometallics* **1987**, *6*, 323.
(138) Swisher, R. G.; Sinn, E.; Grimes, R. N. *Organometallics* **1985**, *4*, 890.
(139) Davis, J. H., Jr.; Benvenuto, M. A.; Grimes, R. N. *Inorg. Chem.* **1991**, *30*, 1765.
(140) Merkert, J. M.; Geiger, W. E.; Davis, J. H., Jr.; Attwood, M. D.; Grimes, R. N. *Organometallics* **1989**, *8*, 1580.
(141) Davis, J. H., Jr.; Sinn, E.; Grimes, R. N. *J. Am. Chem. Soc.* **1989**, *111*, 4776.
(142) Davis, J. H., Jr.; Sinn, E.; Grimes, R. N. *J. Am. Chem. Soc.* **1989**, *111*, 4784.
(143) Fessenbecker, A.; Stephan, M.; Grimes, R. N.; Pritzkow, H.; Zenneck, U.; Siebert, W. *J. Am. Chem. Soc.* **1991**, *113*, 3061.
(144) (a) Plumb, C. A.; Carroll, P. J.; Sneddon, L. G. *Inorg. Chem.* **1991**, *30*, 4678. (b) Weiss, R.; Bryan, R. F. *Acta Crystallogr.* **1977**, *B33*, 588.
(145) Stephan, M.; Davis, J. H., Jr.; Meng, X.; Chase, K. J.; Hauss, J.; Zenneck, U.; Pritzkow, H.; Siebert, W.; Grimes, R. N. *J. Am. Chem. Soc.* **1992**, *114*, 5214.
(146) Benvenuto, M. A.; Sabat, M.; Grimes, R. N. *Inorg. Chem.* **1992**, *31*, 3904. Benvenuto, M. A.; Grimes, R. N. *Inorg. Chem.* **1992**, *31*, 3897.
(147) Dixon, D. A.; Miller, J. S. *J. Am. Chem. Soc.* **1987**, *109*, 3656.
(148) Hanusa, T. P.; Huffman, J. C.; Todd, L. J. *Polyhedron* **1982**, *1*, 77.
(149) Hanusa, T. P.; Huffman, J. C.; Curtis, T. L.; Todd, L. J. *Inorg. Chem.* **1985**, *24*, 787.
(150) Merkert, J. M.; Geiger, W. E.; Attwood, M. D.; Grimes, R. N. *Organometallics* **1991**, *10*, 3545.
(151) Bown, M.; Jelinek, T.; Stibr, B.; Hermanek, S.; Fontaine, X. L. R.; Greenwood, N. N.; Kennedy, J. D.; Thornton-Pett, M. *J. Chem. Soc., Chem. Commun.* **1988**, 974.
(152) Zakharkin, L. I.; Chizhevsky, I. T.; Zhigareva, G. G.; Petrovskii, P. V.; Polyakov, A. V.; Yanovsky, A. I.; Struchkov, Yu. T. *J. Organomet. Chem.* **1988**, *358*, 449.
(153) Bown, M.; Fontaine, X. L. R.; Greenwood, N. N.; Kennedy, J. D.; Thornton-Pett, M. *J. Chem. Soc., Chem. Commun.* **1987**, 1650.
(154) Getman, T. D.; Krause, J. A.; Shore, S. G. *Inorg. Chem.* **1988**, *27*, 2398.
(155) Various authors. In *Advances in Boron and the Boranes*; Liebman, J. F., Greenberg, A., Williams, R. E., Eds.; VCH: New York, 1988.
(156) Ernest, R. L.; Quintana, W.; Rosen, R.; Caroll, P. J.; Sneddon, L. G. *Organometallics* **1987**, *6*, 80.
(157) Quintana, W.; Ernest, R. L.; Carroll, P. J.; Sneddon, L. G. *Organometallics* **1988**, *7*, 166.
(158) Radonovich, L. J.; Klabunde, K. J.; Behrens, C. B.; McCollor, D. P.; Anderson, B. B. *Inorg. Chem.* **1980**, *19*, 1221.
(159) Ditzel, E. J.; Fontaine, X. L. R.; Greenwood, N. N.; Kennedy, J. D.; Sisan, Z.; Stibr, B.; Thornton-Pett, M. *J. Chem. Soc., Chem. Commun.* **1990**, 1741.
(160) Liston, D. J.; Lee, Y. J.; Scheidt, W. R.; Reed, C. A. *J. Am. Chem. Soc.* **1989**, *111*, 6643.
(161) Liston, D. J.; Reed, C. A.; Eigenbrot, C. W.; Scheidt, W. R. *Inorg. Chem.* **1987**, *26*, 2740.
(162) Shelly, K.; Reed, C. A.; Lee, Y. J.; Scheidt, W. R. *J. Am. Chem. Soc.* **1986**, *108*, 3117.
(163) Gupta, G. P.; Lange, G.; Lee, Y. J.; Scheidt, W. R.; Shelly, K.; Reed, C. A. *Inorg. Chem.* **1987**, *26*, 3022.
(164) Shelly, K.; Finster, D. C.; Lee, Y. J.; Scheidt, W. R.; Reed, C. A. *J. Am. Chem. Soc.* **1986**, *108*, 3117.
(165) Nestor, K.; Kennedy, J. D.; Thornton-Pett, M.; Holub, J.; Stibr, B. *Inorg. Chem.* **1992**, *31*, 3339.
(166) Kang, S. O.; Furst, G. F.; Sneddon, L. G. *Inorg. Chem.* **1989**, *28*, 2339.

(167) Stibr, B. *Chem. Rev.* **1992**, *92*, 225.
(168) Plumb, C. A.; Carroll, P. J.; Sneddon, L. G. *Organometallics* **1992**, *11*, 1665.
(169) Plumb, C. A.; Carroll, P. J.; Sneddon, L. G. *Organometallics* **1992**, *11*, 1672.
(170) Plumb, C. A.; Sneddon, L. G. *Organometallics* **1992**, *11*, 1681.
(171) Benfield, F. W. S.; Green, M. L. H. *J. Chem. Soc., Dalton Trans.* **1974**, 1324.
(172) Micciche, R. P.; Briguglio, J. J.; Sneddon, L. G. *Organometallics* **1984**, *3*, 1396.
(173) Wang, Z.; Sinn, E.; Grimes, R. N. *Inorg. Chem.* **1985**, *24*, 834.
(174) Wang, Z.; Sinn, E.; Grimes, R. N. *Inorg. Chem.* **1985**, *24*, 826.
(175) Grimes, R. N.; Sinn, E.; Pipal, J. R. *Inorg. Chem.* **1980**, *19*, 2087.
(176) Hong, F. E.; Eigenbrot, C. W.; Fehlner, T. P. *J. Am. Chem. Soc.* **1989**, *111*, 949.
(177) (a) *Comprehensive Coordination Chemistry*; Wilkinson, G., Gillard, R. D., McCleverty, J. A., Eds.; Pergamon: New York, 1987. (b) *Dictionary of Organometallic Compounds*; Macintyre, J. E., Ed.; Chapman & Hall: New York, 1984; and Suppl. Vols. 1–5, 1985–1989. (c) Cotton, F. A.; Wilkinson, G. In *Advanced Inorganic Chemistry*, 5th ed.; Wiley: New York, 1988 and references therein. (d) Rogers, R. D.; Rogers, L. M. *J. Organomet. Chem.* **1991**, *416*, 201–290.
(178) Evans, W. J. *Adv. Organomet. Chem.* **1985**, *24*, 131.
(179) Manning, M. J.; Knobler, C. B.; Khattar, R.; Hawthorne, M. F. *Inorg. Chem.* **1991**, *30*, 2009.
(180) Manning, M. J.; Knobler, C. B.; Hawthorne, M. F. *J. Am. Chem. Soc.* **1988**, *110*, 4458.
(181) Evans, W. J.; Grate, J. W.; Choi, H. W.; Bloom, I.; Hunter, W. E.; Atwood, J. L. *J. Am. Chem. Soc.* **1985**, *107*, 941.
(182) Evans, W. J.; Grate, J. W.; Levan, K. R.; Bloom, I.; Peterson, T. J.; Doedens, R. J.; Zhang, H.; Atwood, J. L. *Inorg. Chem.* **1986**, *25*, 3614.
(183) Khattar, R.; Manning, M. J.; Knobler, C. B.; Johnson, S. E.; Hawthorne, M. F. *Inorg. Chem.* **1992**, *31*, 268.
(184) Khattar, R.; Knobler, C. B.; Johnson, S. E.; Hawthorne, M. F. *Inorg. Chem.* **1991**, *30*, 1970.
(185) Khattar, R.; Knobler, C. B.; Hawthorne, M. F. *Inorg. Chem.* **1990**, *29*, 2191.
(186) Lebedev, V. N.; Shemyakin, N. F.; Solodovnikov, S. P.; Zakharkin, L. I. *Metalloorg. Khim.* **1988**, *1*, 718; *Chem. Abstr.* **1989**, *111*, 134368v.
(187) Rogers, R. D.; Bynum, R. V.; Atwood, J. L. *J. Organomet. Chem.* **1980**, *192*, 65.
(188) Lamberts, W.; Lueken, H.; Elsenhans, U. *Inorg. Chim. Acta* **1986**, *121*, 81.
(189) Schumann, H.; Kociok-Köhn, G.; Loebel, J. *Z. Anorg. Allg. Chem.* **1990**, *581*, 69.
(190) Fronczek, F. R.; Halstead, G. W.; Raymond, K. N. *J. Am. Chem. Soc.* **1976**, *99*, 1769.
(191) Paxson, T. A.; Hawthorne, M. F. *J. Am. Chem. Soc.* **1974**, *96*, 4674.
(192) Belmont, J. A.; Soto, J.; King, R. E., III; Donaldson, A. J.; Hewes, J. D.; Hawthorne, M. F. *J. Am. Chem. Soc.* **1989**, *111*, 7475.
(193) Baker, R. T.; Delaney, M. S.; King, R. E., III; Knobler, C. B.; Long, J. A.; Marder, T. B.; Paxson, T. E.; Teller, R. G.; Hawthorne, M. F. *J. Am. Chem. Soc.* **1984**, *106*, 2965.
(194) Long, J. A.; Marder, T. B.; Hawthorne, M. F. *J. Am. Chem. Soc.* **1984**, *106*, 3004.
(195) Behnken, P. E.; Belmont, J. A.; Busby, D. C.; Delaney, M. S.; King, R. E., III; Kreimendahl, C. W.; Marder, T. B.; Wilczynski, J. J.; Hawthorne, M. F. *J. Am. Chem. Soc.* **1984**, *106*, 3011.
(196) Behnken, P. E.; Busby, D. C.; Delaney, M. S.; King, R. E., III; Kreimendahl, C. W.; Marder, T. B.; Wilczynski, J. J.; Hawthorne, M. F. *J. Am. Chem. Soc.* **1984**, *106*, 7444.
(197) Kang, H. C.; Hawthorne, M. F. *Organometallics* **1990**, *9*, 2327.
(198) Grimes, R. N. In *Inorganometallic Chemistry*; Fehlner, T. P., Ed.; Plenum Press: New York, 1992; Chapter 6, p 253.
(199) Morandini, F.; Longato, B.; Bresadola, S. *J. Organomet. Chem.* **1982**, *239*, 377.
(200) Hart, F. A.; Owen, D. W. *Inorg. Chim. Acta* **1985**, *103*, L1.
(201) Swisher, R. G.; Sinn, E.; Grimes, R. N. *Organometallics* **1983**, *2*, 506.
(202) Maynard, R. B.; Swisher, R. G.; Grimes, R. N. *Organometallics* **1983**, *2*, 500.
(203) Baumann, F. E.; Howard, J. A. K.; Johnson, O.; Stone, F. G. A. *J. Chem. Soc., Dalton Trans.* **1987**, 2917.
(204) Barker, G. K.; Garcia, M. P.; Green, M.; Stone, F. G. A.; Welch, A. J. *J. Chem. Soc., Dalton Trans.* **1982**, 1679.
(205) Swisher, R. G.; Sinn, E.; Grimes, R. N. *Organometallics* **1985**, *4*, 896.
(206) Swisher, R. G.; Sinn, E.; Butcher, R. J.; Grimes, R. N. *Organometallics* **1985**, *4*, 882.
(207) Chase, K. J.; Bryan, R. F.; Woode, M. K.; Grimes, R. N. *Organometallics* **1991**, *10*, 2631.
(208) Piepgrass, K. W.; Davis, J. H., Jr.; Sabat, M.; Grimes, R. N. *J. Am. Chem. Soc.* **1991**, *113*, 681.
(209) Edwin, J.; Bochmann, M.; Bohm, M. C.; Brennan, D. E.; Geiger, W. E.; Krüger, C.; Pebler, J.; Pritzkow, H.; Siebert, W.; Swiridoff, W.; Wadepohl, H.; Weiss, J.; Zenneck, U. *J. Am. Chem. Soc.* **1983**, *105*, 2582.
(210) Zwecker, J.; Kuhlman, T.; Pritzkow, H.; Siebert, W.; Zenneck, U. *Organometallics* **1988**, *7*, 2316.
(211) Spencer, J. T.; Pourian, M. R.; Butcher, R. J.; Sinn, E.; Grimes, R. N. *Organometallics* **1987**, *6*, 335.
(212) Fessenbecker, A.; Atwood, M. D.; Grimes, R. N.; Stephan, M.; Pritzkow, H.; Zenneck, U.; Siebert, W. *Inorg. Chem.* **1990**, *29*, 5164.
(213) Fessenbecker, A.; Atwood, M. D.; Bryan, R. F.; Grimes, R. N.; Woode, M. K.; Stephan, M.; Zenneck, U.; Siebert, W. *Inorg. Chem.* **1990**, *29*, 5157.
(214) Lewis, Z. G.; Welch, A. J. *J. Organomet. Chem.* **1992**, *430*, C45.
(215) Nestor, K.; Fontaine, X. L. R.; Greenwood, N. N.; Kennedy, J. D.; Plesek, J.; Stibr, B.; Thornton-Pett, M. *Inorg. Chem.* **1989**, *28*, 2219.
(216) Varadarajan, A.; Johnson, S. E.; Gomez, F. A.; Chakrabarti, S.; Knobler, C. B.; Hawthorne, M. F. *J. Am. Chem. Soc.* **1992**, *114*, 9003.